

# Skeletal muscle adaptation in response to chronic oral corticosterone treatment in C57BL/6N mice

A thesis presented to  
The Faculty of Graduate Studies  
of  
Lakehead University  
by  
Paige Perrons

Supervisor: Simon Lees

In partial fulfillment of the requirements  
for the degree of  
Master of Science in Biology

## Abstract

Chronic exposure to elevated glucocorticoid levels represents a significant concern for researchers, healthcare professionals, and the general public. In various disorders and diseases (such as Cushing Syndrome and major depressive disorder), levels of these endogenous stress hormones are chronically elevated. Treatment with glucocorticoids over prolonged periods, as seen in treatment of autoimmune disorders such as rheumatoid arthritis, also results in chronically elevated glucocorticoid levels and poses a significant health concern. While it is generally accepted that chronic glucocorticoid treatment results in skeletal muscle myopathy, less is known about the specific effects of this treatment on functionally different muscle groups and key skeletal muscle structures. The objective of the current study was to determine whether skeletal muscle atrophy is induced in the gastrocnemius/plantaris and soleus by chronic corticosterone (CORT) treatment at doses mimicking physiological stress conditions and to examine the effects of chronic glucocorticoid treatment on key skeletal muscle structures. C57BL/6N mice were dosed with 100 $\mu$ g/mL CORT in drinking water over a period of 4 weeks then compared to naïve (untreated) and vehicle control (<1% ethanol in drinking water) groups. There was a significant decrease in muscle mass and total protein in the CORT group compared to the naïve and vehicle controls in gastrocnemius/plantaris and a smaller, nonsignificant decrease in soleus muscle mass indicating a greater effect of chronic CORT treatment on atrophy in the gastrocnemius/plantaris group, possibly due to muscle recruitment. Relative expression of the contractile proteins myosin and actin were unaffected by treatment. The mitochondrial content biomarker citrate synthase exhibited a nonsignificant increase in relative expression in the gastrocnemius/plantaris but not soleus, indicating possible preservation of mitochondria in chronic stress induced atrophy. Expression of the mitochondrial marker succinate dehydrogenase complex iron sulphur subunit B (SDHB) was unaffected by treatment in gastrocnemius/plantaris and soleus. Significant decreases in relative protein expression of calsequestrin 1 (CASQ1) and

sarcoendoplasmic reticulum ATPase 1 (SERCA1) in the soleus but not gastrocnemius/plantaris indicate potential dysregulation of the sarcoplasmic reticulum (SR) in soleus. The results of this study indicate there is significant atrophy induced in the gastrocnemius/plantaris muscle after 4 weeks of CORT treatment, while the soleus did not exhibit significant atrophy. However, the soleus and not the gastrocnemius/plantaris muscles exhibited decreased expression of proteins involved in SR calcium handling. These data provide further insight into the effects of chronic glucocorticoid levels on skeletal muscles with different fiber type profiles and recruitment patterns.

## Lay Summary

Faculty and students in the Department of Biology at Lakehead University are bound together by a common interest in explaining the diversity of life, the fit between form and function, and the distribution and abundance of organisms. This research supplements the lack of data available for the specific effects of chronic stress induced skeletal muscle atrophy on key muscle components. Namely, it examines changes to the contractile protein content, key markers of mitochondrial content, and critical components of the SR. It also helps fill in gaps in our understanding of the different effects of chronic corticosterone induced atrophy on functionally different muscle types, specifically on the gastrocnemius/plantaris muscle group versus the soleus muscle, which represent fast- and slow-twitch muscles, respectively, and have differences in muscle recruitment and function. Chronic corticosterone exposure can be used as a model of chronic stress and may also be indicative of the effects of low dose treatment with glucocorticoids over long periods of time. The findings of this study suggest that there is a greater effect of chronic corticosterone treatment on the mass of gastrocnemius/plantaris than the soleus, possibly due to differences in muscle recruitment. There was no change detected in relative mitochondrial content or contractile protein content. The relative protein content of key SR indicators remained the same in the gastrocnemius/plantaris muscles, however it was decreased in the soleus muscle. The results from this study supplement existing knowledge on chronic corticosterone treatment and provide a starting point for future studies using this treatment method to compare the effects of corticosterone on skeletal muscle in different muscle groups.

## Acknowledgments

I would like to thank my supervisor Dr. Simon Lees for taking me on and allowing me the opportunity to work in his lab. Even during the most hectic few years, through COVID-19 and project delays, you were there to provide guidance when I needed you. Thank you for making time for my questions even with the hundreds of things you had on the go, and for everything you've taught me.

To my committee members, Dr. Neelam Khaper and Dr. Heidi Schraft, thank you for your patience and your expertise. Your early guidance helped to shape my project and prompted me to dig deeper and expand my understanding of the research, and this project would not have been the same without you. To my external examiner, Dr. Zacharias Suntutres, I cannot thank you enough for your help and willingness to assist on this project.

I would also like to thank Dr. Jocelyn Bel, whose initial efforts and hard work made this project possible. You were a diligent trainer and a wealth of knowledge throughout this process, and I am so grateful for all your support.

Thank you to Sarah Niccoli, for being a friend, a mentor, and an inspiration. Your knowledge of anything and everything relating to technique, research, and lab minutiae is mind boggling. You made long days in the lab fun and were an incredible motivator even in what seemed like the most hopeless situations. I can't thank you enough for your patience and willingness to answer my endless questions.

Thank you to Jake for being my partner in crime during this degree and to Brenda, Courtney, and Reshma, for making my time in the lab (day and night) always enjoyable.

Finally, to my family, thank you for everything. Lexi, Mom, and Dad, thank you for always believing in me and supporting me no matter what. Grandma and Grandpa, thank you for letting me occupy your office to write and for all the love, encouragement, and waffles. To Grandma, for being my most enthusiastic fan. And to Calista, for the good vibes (and the million other things). I love you all.

# Table of Contents

<b>ABSTRACT .....</b>	<b>I</b>
<b>LAY SUMMARY.....</b>	<b>III</b>
<b>ACKNOWLEDGMENTS .....</b>	<b>IV</b>
<b>CHAPTER 1. INTRODUCTION.....</b>	<b>1</b>
1.1 STATEMENT OF PROBLEM .....	1
1.2 SIGNIFICANCE OF STUDY .....	2
1.3 GENERAL RESEARCH QUESTION .....	3
1.4 SPECIFIC AIMS .....	3
<b>CHAPTER 2: LITERATURE REVIEW .....</b>	<b>7</b>
2.1 SKELETAL MUSCLE.....	7
2.1.1 <i>Skeletal Muscle Composition</i> .....	8
2.1.1.1 Contractile Proteins .....	8
2.1.1.2 Mitochondria .....	10
2.1.1.3 Sarcoplasmic Reticulum .....	11
2.2 FAST- AND SLOW-TWITCH FIBERS & MUSCLES.....	13
2.3 MUSCLE RECRUITMENT .....	14
2.4 STRESS RESPONSE AND ACTIVATION OF THE HPA AXIS .....	16
2.4.1 <i>Release of Glucocorticoids under Normal Physiological Conditions</i> .....	18
2.4.2 <i>Corticosteroids</i> .....	19
2.4.2.1 Dexamethasone .....	19
2.4.2.2 Cortisol/ Hydrocortisone .....	21
2.4.2.3 Corticosterone .....	22
2.5 GLUCOCORTICOID INDUCED ATROPHY AND CONTRACTILE PROTEIN .....	22
2.6 GLUCOCORTICOID INDUCED ATROPHY AND MITOCHONDRIA.....	23
2.7 FIBER SPECIFIC DIFFERENCES IN SARCOPLASMIC RETICULUM .....	24
2.8 MODELS OF CHRONIC STRESS .....	24

2.8.1 Stress models using stressful situations.....	24
2.8.2 Chronic GC treatment .....	25
2.9 CUSHING’S SYNDROME .....	25
<b>CHAPTER 3. METHODS .....</b>	<b>27</b>
3.1 INSTITUTIONAL ANIMAL CARE APPROVAL.....	27
3.2 EXPERIMENTAL DESIGN .....	27
3.2.1 Treatments.....	27
3.2.2 Tissue Collection .....	28
3.2.3 Tissue Lysis.....	29
3.2.4 BCA Protein Assay.....	29
3.2.6 Sample Preparation for SDS-PAGE and Western Blot.....	30
3.2.7 Western Blotting.....	30
3.2.8 Coomassie R250 Total Protein Membrane Stain .....	32
3.2.9 Actin vs. Myosin Coomassie G250 Gel Staining .....	33
3.3 LIMITATIONS, BASIC ASSUMPTIONS, AND DELIMITATIONS .....	34
3.3.1 Limitations and Basic Assumptions.....	34
3.3.2 Delimitations.....	35
3.4 STATISTICAL ANALYSIS.....	37
<b>CHAPTER 4. RESULTS .....</b>	<b>38</b>
4.1 DOSING RESULTS .....	38
4.2 ANTHROPOMETRIC RESULTS.....	39
4.2.1 Gastrocnemius/plantaris muscle weight decreases despite increase in body weight in corticosterone treatment group .....	39
4.2.2 Protein yield and muscle mass decrease in parallel in gastrocnemius/plantaris while no significant decreases observed in soleus .....	40
4.2.3 Chronic Corticosterone Exposure Significantly Decreased Skeletal Muscle Wet Weight Normalized to Body Weight in Gastrocnemius/Plantaris but not Soleus .....	41
4.3 CONTRACTILE PROTEIN CONTENT .....	42
4.3.1 Coomassie G250 Gel Stain Results.....	42
4.3.2 Myosin Heavy Chain is Unchanged Relative to Total Protein Content .....	43
4.3.3 Actin is Unchanged Relative to Total Protein Loaded.....	46
4.4 PROTEIN BIOMARKERS OF MITOCHONDRIAL CONTENT .....	48

4.4.1 Citrate Synthase Content is Increased in Gastrocnemius/Plantaris of Corticosterone-treated Mice Relative to Total Protein Content .....	48
4.4.2 SDHB Decreases in Proportion to Total Protein Content .....	50
4.5 PROTEIN BIOMARKERS OF SARCOPLASMIC RETICULUM CONTENT .....	52
4.5.1 CASQ1 Content is Decreased in Soleus of Corticosterone-treated Mice Relative to Total Protein Content .....	52
4.5.2 SERCA1 Content is Decreased in Soleus Relative to Total Protein Content.....	54
<b>CHAPTER 5. DISCUSSION .....</b>	<b>57</b>
5.1 DOSING EFFECTS .....	58
5.2 SAMPLE POPULATION CONSIDERATIONS .....	59
5.3 OVERALL EFFECT OF TREATMENT ON MUSCLE WET WEIGHT AND TOTAL PROTEIN CONTENT .....	59
5.4 ATROPHY EFFECT ON FUNCTIONALLY DIFFERENT MUSCLE GROUPS .....	60
5.5 CONTRACTILE PROTEIN.....	61
5.6 MITOCHONDRIAL CONTENT.....	62
5.7 SARCOPLASMIC RETICULUM CONTENT.....	63
<b>CHAPTER 6. CONCLUSION .....</b>	<b>65</b>
<b>CHAPTER 7. FUTURE DIRECTIONS .....</b>	<b>66</b>
<b>CHAPTER 8. REFERENCES.....</b>	<b>67</b>
<b>CHAPTER 9. APPENDIX .....</b>	<b>81</b>
9.1 LIST OF ABBREVIATIONS.....	81
9.2 ISOFLOURANE ANAESTHESIA IN RODENTS.....	82
9.3 POWER ANALYSIS.....	86
9.4 LEES LAB WESTERN BLOT SOP .....	86
9.5 COOMASSIE G250 MEMBRANE STAINING SOP .....	102
9.6 ADDITIONAL TABLES AND FIGURES.....	104



## List of Figures

Figure 1. Muscle fiber composition. ....	7
Figure 2. Sarcomere and Contractile Proteins. ....	10
Figure 3. HPA Axis .....	16
Figure 4. GR Activation by Glucocorticoids.....	17
Figure 5. Corticosterone Dose Administered.....	38
Figure 6. Body and muscle weights of treated mice.....	39
Figure 7a. Gastrocnemius/Plantaris Muscle Weight .....	41
Figure 7b. Soleus Muscle Weight.....	42
Figure 8. Myosin and Actin in Coomassie Stained Gels. ....	43
Figure 9. Myosin Heavy Chain Expression in Gastrocnemius/Plantaris Western Blot. ....	44
Figure 10. Myosin Heavy Chain Expression in Soleus Western Blot. ....	45
Figure 11. Actin Expression in Gastrocnemius/Plantaris Western Blot. ....	46
Figure 12. Actin Expression in Soleus Western Blot. ....	47
Figure 13. Citrate Synthase Protein Expression in Gastrocnemius/Plantaris .....	49
Figure 14. Citrate Synthase Protein Expression in Soleus.....	50
Figure 15. SDHB Protein Expression in Gastrocnemius/Plantaris.....	51
Figure 16. SDHB Protein Expression in Soleus .....	52
Figure 17. CASQ1 Protein Expression in Gastrocnemius/Plantaris.....	53
Figure 18. CASQ1 Protein Expression in Soleus .....	54
Figure 19. SERCA1 Protein Expression in Gastrocnemius/Plantaris .....	55
Figure 20. SERCA1 Protein Expression in Soleus.....	56

## List of Tables

Table 1. Western Blot Details	32
Table 2. Average muscle mass and protein yield in milligrams of combined gastrocnemius/plantaris muscles in each treatment group.	40
Table 3. Average muscle mass and protein yield in milligrams of combined left and right soleus muscles in each treatment group.	40

## Chapter 1. Introduction

### 1.1 Statement of Problem

Glucocorticoids are a class of corticosteroids which are produced in the adrenal cortex in response to stress [5]. Under normal physiological conditions, these steroid hormones help to regulate metabolic homeostasis including through regulation of protein, carbohydrate, and lipid metabolism; tissue repair; and immune stability [11]. The three major endogenous glucocorticoids are cortisol, corticosterone, and cortisone [6,7]. In humans, the primary ligand of the glucocorticoid receptor (GR) is cortisol, whereas in rodent species including rats and mice the primary ligand of the GR is corticosterone [19]. Glucocorticoids are crucial for controlling appropriate responses to stress, regulating energy homeostasis, and limiting inflammation [12, 13, 14], however, prolonged periods of elevated endogenous glucocorticoid levels, as seen in chronic stress models and disorders such as Cushing's syndrome (a disorder characterized by prolonged, disproportionately high levels of glucocorticoids), can negatively impact overall health and induce muscle atrophy [10,19].

Muscle atrophy is defined as loss of muscle mass and is a serious problem in many aspects of health. It can occur progressively as we age (sarcopenia), as the result of a disease or disorder, or as a side-effect of certain medications or treatments [32, 33, 34, 35, 36]. The loss of muscle mass in elderly individuals leads to an increased likelihood of falls resulting in sprains or fractures, loss of independence and mobility, and increased recovery times following operations [14]. In cancer patients, a higher degree of cancer- or chemotherapy-related muscle loss (i.e. cachexia) has been linked to increased chemotherapy-related toxicities in patients and reduced quality of life [15]. The degree of severity of muscle loss in cancer patients has also been reported to negatively impact a patient's prognosis [16].

As a result of their anti-inflammatory and immunosuppressant capabilities, glucocorticoids are commonly used in the treatment of various inflammatory and autoimmune diseases, including rheumatoid arthritis, multiple sclerosis, Duchene's

muscular dystrophy, and many others [1]. Despite their widespread use and positive effects, chronic treatment with glucocorticoids in a medical setting can lead to negative health outcomes, most notably a loss of skeletal muscle mass [8]. To boost the efficacy of glucocorticoid treatment, synthetic glucocorticoids have been developed which have a higher affinity for GRs and minimal affinity for mineralocorticoid receptors (MRs) including Dexamethasone (DEX), which has 30x the affinity of hydrocortisone for the GR [20]. The selectivity and high affinity of DEX for GR have led to it becoming one of the most popular glucocorticoid treatments in medicine and thus one of the most widely studied glucocorticoids in the literature [32-34]. While synthetic glucocorticoid models are useful to understand the effects of prolonged glucocorticoid treatment in a clinical setting, they are less applicable when studying the effects of chronic stress and health disorders, as they have a far greater affinity for the GR receptors than naturally occurring stress hormones such as corticosterone. This creates a gap in the literature relating to the specific effects of chronically elevated levels of endogenous stress hormones on the skeletal muscle.

## 1.2 Significance of Study

While studies have been done demonstrating *in vivo* loss of skeletal muscle mass following prolonged treatment with synthetic glucocorticoids, there is limited research into the effect of chronic corticosterone treatment on functionally different muscle types. What research exists is often contradictory, and therefore this study provides valuable data regarding the differential effects of chronic glucocorticoid treatment, especially chronic corticosterone treatment, on atrophy. For example, in one study chronic corticosterone treatment resulted in a greater degree of atrophy in slow-twitch than fast-twitch muscle [25]. Another group reported that fast-twitch muscle fibers (and by extension fast-twitch muscles) are decreased to a greater degree than other muscular proteins [23]. Moreover, the majority of the literature has investigated

supraphysiological treatments using dexamethasone. By determining the specific effects of naturally occurring glucocorticoids such as corticosterone on skeletal muscle, a better understanding of stress-induced muscle atrophy may be determined.

There is also a paucity of papers discussing the atrophic effects of glucocorticoids which include treatment with endogenous glucocorticoids, and/or treatment at doses which fall in or near the physiological range (i.e., at a level which could be reasonably expected to occur within an organism, whether healthy or diseased). By using a dose designed to mimic corticosterone levels seen in mice under high stress conditions, we are able to determine the anticipated *in vivo* effects of stress-induced corticosterone on skeletal muscle.

Therefore, the objective of this thesis was to determine whether skeletal muscle atrophy is induced in gastrocnemius/plantaris and soleus of C57BL/6N mice by chronic oral corticosterone treatment at doses mimicking physiological stress conditions, and to examine the phenotypical effects of chronic glucocorticoid treatment on key skeletal muscle structures (contractile protein, mitochondria, and sarcoplasmic reticulum).

### 1.3 General Research Question

1. What are the specific adaptations seen in soleus and gastrocnemius/plantaris skeletal muscles in response to chronic oral corticosterone treatment?

### 1.4 Specific Aims

1. *Determine the effect of chronic oral corticosterone treatment on muscle mass in the soleus muscle and the gastrocnemius/plantaris muscle group.*

**Hypothesis 1:** Chronic corticosterone treatment will lead to a decrease in muscle mass in both the soleus and the gastrocnemius/plantaris muscle group, with a greater amount of atrophy seen in the gastrocnemius/plantaris muscle group.

**Rationale:** Skeletal muscle acts as a reservoir for amino acids and in times of stress proteins can be broken down into amino acids which are then converted through gluconeogenesis into glucose in the liver [5]. Glucocorticoids are known to degrade proteins into amino acids to provide energy as a response to stress or danger stimuli [11, 59]. Muscles composed mainly of fast-twitch fibers, such as the gastrocnemius and plantaris muscles, are recruited more for short, quick bursts of movement, whereas muscles composed mainly of slow-twitch fibers, such as the soleus, are recruited for extended, less intense postural contractions involved in standing [60, 61, 125]. The soleus is a major postural muscle needed to hold the body upright at the ankle, therefore it is recruited during standing in both humans and mice [61, 123, 125]. Since the gastrocnemius/plantaris muscles are not recruited as frequently as the soleus, it is expected that glucocorticoids will cause greater protein catabolism in the gastrocnemius/plantaris group, compared to the soleus.

*2. Determine phenotypic adaptations of skeletal muscle to chronic oral corticosterone treatment, including:*

*2a) Contractile protein content*

**Hypothesis 2a):** Chronic corticosterone treatment will decrease contractile protein content at a faster rate compared to non-contractile proteins in the skeletal muscle. It is expected that both myosin and actin will decrease at the same rate. Myosin and actin will be reduced to a greater extent in the gastrocnemius/plantaris than in the soleus.

**Rationale:** Contractile proteins comprise the majority of the non-water weight of a muscle, with myosin and actin making up approximately 50% of the total protein mass of the muscle [9]. Since the entire volume of contractile protein is not necessary to maintaining the muscle and it can increase or decrease depending on conditions, it is less strictly necessary for survival. Therefore, contractile proteins may be the first catabolized for energy. In some studies, myosin was reported to decrease more than actin [19, 40], whereas in other research models, myosin and actin degraded at the

same rate [38]. Since myosin and actin function as a contractile unit, it is logical to assume that they will decrease in parallel. Since the bulk of the muscle mass loss is expected to occur in gastrocnemius/plantaris, it is expected that the contractile protein loss will be greater in these than the soleus.

### *2b) Sarcoplasmic reticulum (SR) content*

**Hypothesis 2b:** Sarcoplasmic reticulum (SR) content will be increased in gastrocnemius/plantaris and soleus relative to total protein content.

**Rationale:** SR is essential to muscle contraction and relaxation, as it releases, stores, and retrieves calcium ions to enable excitation-contraction coupling [41]. Calsequestrin (CASQ) is the most abundant  $\text{Ca}^{2+}$  binding protein which functions to maintain a constant supply of  $\text{Ca}^{2+}$  in SR for muscle contraction. As such, it can be seen as an important indicator of functional SR volume. According to Hunter et al 2001, hind limb unloading led to an increase in CASQ at both the mRNA (68%) and protein (24%) levels in the soleus of female Wistar rats [39]. Conversely, calsequestrin 1 (CASQ1) knockout models show moderate but significant muscle atrophy in extensor digitorum longus (EDL) muscles and not in soleus muscles, indicating a potentially muscle-specific link between muscle atrophy and CASQ1 content [63]. An important consideration when interpreting these studies is that if contractile protein is selectively reduced in the skeletal muscle, the other non-contractile proteins will increase relative to total protein content. Sarcoplasmic/endoplasmic reticulum calcium ATPase 1 (SERCA1) is a crucial  $\text{Ca}^{2+}$  transporter necessary for signalling in muscle contractions. Previous research reported that SERCA1 is increased relative to total protein content in disuse atrophy, as well as in space-flight atrophy models [67, 76]. In our model of chronic corticosterone treatment, SERCA1 protein is expected to be increased in the corticosterone group relative to control in both gastrocnemius/plantaris and soleus.

### *2c) Mitochondrial content*

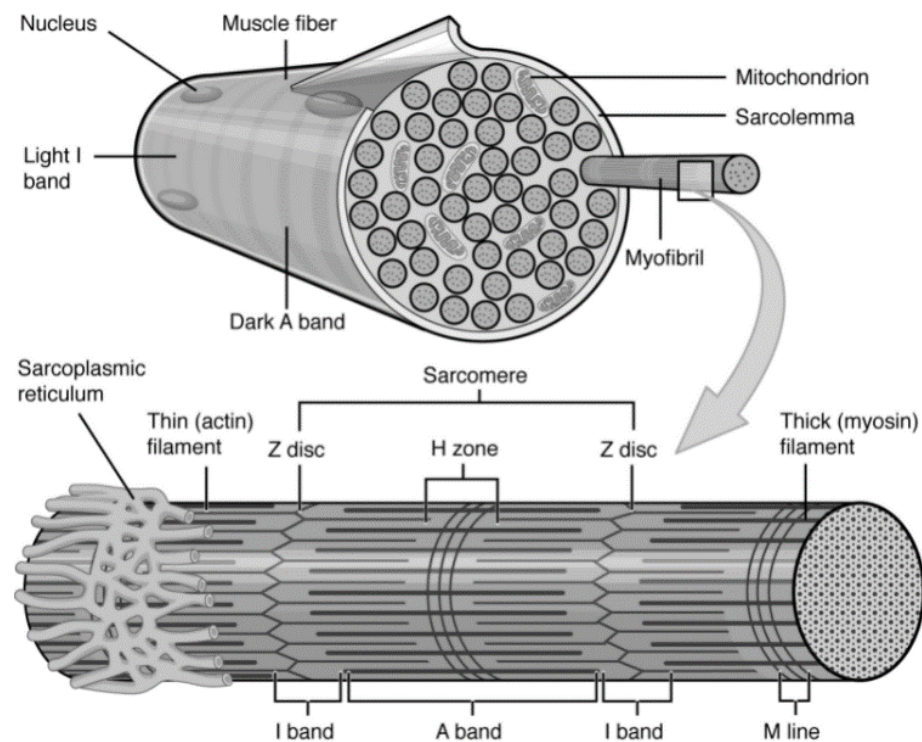
**Hypothesis 2c:** Mitochondrial content will be reduced in gastrocnemius/plantaris but not soleus.

**Rationale:** Chronic stress and stress hormones have been reported in some studies to result in mitochondrial dysfunction via dysregulated exchange between mitochondria and endoplasmic reticulum or reduced mitochondrial biogenesis and quality control [26, 27]. Additional evidence suggests that mitochondrial content is decreased in more extreme atrophy models such as denervation [28]. Markers of functional mitochondrial content such as citrate synthase and succinate dehydrogenase (also called SDH or Complex II), key components of the Krebs cycle, have both been used as indicators of functional mitochondrial content and will provide insight into the effect of chronic corticosterone on mitochondrial content [18, 28, 29]. As it is hypothesized that the gastrocnemius/plantaris group will be more susceptible to corticosterone-induced atrophy, compared to the soleus, it is expected that a decrease in mitochondrial content will be observed in the gastrocnemius/plantaris.

## Chapter 2: Literature Review

### 2.1 Skeletal Muscle

The primary function of skeletal muscle is to produce force to support movement and posture [31]. Skeletal muscle is composed primarily of contractile thick and thin filaments, which contain myosin and actin, respectively. These thick and thin filaments interact to generate force when stimulated by the nervous system [31]. The loss of these contractile fibers leads to reduced generation of force and a weakening of the muscles, as seen in atrophy induced by any model, condition or disease, such as cancer cachexia [30, 40].



**Figure 1. Muscle fiber composition.**

Image taken from Relaix and Zammit 2012 showing the basic composition and levels of organization of a typical skeletal muscle including SR, mitochondria, and myosin and actin filaments [69].



### 2.1.1 Skeletal Muscle Composition

Skeletal muscle can be broken down into several levels of organization as seen in Figure 1. Individual muscle cells- also known as myocytes or muscle fibers- are bundled together in a fascicle surrounded by perimysium. Many fascicles are bunched together and surrounded by epimysium to form a skeletal muscle [8]. Each muscle fiber is a single large cell with hundreds of myonuclei and mitochondria which is first formed during development from the fusion of many myoblasts into myotubes which then further develop and become innervated to form muscle fibers [16]. Each individual muscle fiber is surrounded by the inner plasma membrane and extracellular matrix referred to as the outer basal lamina [16]. Between these two membranes lie the satellite cells, which are a self-maintaining population of multipotent stem cells which help to control muscle growth and repair in post-natal skeletal muscle [4].

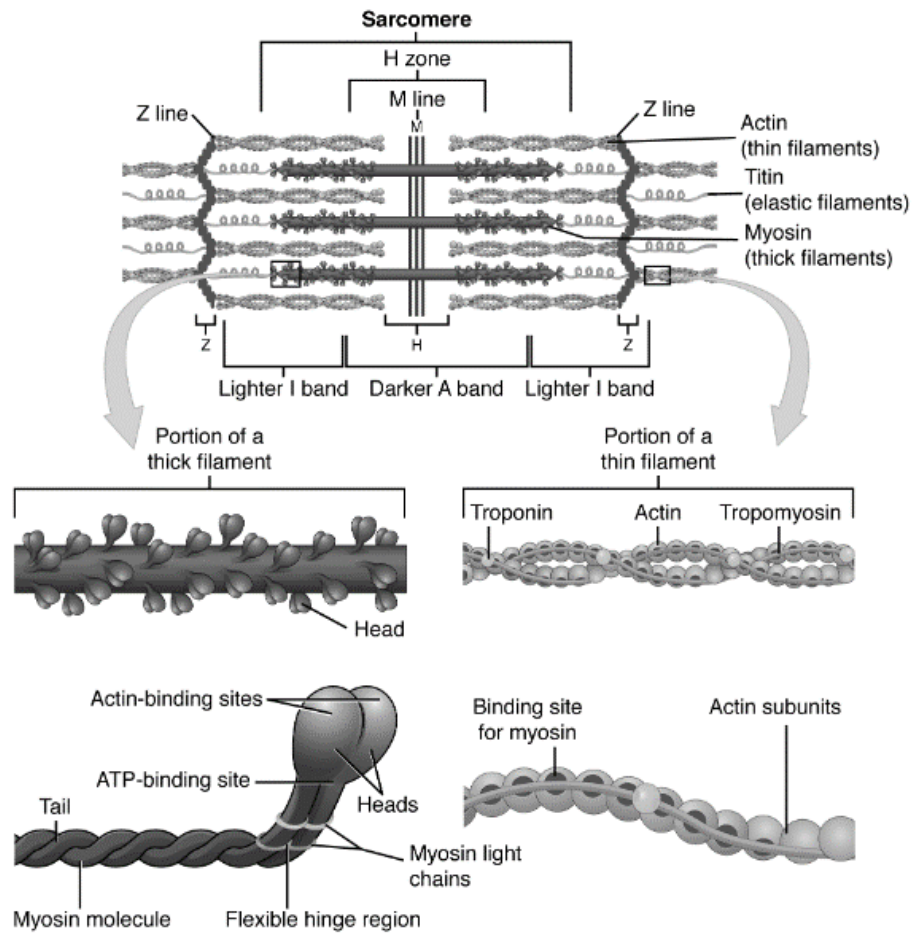
#### 2.1.1.1 Contractile Proteins

Within the plasma membrane there are many myofibrils, columns made up of bundles of myofilaments, primarily composed of two main contractile proteins--actin and myosin— which make up roughly half of the total protein mass of skeletal muscle [9]. Myofibrils are divided into functional units called sarcomeres by Z-discs [21]. These sarcomeres form the basic contractile unit of striated muscle and are depicted in Figure 2. Each sarcomere contains organized thick and thin filaments containing a darker A band composed primarily of myosin (thick filament) and a lighter I band composed primarily of actin (thin filament). Titin is an elastic protein that makes up part of the cytoskeleton; it is anchored at the M line, runs along the length of the myosin filament and attaches to the Z disk to help align the thick filament. Desmin, an intermediate protein located mainly near the Z disks which connects the Z disks to the sarcolemma, mitochondria, and nuclear membrane, is another cytoskeletal protein important for the alignment and organization of the sarcomeres and myofibrils [33, 77]

The thick filaments are composed of myosin protein complexes containing two myosin heavy chain (MHC) and four myosin light chain molecules. The heavy chain

contains a head with an actin-binding site and a binding site for ATP, a hinge region, and a tail region while the light chains help to regulate the hinge region. The thick filament is anchored at the M-line by myomesin [77]. Myosin exists in different isoforms which are different in type I and type II muscle fibers (MYH1, MYH2, MYH3, MYH4, and MYH8, found in type II fibers and MYH7 in type I) [31, 77].

The thin filaments consist of two filamentous actin chains (F-actin) made up of repeating globular actin monomers (G-actin) which are anchored at the Z disk by  $\alpha$ -actinin and extend toward the center of the sarcomere. Actin exists in six isoforms in mammals, of which  $\alpha_{\text{skeletal}}$ -actin is the skeletal muscle isoform and is contained in the actin filaments [79]. Cardiac  $\alpha$ -actin is 99% structurally similar to skeletal  $\alpha$ -actin but is found in the cardiac muscle and in early adult skeletal muscle [79, 80].  $\beta_{\text{cyto}}$ -actin and  $\gamma_{\text{cyto}}$ -actin are the cytoskeleton proteins which are ubiquitously expressed [80]. Each G-actin has a myosin binding site to allow for contraction and is connected to troponin and tropomyosin, which run alongside the actin filaments and control when the actin binding sites will be exposed for myosin binding. Troponin protein complexes contain three polypeptides: troponin I (TnI), troponin T (TnT), and troponin C (TnC) which bind to actin, tropomyosin, and calcium ions respectively [77]. Each troponin subunit exists in muscle- and fiber-specific fast and slow isoforms, however the amount of each isoform varies by muscle type [81]. Other contractile proteins have varying expression in different muscle types as well, although for the purposes of this review we will focus on myosin and actin.



**Figure 2. Sarcomere and Contractile Proteins.**

Image from Biga et al 2019 showing the general structure of the sarcomere as well as closeups of the thick filament (bottom left) and thin filament (bottom right) [31].

### 2.1.1.2 Mitochondria

Millions of mitochondria are interspersed between the myofibers of skeletal muscle to provide the energy needed for muscle contraction (Figure 1). They do this through the production of the precursors NADH and FADH<sub>2</sub> in glycolysis and the Krebs cycle and the direct production of ATP through oxidative phosphorylation. The ATP produced by the mitochondria is hydrolyzed to produce energy which fuels cross-bridge coupling of myosin and actin, allowing for the contraction of the skeletal muscles (along with all other energy-dependent processes in the cells). Several proteins are involved in the mitochondrial energy production processes, including citrate synthase and succinate

dehydrogenase (SDH). Citrate synthase is a Krebs cycle enzyme which catalyzes the synthesis of citrate from oxaloacetate and acetyl coenzyme A; it is a rate limiting enzyme and is found in nearly all cells capable of oxidative metabolism. It is commonly used as a marker of intact mitochondria, as it is present in high amounts in cells and is essential to proper function of a living mitochondria. Although the activity of citrate synthase is more commonly used as an indicator than protein expression, nearly all studies which have examined both citrate synthase activity and citrate synthase protein expression found that activity and expression increased and/or decreased together [18,28].

The SDH enzyme complex is composed of four nuclear-encoded subunits including SDH iron sulfur subunit B (SDHB) and plays a critical role in the mitochondria. SDH converts succinate to fumarate which releases electrons as part of the Krebs cycle. It also provides an attachment site for released electrons to be transferred to the oxidative phosphorylation pathway and is therefore a key part of the electron transport chain. SDH helps with oxygen-related gene regulation through its conversion of succinate, which is an oxygen sensor that stabilizes the hypoxia-inducible factor 1 (HIF1) transcription factor [108]. Staining for SDH activity is often used as a marker of mitochondrial content in histology, and although less commonly used, SDH protein content is also used as a marker of mitochondrial content [37, 109]. Additionally, due to its role in the electron transfer chain, it is sometimes used as a marker of muscle oxidative capacity [37].

#### *2.1.1.3 Sarcoplasmic Reticulum*

The sarcoplasmic reticulum is an organelle comprised of a network of interconnected tubules that surrounds each myofiber (Figure 1). It is responsible for the storage, release, and retrieval of calcium ions in skeletal muscle. Calcium ions are important secondary messengers that control several vital processes including programmed cell death, gene transcription, and protein synthesis and breakdown [24]. In muscle, the SR plays a central role in excitation contraction coupling by providing  $\text{Ca}^{2+}$

ions to allow cross-bridge formation and contraction of myofilaments and retrieves  $\text{Ca}^{2+}$  ions from the myoplasm to allow for relaxation [43].

Within the SR, calcium-binding proteins function as a calcium buffer. These proteins help hold calcium in the cisterna of the SR after a muscle contraction, even though the concentration of calcium in the SR is much higher than in the surrounding cytosol. In the lumen of the intracellular stores, large amounts of  $\text{Ca}^{2+}$  are buffered by calcium binding proteins such as calsequestrin and calreticulin. Calsequestrin is the major  $\text{Ca}^{2+}$ -binding protein in skeletal and cardiac muscle and is localized in the terminal cisternae of the SR of skeletal muscle [44, 45]. Calsequestrin is present in skeletal muscle in two isoforms: CSQ1 (the main isoform) and CSQ2. CSQ1 is a major determinant of maximal SR  $\text{Ca}^{2+}$  capacity in skeletal muscle fibers [45]. In skeletal muscle-- especially fast twitch muscle--there must be a large amount of  $\text{Ca}^{2+}$  on hand at all times to produce quick contractions and a large amount of sarcoendoplasmic reticulum calcium ATPase (SERCA) pumps (discussed below) present to allow release of  $\text{Ca}^{2+}$  for rapid muscle relaxation. Since SERCA pumps leak  $\text{Ca}^{2+}$  and a great deal of ATP is needed to pump the  $\text{Ca}^{2+}$  back into the SR, calcium binding proteins such as CSQ1 are essential to keep the amount of free  $\text{Ca}^{2+}$  low while also keeping a large store of  $\text{Ca}^{2+}$  on hand for rapid release [45]. By reducing the calcium binding capacity of the muscles, the efficiency of contraction and relaxation is reduced. It is worth noting, however, that in one study of CSQ1-null mice, the mice remained viable with little or no change in twitch and tetanic peak force, and only moderate slowing of the rise time and decay of the twitch [47]. They also showed no increase in the other calsequestrin isoform, CSQ2. This may be explained by the other calcium binding proteins present in the sarcoplasm but could also indicate an increased role of SERCA2b pumps with modified SERCA1 properties, which has not been measured [45]. Some studies have indicated that in disuse (denervation) atrophy, there is an increase in calcium sequestration capacity of the muscles, although the effects on less severe atrophy models are as yet unknown [39].

The most abundant protein in the SR is the sarcoendoplasmic reticulum calcium ATPase (SERCA) pump, which transports  $\text{Ca}^{2+}$  from the cytosol back to the SR following muscle contraction [122]. The SERCA protein is localized on the SR membrane and exists in three known isoforms: SERCA1, SERCA2, and SERCA3. SERCA1 is the fast-twitch skeletal muscle isoform and is further divided in SERCA1a (the adult isoform) and SERCA1b (the fetal isoform, not found in adult muscle). SERCA1a is expressed only in fast twitch fibers, while SERCA2a is predominantly expressed in cardiac and slow-twitch muscle fibers and SERCA2b is expressed at low levels in all tissues, including muscle. SERCA3 is not present in muscle [101].

The reduced activity of SERCA1, an essential  $\text{Ca}^{2+}$  pump, has strong ties to muscle atrophy and weakness and can lead to SR stress and mitochondrial dysfunction [64]. The ATP consumed by SERCA pumps contributes to 50% of the resting metabolic rate of muscles in mice, and thus it can be understood that SERCA creates a large energy demand [49]. An increase in the number of SERCA transporter proteins leaking  $\text{Ca}^{2+}$  and increasing energy demand on the muscle could make it an important contributing factor in characterizing atrophy. Previous research has reported that SERCA1 is increased in disuse atrophy, as well as in space-flight models [67, 76]. In one study examining the effect of disuse on SERCA1 content, researchers observed an approximately 120% increase in SERCA1 protein content of the vastus lateralis following 23 days of unilateral lower limb suspensions in humans [76]. In a spaceflight model, mice showed statistically significant impairments in  $\text{Ca}^{2+}$  uptake despite having increases in SERCA1 protein content [67]. Contradictorily, in a model of heart failure, SERCA1 protein levels were reported to decrease by 46%, 64% and 42% respectively in the tibialis anterior (TA), diaphragm, and gastrocnemius, while muscle wasting of ~15% was seen in the gastrocnemius, TA, and plantaris, indicating a potential correlation between decreased SERCA1 protein and muscle wasting in this model [71].

## 2.2 Fast- and Slow-twitch Fibers & Muscles

There are two main types of skeletal muscle fibers: slow-twitch (type I) and fast-twitch (type II). Type I fibers contract relatively slowly and use aerobic respiration

(oxygen and glucose) to produce ATP, while type II fibers have relatively fast contractions and have a larger capacity for anaerobic glycolysis to provide for the large, often sudden ATP demands for the faster contraction velocities, although this high energy output cannot be sustained by anaerobic metabolism in the long-term [30, 38, 111]. Type II fibers can also be further divided into type 2a (fast oxidative) and type 2b (fast twitch glycolytic) [30].

All skeletal muscles have a mixture of these different fiber types but are sometimes classified as fast- or slow-twitch muscles based on the relative amount of each fiber type present. Slow-twitch muscles have more type I fibers, higher levels of mitochondria, and are important to posture ex. soleus [45]. Fast-twitch muscles have more type II fibers, lower levels of mitochondria, and produce greater, quicker force for movement activities ex. gastrocnemius, plantaris [38]. Fast and slow twitch muscles often respond differently to atrophy [30, 38, 111]. In a study of the fiber type composition of C57BL6J mice (the same strain used in our study but a different substrain), the gastrocnemius muscles contained around 95% type II fibers and only 5% type I and the soleus muscle contained roughly 40% type I and 60% type II muscle fibers [112].

### 2.3 Muscle Recruitment

Gastrocnemius and plantaris can also be differentiated from soleus because they are both more movement than posture-oriented and are typically recruited for movements such as jumping and running [48, 65, 125]. Soleus muscle is a postural muscle located deep to the gastrocnemius and plantaris. It is recruited for normal weight bearing activities and to maintain posture [48, 65, 123, 124]. As a typically highly active species, mice often engage in voluntary wheel running and other activity when the options are provided. When examining the effects of high frequency running program (HRP; twice per day) and low frequency running program (LRP; once per day) treadmill running programs on the muscle mass of gastrocnemius and soleus muscles in aged mice with low voluntary movement, there was a significant increase in the

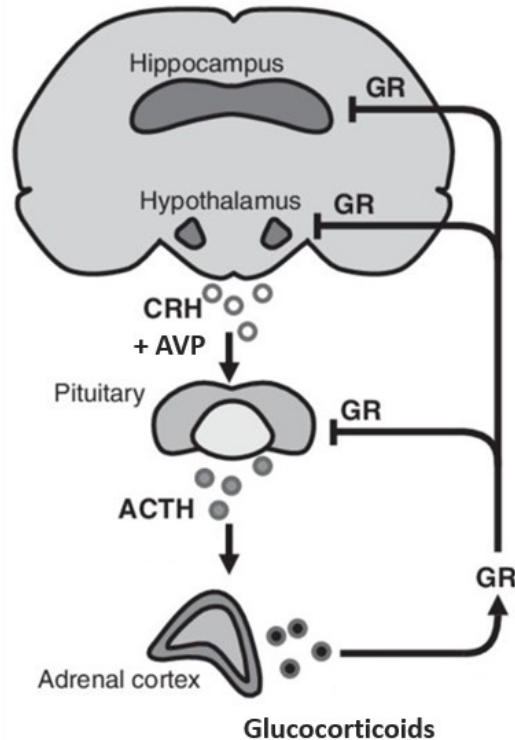
gastrocnemius wet weight in the HRP group compared to control while no significant changes in soleus wet weight were observed in either running group compared to control [75]. This indicates that gastrocnemius muscles are more sensitive to increased voluntary movement than soleus muscles.

Karatsoreos et al examined the effect of low (25µg/mL) and high (100µg/mL) doses of corticosterone over a period of four weeks and found the overall home-cage locomotor activity of C57BL/6 rats was significantly decreased compared to control [53]. In another study by DeVallance et al, mice exposed to the Unpredictable Chronic Mild Stress (UCMS) model over a period of 8 weeks showed reduced voluntary wheel running behaviour with running time, distance, and work all significantly decreased in the stressed versus the unstressed groups [50]. In support of this, other studies have also demonstrated that during periods of chronic stress in mice, voluntary exercise is reduced and depressive, sleep-like periods of reduced activity occur during dark cycles when mice are typically most active [51, 52]. As mice are exposed to stress hormones over an extended period, they will engage in less activity requiring the recruitment of the gastrocnemius and plantaris muscle group while the soleus muscle will continue to be used for weightbearing throughout treatment as mice move freely about the cage, even as activities such as wheel running are reduced. Importantly, this continued recruitment of the soleus for weightbearing represents a marked difference from atrophy studies using a hindlimb unloading or denervation atrophy model, where all leg muscles including the soleus are not used at all.

As mice become more sedentary throughout the treatment, muscles which are not in use will be broken down sooner as a source of amino acids for gluconeogenesis [5,11,18,40]. Therefore, due to regular recruitment of the soleus for weightbearing, it is accepted that there is less atrophy in the soleus than the gastrocnemius and plantaris in response to chronic stress (the soleus muscle continues to be used and therefore will be spared) and therefore any adaptations to skeletal muscle morphology should be seen first/ to a greater degree in the gastrocnemius/plantaris.



## 2.4 Stress Response and Activation of the HPA Axis



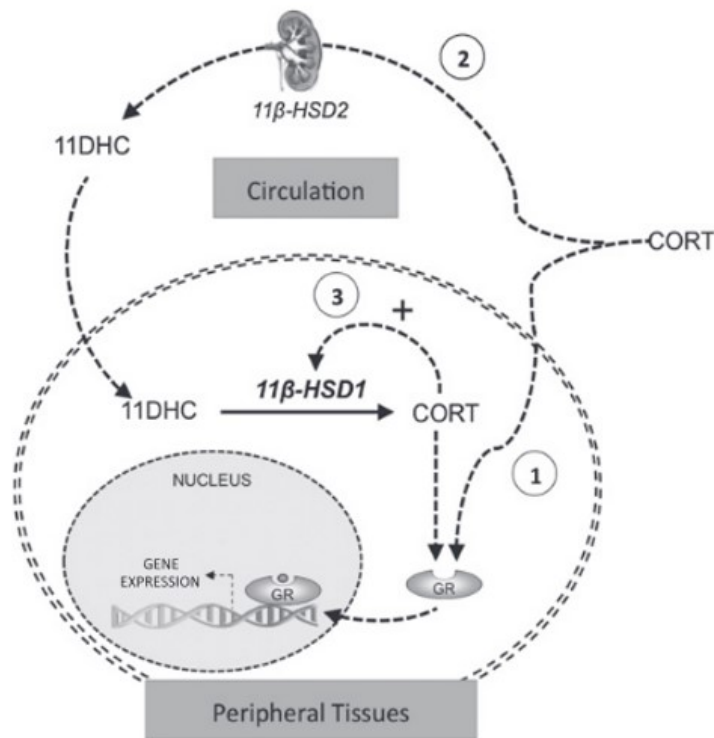
**Figure 3. HPA Axis**

Figure adapted from Kitraki et al showing the stages of glucocorticoid release by the HPA axis [97].

When presented with a stressor (which can be any perceived threat, real or imagined) the hypothalamus-pituitary-adrenocortical (HPA) axis will be activated. The HPA axis is the primary driver of the endocrine stress response and it is affected in some way by all types of stressors, therefore its activation is a hallmark of the body's reaction to stress. Upon activation of the HPA axis, the hypothalamus releases corticotropin releasing hormone (CRH) and arginine vasopressin (AVP) which stimulates the anterior pituitary to secrete adrenocorticotrophin hormone (ACTH) (Figure 3). ACTH then stimulates the synthesis and release of glucocorticoids from the cortex of the adrenal glands [72]. The adrenal cortex has 3 cellular zones- the zona glomerulosa, the zona fasciculata, and the zona reticularis which each secrete their own set of hormones: the

zona glomerulosa is the main site for mineralocorticoids, the zona reticularis for androgens, and the zona fasciculata for glucocorticoids [58].

After being released from the zona fasciculata of the adrenal cortex, glucocorticoids activate glucocorticoid receptors (GRs) using three main pathways, as demonstrated in Figure 4. Key regulator 11beta-hydroxysteroid dehydrogenase type 1 (11 $\beta$ -HSD1) converts inactive cortisone (11-dehydrocorticosterone in rodents) to active cortisol in humans or to corticosterone in rodents, while 11beta-hydroxysteroid dehydrogenase type 2 (11 $\beta$ -HSD2) converts active cortisol to inactive cortisone [82, 100].



**Figure 4. GR Activation by Glucocorticoids**

Signalling Image taken from Morgan et al 2013 [100]. Circulating endogenous glucocorticoids such as corticosterone in rodents (CORT) can activate the GR by three main mechanisms: (1) Circulating corticosterone binds to the GR in peripheral tissues; (2) Circulating CORT is inactivated by 11 $\beta$ -HSD2, then reactivated in peripheral tissues

by 11 $\beta$ -HSD1; and (3) GR activation increases 11 $\beta$ -HSD1 expression and activity, further amplifying intracellular CORT availability.

The release of glucocorticoids is controlled by glucocorticoid negative feedback, which is primarily read by the GR, and therefore the GR is assumed to control the bulk of feedback regulation [73]. In this negative feedback loop, glucocorticoid binding to the GR receptors in the brain and pituitary gland prevents the production of CRH and ACTH, stopping the production and release of more glucocorticoids [73]. The main glucocorticoid produced in humans is cortisol, whereas in rodents (which lack the adrenocortical zona fasciculata enzyme 17- $\alpha$  hydroxylase (*CYP17*) necessary for high amounts of cortisol production) corticosterone is the main corticosteroid [74]. Both cortisol and corticosterone have broad physiologic effects on the body and are widely accepted to have approximately equivalent downstream signalling and affinities for the GR ( $K_d \approx 5.0$  nM) [126, 127].

In addition to activation of the HPA axis, a typical stress response will also activate the sympathetic nervous system (SNS) axis which prompts the release of epinephrine and norepinephrine from the medulla of the adrenal glands, and together with glucocorticoids these trigger changes in blood pressure, heart rate, glucose metabolism, and many more wide-ranging effects [99].

#### 2.4.1 Release of Glucocorticoids under Normal Physiological Conditions

In healthy humans, the primary stress hormone, cortisol, follows a diurnal pattern where the cortisol level is higher after waking, increases significantly and peaks around thirty minutes after waking, then steadily decreases throughout the day, reaching its lowest point in the middle of the night during the rest phase [55, 56]. In most mammals, the release of glucocorticoids follows a circadian cycle with GC levels peaking right after waking and decreasing steadily to reach nadir sometime in the rest phase (whether this is during the night or day depends on if the animal is nocturnal or not) [56]. Normal values for serum cortisol in humans taken at 8:00am near the peak are

between 140 and 690nmol/L but can vary depending on the laboratory running the tests, medications being taken, or other if other tests are being run concurrently [57]. Values below these levels can indicate adrenal insufficiency, hypopituitary disorders, etc., while values above can indicate stress, Cushing disease, tumors of the adrenal gland, etc. [57].

#### 2.4.2 Corticosteroids

Corticosteroids are a class of steroid hormones which are released by the adrenal glands. Of note, although this class technically includes both mineralocorticoids (MCs) and glucocorticoids (GCs), the designation “corticosteroid” is often used interchangeably with “glucocorticoid”. GCs produced have different metabolic effects on different tissues and communicate signals through GC receptors (GR) scattered throughout the body. In skeletal muscle, the main function of GCs is regulation of protein and glucose metabolism. When GC levels are increased in stressful conditions, the rate of protein synthesis is decreased and protein degradation is increased to provide precursors for hepatic gluconeogenesis [5, 11]. Cortisol and corticosterone have equal binding affinity for the mineralocorticoid receptor (MR) and GR [5]. In addition to these two key endogenous glucocorticoids, several synthetic glucocorticoids have been synthesized in recent years which have similar effects, including prednisolone and dexamethasone. Naturally occurring primary stress hormones bind to GRs located throughout the body, but also share an approximately equal affinity with mineralocorticoid receptors, making them far less selective for GRs than synthetic glucocorticoids including Dexamethasone which have a much greater affinity for the GR [5, 20].

##### 2.4.2.1 Dexamethasone

Dexamethasone (DEX) is a synthetic glucocorticoid first discovered by Phillip Showalter Hench which is commonly used to treat autoimmune diseases. It is popularly used in animal studies, as it is commonly prescribed in healthcare, making the

characterization of its effects and mechanism of action very valuable. In recent years, glucocorticoids including DEX and Prednisone have also been trialed as a therapy for severe cases of COVID-19, to mixed success [2,3]. Whereas in acute treatment, daily DEX treatment for up to 10 days lowered mortality rates in patients requiring oxygen or invasive ventilation [3], other data suggest chronic glucocorticoid use may increase the odds of hospitalization or death in people who contract the COVID-19 virus [4,17]. In atrophy studies, DEX has been reported to decrease the proliferation of C2C12 myogenic cells; adding doses of DEX at 0, 25, 50, 75, 100, 150, or 200 nM to medium with or without 5% horse serum decreased proliferation in each treatment compared to controls, increased protein degradation, and decreased protein synthesis [33].

MURF-1 is a ubiquitin ligase which controls proteasome-dependent degradation of muscle proteins. Since glucocorticoids typically increase muscle protein degradation in the muscle atrophy process, elevated MURF-1 levels may be used as an indicator of muscle wasting. Bodine et al induced muscle atrophy and treated rats orally with 6µg/mL DEX for nine days, then used northern blots to determine the amount of mRNA of two ubiquitin ligases: MURF-1 and MuFbx. Results indicated that there was a greater than 10-fold increase of mRNA in both molecules in atrophied muscle versus the control [70]. Another study used L6 and C2C12 myotubes with 1 µM dexamethasone (DEX), or 1 µM corticosterone (CC) for 24 and 48 h. It was reported that there was a dose-dependent increase in protein degradation rates in both cell lines with DEX. The MURF1 mRNA level in L6 myotubes increased 2-to-3-fold, but no increase was observed in C2C12s with either treatment. The Atrogin-1 mRNA level increased 2 to 2.5 fold in L6 and C2C12 myotubes, however a lower sensitivity to CORT was reported in C2C12 myotubes (needed 10uM vs 0.1uM dose to increase mRNA) [32].

In Barel et al, the effect of exercise training on DEX induced atrophy and other symptoms was observed. Rats which were given dexamethasone treatment (1 mg/kg per day, interperitoneally for 10 days) exhibited body weight loss (-24%), with muscular atrophy in the tibialis anterior (-25%) and the extensor digitorum longus (-15%),

however there was no significant atrophy in the soleus. Dexamethasone also increased fasting serum insulin levels by 5.7-fold and glucose levels by 2.5-fold compared to control, and decreased muscular glycogen (41%) [87].

#### 2.4.2.2 Cortisol/ Hydrocortisone

Cortisol (or hydrocortisone as it is referred to when prescribed in a clinical setting) is the main glucocorticoid in humans. It is commonly studied in chronic stress models both *in vitro* and *in vivo*, although it is less appropriate as a chronic stress model in rodent studies as it is not the primary stress hormone in rodents. Despite its limitations, its similar function in human chronic stress response makes it valuable in understanding the effects of chronic corticosterone treatment on mice. Fimbel et al. subcutaneously injected young, growing, male Wistar rats with hydrocortisone acetate (5 mg kg<sup>-1</sup> day<sup>-1</sup>) daily and exercise programs of varying intensities were investigated. After 8 weeks, they reported that final body weight in control and cortisol rats was similar (with or without training); that the specific carcass mass (1g carcass/100g body weight) was significantly lowered 4-7% by corticoid treatment; that absolute mass of studied muscles was significantly reduced only in fast-type plantaris, EDL, and tibialis anterior muscles with no effect on the soleus (slow-type muscle); that total muscle protein content was significantly reduced (9-13%) in the fast type muscles; that cross-sectional myofiber area was 12-18% reduced in Type 2b fibers; and that carcass lipid content was reduced in steroid-treated rats ( $p < 0.01$ ) [86].

Ferguson et al. treated New Zealand White rabbits with the cortisol precursor cortisone using intramuscular injections into their right lower extremity of either cortisone acetate (10 mg/kg/day, Cortone, 50 mg/ml [Merck, Sharp & Dohme, West Point, PA]) or normal saline (0.6 ml/day) for 3 weeks. After 3 weeks, they observed a significant decrease in the body weight and muscle mass of the diaphragm, sternocleidomastoid, and EDL of the cortisone acetate treated group but no effect on the soleus. Likewise, muscle fiber volume of the cortisone group decreased significantly

(around 40% compared to control) in all the previous muscles except soleus. The number of muscle fibers and composition of muscle fiber types remained unchanged. [87].

Brotto et al. treated C2C12 cells and human primary muscle cells with cortisone, allowing 11beta-HSD1 to convert the corticoid to its active form (while also studying cells with the 11beta-HSD1 gene knocked out to ensure the effect observed was a result of the cortisone being converted). In cells without 11beta-HSD1, the cortisone was not converted to its active form, and atrophy did not occur. In cells with functional 11beta-HSD1, protein degradation increased 20%, MURF1 mRNA expression increased, and Atrogin-1 mRNA expression increased [78].

#### 2.4.2.3 Corticosterone

Corticosterone (CORT) is the primary endogenous stress hormone in rodents. It is best used when replicating a chronic or acute stress model, compared to DEX or cortisol. It has been used in a number of stress and atrophy studies, both *in vitro* and *in vivo*. Menconi et al used L6 (rat) and C2C12 (mouse) myotubes with 1  $\mu$ M dexamethasone or 1  $\mu$ M corticosterone for 24 and 48 h and found a dose-dependent increase in protein degradation rates in both cell lines with CORT. The MURF1 mRNA level in L6 myotubes increased 2-to-3-fold, however no increase was observed in C2C12s with either treatment. The Atrogin-1 mRNA level increased 2-to-2.5-fold in L6 and C2C12 myotubes and had lower sensitivity to CORT in C2C12 (needed 10uM vs 0.1uM dose to increase mRNA) [32].

## 2.5 Glucocorticoid Induced Atrophy and Contractile Protein

It is generally accepted that prolonged exposure to glucocorticoids has a catabolic effect on muscle protein metabolism and will lead to decreased muscle protein synthesis and increased muscle protein breakdown [102]. Since skeletal muscle myosin and actin form a contractile unit, their degradation should theoretically happen

at approximately the same rate if tied primarily to disuse, although different degradation pathways may also be a factor [103, 104]. There are conflicting reports in the literature regarding the relative rate of degradation of myosin and actin during skeletal muscle atrophy, with myosin sometimes being reported to decrease quicker than actin [19, 40] or other times with myosin and actin degrading at the same rate [38]. One study showed that C2C12 mouse myotubes atrophied when treated with DEX for 24 hours, as measured by a decrease in diameter and a loss of insoluble protein, and the amount of both fast- and slow-twitch myosin heavy chain protein isoforms (MYH1, MYH2, MYH3, MYH4, and MYH8 in fast-twitch and MYH7 in slow-twitch fibers) was decreased, whereas actin levels remained unchanged [77].

The effect of DEX on the myosin heavy chain isoforms' turnover in skeletal muscle of rats was determined using a dexamethasone treatment of 200 µg/ml DEX with 0.15 M NaCl administered intraperitoneally (100 µg/100 g body weight). The degradation rate of muscle contractile proteins increased from 2.0 to 5.9% per day ( $P < 0.001$ ), the MHC IIB isoform degradation increased, and synthesis rate of MHC type II isoforms decreased in the plantaris muscle [83].

## 2.6 Glucocorticoid Induced Atrophy and Mitochondria

Previous research has indicated that in some atrophy models, skeletal muscle biochemistry and histology relative to fiber type is altered and abnormalities in muscle metabolism can occur, including a reduction in several indicators of functional mitochondrial content such as citrate synthase activity [48, 66]. In a study of skeletal muscle atrophy induced by left ventricular dysfunction (LVD) conducted by Delp et al, moderate LVD decreased the activity of mitochondrial enzymes citrate synthase and phosphofructokinase (PFK) in a muscle composed of type IIB fibers but did not modify fiber composition or size of any muscle studied, whereas severe LVD decreased mitochondrial enzyme activities regardless of muscle fiber composition, and caused a reduction in PFK activity in type IIB muscle and atrophy of type I, IIA, and IIB fibers [48].



The difference in functional mitochondrial content relative to muscle fiber type composition in a chronic stress model is still unclear.

## 2.7 Fiber Specific differences in Sarcoplasmic Reticulum

In fast twitch muscle (ex. EDL), CASQ1 comprises nearly all of the calsequestrin detectable while in slow twitch muscle (ex. soleus) there is a higher ratio of CASQ2 (approximately 3:1 CASQ1 to CASQ2 in rabbits), although CASQ1 remains the dominant isoform in both muscle types [45, 46]. There is on average 3 to 4 times the CASQ1 content found in the EDL of rats compared to soleus [45].

In EDL and gastrocnemius muscles there is a high density of SERCA1 whereas in whole muscle homogenate of soleus, which has predominantly slow-twitch type I muscle fibers, there is ~20% the SERCA1 content detected in the fast muscle types which is consistent with the ratio of type I and II fibers [45]. In Type II fibers of any muscle type there is a high amount of the SERCA1 protein, whereas there is almost no SERCA1 present in type I fibers of soleus muscles. When examining whole muscle homogenates, SERCA2 is not detectable in EDL homogenates but does show a strong signal in soleus homogenates [45].

## 2.8 Models of Chronic Stress

### 2.8.1 Stress models using stressful situations

To study chronic stress, many researchers will try to repeatedly induce stress using methods known to increase serum cortisol in study animals. Common methods include cage-switching, forced exercise (such as running or swimming), social stress (wherein a more aggressive animal is introduced), or a combination of these. This method has some merits as it will activate other aspects of the stress response in addition to glucocorticoid release, however, it is difficult to ensure the level of stress is kept chronically elevated and the response to various stressors is variable between sexes and strains of animals. One study examining two models of stress in rats (restraint and cage-switching stress) indicated daily psychological stress induced atrophic gene expression and muscle atrophy [21]. Allen et al. determined that restraint stress significantly

decreased muscle mass in the tibialis anterior (TA) and soleus (SOL) after 3 and 7 days, and cage-switching stress significantly decreased SOL muscle mass after 7 days [21]. In teleost fish, chronic stress induced by crowding resulted in elevated endogenous cortisol at 4 weeks, upregulation of the ubiquitin-proteasome and intrinsic apoptotic pathways at 4 weeks; and autophagy and downregulation of the growth hormone/IGF system (which promotes muscle growth through anabolic pathways) at 7 weeks [22].

### 2.8.2 Chronic GC treatment

Chronic glucocorticoid treatment as a model of chronic stress has been widely used for many years. Researchers use various methods including subcutaneous injections, slow-release pellet implantation, and oral dosing using drinking water to administer glucocorticoids. In a recent comparative study of the various methods of chronic glucocorticoid treatment, pellet implantation, which has predominated in the literature in recent years, was proven to be a far less reliable method of chronic glucocorticoid release than previously thought. In this study by Gasparini et al., drinking water versus pellet implantation as a mode of delivery for corticosterone, and the effects of different dose ranges (25, 50, 75 and 100 µg CORT/mL via drinking water at av. 4.5mL water per day for weekly dose of 0.8, 1.6, 2.4 and 3.2 mg) in drinking water or of 1.5mg CORT through slow-release pellets were examined. After 4 weeks, the percent increase in lean mass from baseline (using densitometer and measuring change from baseline) showed that while the control increased 10%, all oral doses showed less than 3% increase (a significant change and decrease in lean mass) and the pellet group showed a 5% increase [25].

### 2.9 Cushing's Syndrome

Cushing's syndrome is a disorder caused by hypersecretion of adrenocorticotrophic hormone (ACTH) which causes hypercortisolism by overstimulating the adrenal glands [10]. To diagnose Cushing's syndrome, serum cortisol can be taken at midnight and a value higher than 140nmol/L while the patient is asleep or higher than 207nmol/L while

the patient is awake will lead to a positive diagnosis, while a value lower than 50nmol/L rules out Cushing syndrome [10]. In patients with Cushing's syndrome, the normal diurnal variation in serum cortisol seen in healthy adults is absent [10]. In women with Cushing syndrome, muscle tissue is comprised of a relatively low proportion of type I fibers (30%) and a relatively high proportion of type IIx fibers (reported at the time of the initial study as IIb, although classification of human muscle fibers has since changed from IIb to IIx) [84]. In a study of two patients with Cushing's syndrome, a decrease in muscle fiber diameter indicated atrophy was more prominent in type II than type I fibers [85].

Kang et al. studied a breed of transgenic mice (Corticotropin releasing factor-overexpressing (CRF-OE) mice), which exhibit increased plasma corticosterone levels and Cushing's syndrome, as a model of chronic stress. Cushing's mice exhibited muscle weakness as evidence by decreased muscle grip strength in the wire hang. No difference in skeletal muscle mass was observed after 7 weeks, but after 19 weeks the CRF-OE muscle mass decreased by 30%. Compared to control, the CRF-OE cross-sectional myofiber area was decreased, total muscle protein content was lower, HOMA-IR was elevated, and Atrogin and MURF1 mRNA were increased, while there was no difference in body weight [65].

## Chapter 3. Methods

### 3.1 Institutional Animal Care Approval

Male C57BL/6NCrI mice (Charles River) aged four weeks old were received from Charles River and allowed to acclimate for two weeks after arriving at the LUACF (Lakehead University Animal Care Facility) in Thunder Bay before treatment. Mice were held at 40-70% humidity and caged in groups of three to four per cage. Mice were kept on a standard 12:12-hour light: dark cycle and given unlimited access to a standard chow and water. Institutional animal care approval was received from Lakehead University Animal Care Committee (AUP 1467374).

### 3.2 Experimental Design

#### 3.2.1 Treatments

Mice were randomly divided into three treatment groups with ten mice each. All treatments were administered through a water bottle and mice were given *ad libitum* access over a 4-week period. Naïve control mice were given normal drinking water, vehicle control mice were given <1% ethanol in water (using 95% Ethanol from Cedarlane, Cat# 40120791-3), and corticosterone treatment mice were given corticosterone (Sigma Aldrich, cat #27840) dissolved in 1% ethanol via drinking water at 100µg/mL at the beginning of the study lowered to 50 µg/mL on day 20. This concentration was used to achieve an average target dose of 500 µg/mouse/day, which previous studies indicated induced atrophy and mimicked elevated serum corticosterone levels seen in stress models [42, 106, 107]. Previous studies have reported that oral dosing provides a consistent response and reduces additional stress to the animal [25, 42, 106,107].

Drinking water treatments were prepared fresh every 3-4 days and mice were monitored for dose consumption and adjusted accordingly. The appropriate amount of corticosterone powder was added to ethanol in conical tubes which were then placed in a 37°C bead bath until the powder fully dissolved. Treatment solutions were then added to autoclaved water to give a final concentration of 100µg/mL for corticosterone, or 50 µg/mL corticosterone in the later part of the study. Vehicle water was prepared so that the final concentration of ethanol in the bottle was <1%. Naïve control water bottles were prepared using autoclaved water only. Treatments were administered to the mice through water bottles that were pre-weighed in order to track water consumption and weighed again to find the weight of water consumed. The amount of water consumed was divided by the number of mice in the cage for approximate water amount consumed per mouse. The corticosterone-treated animals began to drink significantly more of the treatment water than control groups by day 21, which led to the administered dose exceeding the target. In response to concerns for animal health and to keep doses within the bounds of the experiment, the corticosterone concentration in the treatment water was decreased to 50µg/ml on day 20 so animals could receive the targeted dose of 500µg per day, after which point the drinking water consumption stabilized. Two corticosterone-treated mice perished during the study, possibly due to corticosterone-induced complications, however this was not tested. One vehicle mouse was removed from the study due to unrelated health complications.

### 3.2.2 Tissue Collection

(See Appendix for R-18-LUACF anesthesia SOP)

Mice were anesthetized with inhaled 3% isoflourane following the LUACF standard operating procedure R-18-LUACF and their hearts were removed under the effects of the anesthetic. After removal of the heart, the soleus and the gastrocnemius/plantaris muscle group were dissected and weighed, then frozen in liquid nitrogen before being placed in storage at -80°C until use.

### 3.2.3 Tissue Lysis

Soleus samples were removed from -80°C and homogenized and disrupted in ice-cold Pathscan buffer (10mL 1M pH 7.5 Tris, 380 mL DW, 1.75g NaCl (Sigma Life Science, St. Louis, Missouri, USA), 4mL Triton X-100 (Thermo Scientific, cat # 28313), and PMSF protease inhibitor (ThermoFisher Scientific, cat #36978) with 600 mM KCl (Sigma Life Science, St. Louis, Missouri, USA)). Disruption and homogenization were completed using the Qiagen TissueLyser using two rounds lasting two minutes each at a frequency of 30Hz, placing samples on ice for 5 minutes in between to keep cool. Samples were then centrifuged at 16,000g for 10 minutes at 4°C and supernatant was collected and frozen at -80°C for further analysis.

Gastrocnemius/plantaris muscle group samples were removed from -80°C and kept on ice throughout homogenization in ice-cold Pathscan buffer (10mL 1M pH 7.5 Tris, 380 mL DW, 1.75g NaCl (Sigma Life Science, St. Louis, Missouri, USA), 4mL Triton X-100 (Thermo Scientific, cat # 28313), and PMSF protease inhibitor (ThermoFisher Scientific, cat #36978) with 600 mM KCl (Sigma Life Science, St. Louis, Missouri, USA)). Samples were homogenized on ice using the Kinematica Polytron PT 1200 at speed 2 for 1.5 minutes. Samples were then centrifuged at 16,000 g for 10 minutes at 4°C and supernatant was collected and stored at -80°C for further analysis.

### 3.2.4 BCA Protein Assay

A BCA protein assay was used to determine protein concentration in the supernatant. The assay was conducted according to Pierce BCA Protein Assay Kit protocol. To summarize: 10 µL of diluted samples (in duplicate) and bovine serum albumin standards (in triplicate) were loaded into a 96 well flat bottom plate (model# 9017). Once all samples were loaded, 200µl of working reagent (prepared 50:1 reagent A:B) was added to each well with standard or sample. The plate was sealed and mixed on the plate shaker at 200rpm for 30 seconds. After mixing, the plate was incubated at 37°C for 30 minutes. The plate was then cooled to room temperature and read at

562nm on a Bio Tek Power Wave XS microplate reader using Gen5 data analysis software.

### 3.2.6 Sample Preparation for SDS-PAGE and Western Blot

The muscle samples were prepared for sodium dodecyl sulfate polyacrylamide gel electrophoresis (SDS-PAGE) and western blots in two concentrations-- 0.2mg/mL (used for actin, MHC, and SERCA1) and 1 mg/mL (used for CASQ1, SDHB, and citrate synthase)-- depending on the amount of protein being loaded for each target. The [0.2 mg/mL] samples were used to image SERCA1, as the higher [KCl] in the [1mg/mL] samples caused imaging issues in SERCA1 westerns. Samples were kept on ice for the duration of the preparation. A 1mL aliquot of sample reducing buffer (4X Laemmli buffer) was thawed at room temperature before adding 110µl of 100mM dithiothreitol (DTT) (Fisher Scientific, Fair Lawn, NJ, cat# BP172-25) to the buffer. The appropriate amount of sample for each concentration was added to the corresponding 1.5ml tube, along with the appropriate volumes of sample reducing buffer and distilled water. The tubes were heated at 100°C for 5 minutes and centrifuged at 16,000xg at room temperature for 30 seconds. Prepared samples were stored at -80°C until western blots were performed.

### 3.2.7 Western Blotting

(see Appendix for full Lees Lab Western Blot SOPs)

Polyacrylamide gels were prepared using a 5% acrylamide (for MHC analysis), 7.5% acrylamide (for SERCA1 analysis), or 10% acrylamide (for actin, calsequestrin, citrate synthase, and SDHB analysis) separating gel, and a 4% stacking gel for all samples. The acrylamide concentration of the separating gel was chosen based on the antigen molecular weight. Gels were 1.0mm thick except in the case of MHC, which was 1.5mm thick. Samples prepared as described in section 3.2.6 were thawed briefly at 37°C until transparent. 5µl of BLUelf pre-stained protein ladder (FroggaBio, Canada, cat

#PM008-500) was used for molecular weight determination. Samples were loaded by alternating treatment groups, with soleus and gastrocnemius/plantarum on separate gels to prevent over- or under-exposure of bands due to large differences in the amount of target proteins typically found in the different muscle types. Designated samples (either soleus or gastrocnemius/plantarum from naïve mouse one depending on target protein) were repeated across gels as loading controls. Gels were run for approximately 1 hour at 200 volts until the dye front ran off the gel.

Each gel was transferred to a polyvinylidene fluoride (PVDF) membrane and briefly stained with Ponceau S total protein stain to verify successful protein transfer and scanned. Membranes were then blocked for one hour using 5% powdered non-fat dry milk in 1X TBST (1X Tris buffered saline with 0.1% TWEEN-20) (TBST: Tris Base, Molecular Biology Grade, Fisher Scientific, Fair Lawn, NJ, cat # BP152-5 + Tris Hydrochloride, Fisher Scientific, Fair Lawn, NJ, cat # BP153-500 + Tween 20, Bio Rad, Hercules, CA, USA, cat # 1706531). Western blotting was performed using the following primary antibodies: myosin heavy chain antibody, skeletal muscle actin antibody, citrate synthase antibody, succinate dehydrogenase subunit B antibody, calsequestrin 1 antibody, and sarcoendoplasmic reticulum calcium ATPase 1 antibody according to Table 1.

After incubation in primary antibody, the secondary antibody Stabilized Peroxidase Conjugated Goat Anti-Mouse (H+L) (Invitrogen, cat# 32430) was used for MHC, actin, SERCA1, and SDHB, and secondary antibody IgG (H+L) Goat anti-Rabbit, HRP (Invitrogen, cat#PI31460) was used for citrate synthase and calsequestrin. Enhanced chemiluminescence (ECL) (ChemiDoc XRS, Bio-Rad, Hercules, CA, USA) was used to detect target proteins. All western blots were then imaged using the BioRad ChemiDoc Imaging System at an optimized exposure time which was kept consistent for each treatment and quantified using ImageLab version 6.0 software according to manufacturer's instructions. Molecular weight was also determined using ImageLab 6.0 software according to manufacturer's instructions and validated against antibody



product information and antibody testing data and/or previously published western data where available. Loading controls were used for normalization between membranes, and Coomassie R250 total protein membrane stain was used as an indicator of equal loading.

**Table 1. Western Blot Details**

Target	Total Protein Loaded (ug)	Gel Concentration	Primary Antibody	Primary Antibody Concentration	Secondary Antibody	Secondary Antibody Concentration
<b>Myosin Heavy Chain</b>	1	5%	MF-20 deposited to the DSHB by Fischman, D.A.	1:2500	Stabilized Peroxidase Conjugated Goat Anti-Mouse (H+L), Invitrogen, cat# 32430	1:100
<b>Alpha-Actin</b>	1	10%	Skeletal Muscle Actin Monoclonal Antibody (5C5.F8.C7 (alpha-Sr-1), Invitrogen, cat#MA5-12542	1:2500	Stabilized Peroxidase Conjugated Goat Anti-Mouse (H+L), Invitrogen, cat# 32430	1:100
<b>Citrate Synthase</b>	5	10%	Recombinant Anti-Citrate synthetase antibody abcam, cat# ab129095	1:100,000	IgG (H+L) Goat anti-Rabbit, HRP (Invitrogen, cat#PI31460)	1:500,000
<b>SDHB</b>	5	10%	Anti-SDHB antibody [21A11AE7], abcam, cat# ab14714	1:1000	Stabilized Peroxidase Conjugated Goat Anti-Mouse (H+L) (Invitrogen, cat# 32430)	1:1000
<b>CASQ1</b>	10	10%	Recombinant Anti-Calsequestrin 1 antibody, abcam, cat# ab191564	1:20,000	IgG (H+L) Goat anti-Rabbit, HRP (Invitrogen, cat#PI31460)	1:100,000
<b>SERCA1</b>	3	7.5%	CaF2-5D2 deposited to the DSHB by Fambrough, D.M.	1:4000	Stabilized Peroxidase Conjugated Goat Anti-Mouse (H+L) (Invitrogen, cat# 32430)	1:10,000

### 3.2.8 Coomassie R250 Total Protein Membrane Stain

Following antigen detection by ECL, membranes were stained with Coomassie R250 membrane stain according to the protocol outlined in Current Protocols in Science- Electrophoresis 1.5.3 [88]. In summary, stock Coomassie R250 staining solution was prepared with 4.8g of Coomassie Blue R250 powder (BioRad), 120mL of methanol

and 24mL of acetic acid and then used to prepare membrane staining solution with 75 mL of stock Coomassie R250 solution, 400mL of methanol, 70mL acetic acid and 522.5mL of distilled water. De-staining solution was prepared with 500mL of methanol, 70mL of acetic acid, and 430mL of distilled water to create a 15% methanol/10% acetic acid volume/volume solution. All solutions were stored at room temperature for a maximum of 2 weeks before use.

After membranes were imaged with ECL they were washed 2 times for 5 minutes each time in fresh 1X TBST, then washed 3 times with distilled water for 15 minutes total before being covered with staining solution and being placed on a Belly Dancer shaker at speed 1 for 5 minutes. The staining solution was then removed and destaining solution was added along with a folded Kimwipe in the corner of the container (to absorb some of the dye during the de-staining process). The membrane was then destained for 10 minutes at speed 3 on a Belly Dancer shaker. After 10 minutes, the kimwipe and destain was refreshed and the destaining step was repeated for another 10 minutes. The membranes were then quickly rinsed 5-10 times with distilled water and left to dry on a flat surface at room temperature overnight. Once dry, membranes were imaged using the BioRad ChemiDoc Imager using the colorimetric setting. Coomassie stained images are included as markers of equal protein loading. Coomassie total protein staining was chosen instead of other loading controls because frequently used housekeeping proteins (such as GAPDH and  $\beta$ -actin) vary between fiber types and can be influenced by various experimental conditions and as such may not accurately reflect total protein loads [89-91].

### 3.2.9 Actin vs. Myosin Coomassie G250 Gel Staining

(See Appendix for full Coomassie G250 Gel Staining Protocol)

7.5% Tris-glycine gels were run at 200V for one hour, fixed with a solution of 50% methanol and 10% acetic acid for 15 minutes, and stained for 16 hours with QC Colloidal Coomassie G250 (BioRad, cat#1610803) stain to visualize protein content of samples, including myosin and actin content. MHC and actin bands were determined by

molecular weight and relative band volume of MHC and actin in each treatment was quantified using ImageLab version 6.0 software.

### 3.3 Limitations, Basic Assumptions, and Delimitations

#### 3.3.1 Limitations and Basic Assumptions

Mice were regularly monitored, however, as with any animal model a certain degree of variability is inevitable. Based on monitoring, it is assumed that all mice consumed a similar amount of food, however, mice in the corticosterone treatment group drank more than mice in vehicle and naïve control groups as the study progressed. This was accounted for by adjusting the concentration of corticosterone in the water from 100µg/mL to 50 µg/mL in the final week, to bring the average dose of corticosterone administered over the 4-week period back in line with the target dose. In studies using pellet implantation and other similar methods of corticosterone delivery, data monitoring the dose released throughout the treatment period is rarely included and dose adjustment during the treatment period is not possible. This strain of mouse is thought to represent healthy, normal physiological conditions and is assumed to be pathogen and disease free. Other limitations include environmental factors that affect the animals such as the initial transport of mice to the lab and any incidental disruption to light/dark cycles.

All mice were kept in the same environment at the Lakehead University Animal Care Facility following the Canadian Council on Animal Care guidelines but may have been unknowingly exposed to stressors that may cause uncontrollable variation in results. During the treatment period, three mice died—two from the corticosterone treatment group and one from the vehicle control group. The ideal size of each treatment group according to *a priori* power analysis is 10 per group, meaning that the death of these mice reduced the power of the study. With animal studies, unpredictable issues such as this are common, and we chose to accept the reduction in power to reduce the number of animals used in this study. The sample size may not have been

large enough to detect relatively small changes (e.g., citrate synthase), that may still be physiologically relevant.

In early loading tests, the MHC antibody used appeared to show a higher specificity for Type I myosin fibers. This caused soleus bands to appear to have more myosin heavy chain than gastrocnemius/plantaris bands when equal volumes of protein were loaded, contrary to established contractile protein levels. SDS-PAGE gels run for three separate test samples confirmed approximately the same ratio of MHC: other proteins in both soleus and gastrocnemius/plantaris muscle types, making it unlikely to be a loading error or due to muscle-specific differences in MHC content. As a result, western blots were not used to compare MHC between the soleus and gastrocnemius/plantaris muscles.

### 3.3.2 Delimitations

This study could not be carried out on humans, therefore a mouse stress model was used to study the effect of chronic oral corticosterone treatment. While this study is not performed in humans, the mouse model has been widely studied as representative of human stress. Animal study also accounts for the many *in vivo* effects of the drug as opposed to an *in vitro* study, allowing for a deeper understanding of the effects of whole body response in response to treatment. Mice have a different primary stress hormone than humans, and therefore corticosterone was used for the model rather than cortisol. By using the primary endogenous stress hormone of the study animals, we can better replicate the conditions of chronically elevated endogenous stress hormones in humans. For our study, C57BL/6NCrI mice from Charles River Laboratories were used. This strain of mice is the most commonly used in medical research and although there are strain differences between the C57BL/6NCrI sub-strain and the more frequently reported sub-strain C57BL/6J, this model was selected due to availability and the selected treatment application [92-94]. Namely, the C57BL/6NCrI strain does not show the same increased ethanol consumption as the C57BL/6J strain, and therefore is a more appropriate choice

for our treatment delivery method (i.e., dissolved in ethanol) [93]. This strain is also a suitable model of mitochondrial function, and chronic stress [18, 25]. This study only examines the effect of chronic oral corticosterone treatment on male mice. Male and female mice respond differently to stress, and historically more chronic stress research is conducted on males than females [95, 96, 98].

This model also only examines one time point (at 4 weeks). Including more time points at longer durations may have resulted in changes to different markers of atrophy. This time point was based on previously reported studies, and although differences in some measurements can be seen, increasing the duration of the study may have allowed further statistically significant changes to develop in the muscle tissue. The use of drinking-water based treatment delivery was also a delimitation. The treatments were administered to mice using pre-weighed water bottles provided to each cage. Bottles were weighed and fresh treatment water replaced every few days, and the amount of water consumed was divided by the number of mice in the cage to find the approximate amount consumed per mouse. This resulted in an approximation for the dosage each animal received within the cage. This method offers less control over water consumption and dosing than methods such as oral gavage or injection but does allow for the diurnal rhythm of corticosterone to be maintained and reduces the amount of physical stress placed on animals as they do not need to be regularly restrained for treatment. The use of injections and studies involving stressors (ex. UCMS) can result in the release of confounding stress-related hormones and factors such as epinephrine, norepinephrine, corticotropin-releasing hormone, adrenocorticotrophic hormone, and endorphins [42].

Western analysis was done by one individual to ensure consistent interpretation of the results, given the subjective nature of the analysis software. Using the same individual for all measurements does not allow for comparison to account for bias or skew in analysis but helps to limit variation and maintain consistency in measurements.

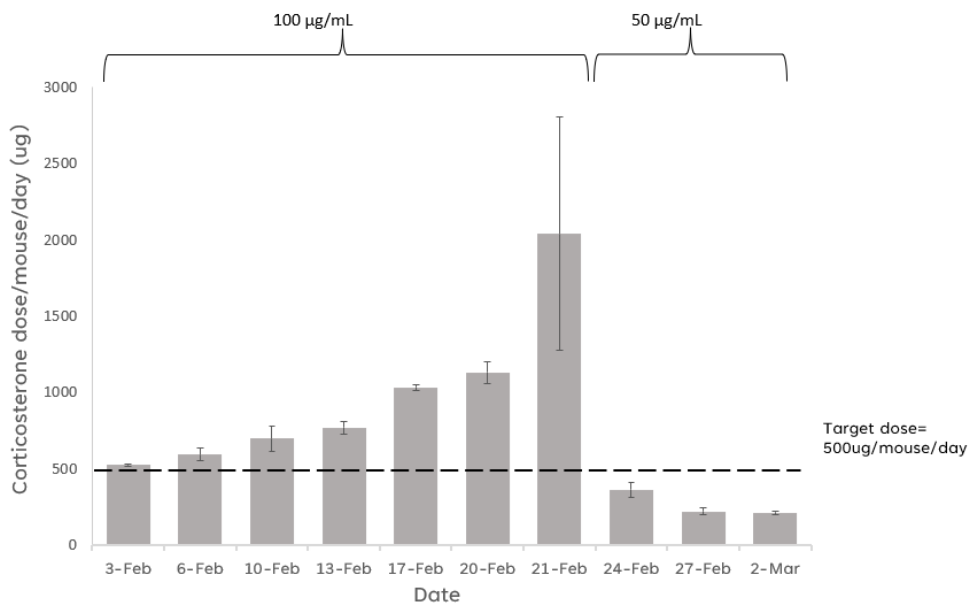
### 3.4 Statistical Analysis

Statistical analysis was done using RStudio software. Values are presented as mean  $\pm$  SD. Comparisons between treatments were made using one-way ANOVA. Post-hoc analysis was done using Fisher's LSD test. For both the ANOVA and Fisher's LSD a p-value of less than or equal to 0.05 was considered statistically significant.

## Chapter 4. Results

### 4.1 Dosing Results

Based on previous studies, the target dose of corticosterone for this study was set at 500  $\mu\text{g}/\text{mouse}/\text{day}$  [25]. Monitoring of treatment water consumption indicated mice in the corticosterone treatment group began drinking more water midway through the study, and so on day 20 the concentration of corticosterone in the drinking water was lowered from 100  $\mu\text{g}/\text{mL}$  to 50  $\mu\text{g}/\text{mL}$  to bring the average dose of corticosterone administered per mouse in line with the target (Figure 5). After the concentration change, the drinking behaviour of the corticosterone mice became similar to the naïve and vehicle controls and the amount of water and corticosterone consumed became more similar to target levels.



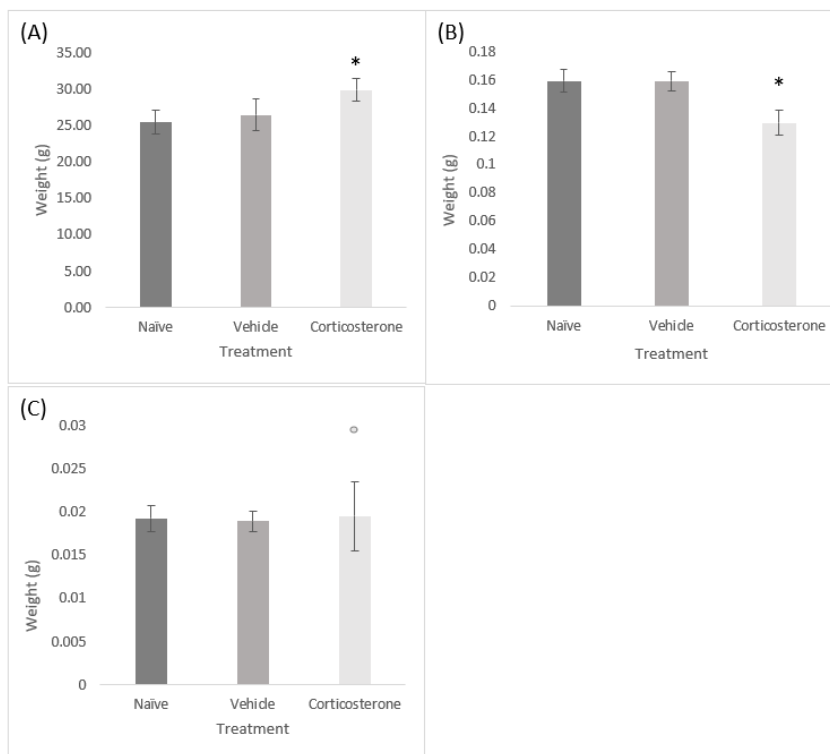
**Figure 5. Corticosterone Dose Administered**

Average corticosterone dose administered via drinking water per mouse per day over treatment period. Drinking water was monitored and refreshed every 3-4 days, at which time the amount of water consumed was measured and averaged for the number of days and number of mice in the cage. The concentration of corticosterone in drinking water was changed from 100  $\mu\text{g}/\text{mL}$  to 50  $\mu\text{g}/\text{mL}$  on Feb. 21 (day 20). Data presented as mean  $\pm$  SD (n=8).

## 4.2 Anthropometric Results

### 4.2.1 Gastrocnemius/plantaris muscle weight decreases despite increase in body weight in corticosterone treatment group

A significant increase was observed in the body weight of corticosterone treated mice compared to naïve and vehicle controls (Figure 6A). The mass of the gastrocnemius/plantaris muscle group was significantly decreased in corticosterone-treated mice compared to naïve and vehicle controls (Figure 6B), while there was no significant difference in soleus mass between the corticosterone-treated mice and naïve and vehicle controls (Figure 6C). It is important to note that the soleus weight data includes an outlier of 0.029g as identified by Normal Q-Q plot and Interquartile Range which was left in the analysis.



**Figure 6. Body and muscle weights of treated mice**

The body weight at tissue collection (A), gastrocnemius/plantaris muscle wet weight (B), and soleus muscle wet weight (C) of naïve, vehicle, and corticosterone treated mice. Data presented as mean  $\pm$  SD (n=8). \*Significant difference ( $p \leq 0.05$ ) from naïve and vehicle control groups. An outlier of 0.029g is seen in the corticosterone group.



4.2.2 Protein yield and muscle mass decrease in parallel in gastrocnemius/plantaris while no significant decreases observed in soleus

The muscle wet weight of mice at the time of euthanasia was found to decrease in parallel with the protein yield obtained via protein extraction in the gastrocnemius/plantaris (Table 2), while there was no significant change in either measure in the soleus (Table 3). The percent of muscle wet weight recovered as protein averaged around 15% in treatment groups of gastrocnemius/plantaris and 16% in soleus (Tables 2 and 3) with no significant difference between groups.

**Table 2. Average muscle mass and protein yield in milligrams of combined gastrocnemius/plantaris muscles in each treatment group.** Percent yield indicates percent of muscle wet weight recovered as protein. Data are presented as mean  $\pm$  SD \*Significant difference ( $p \leq 0.05$ ) from control

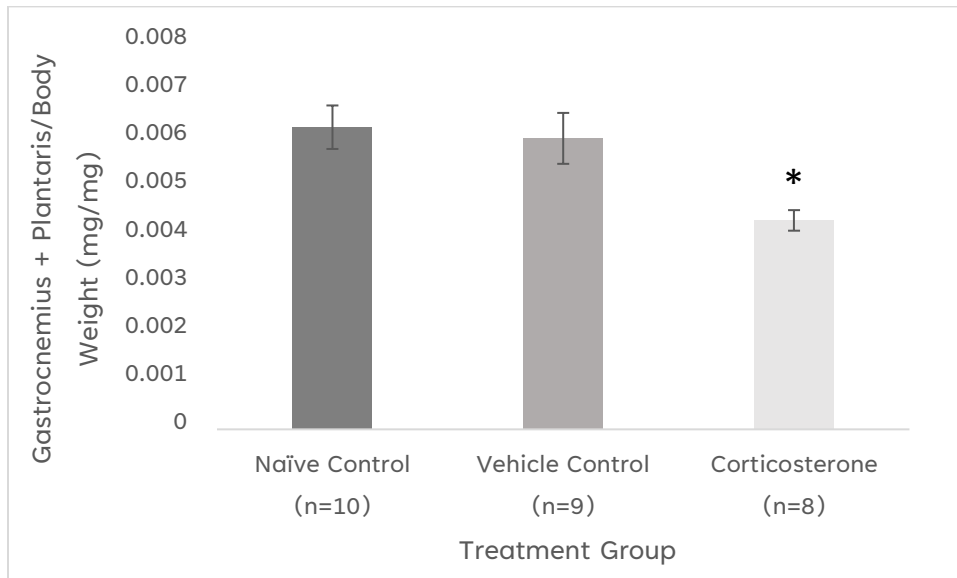
Treatment	Average Muscle Mass (mg)	Average Protein Yield (mg)	Average Percent Protein Yield (%)
Naïve	159.3 $\pm$ 7.8	25.3 $\pm$ 1.8	15.9 $\pm$ 0.8
Vehicle	159.0 $\pm$ 7.1	23.8 $\pm$ 1.4	14.9 $\pm$ 0.6
Corticosterone	129.6 $\pm$ 8.9*	19.7 $\pm$ 2.0*	15.2 $\pm$ 1.5
<hr/>			
% Difference CORT vs Naïve	-20.5	-25.1	
% Difference CORT vs Vehicle	-20.4	-18.9	

**Table 3. Average muscle mass and protein yield in milligrams of combined left and right soleus muscles in each treatment group.** Percent yield indicates percent of muscle wet weight recovered as protein. Data are presented as mean  $\pm$  SD \*Significant difference ( $p \leq 0.05$ ) from control

Treatment	Average Muscle Mass (mg)	Average Protein Yield (mg)	Average Percent Protein Yield (%)
Naïve	19.2 $\pm$ 1.5	3.11 $\pm$ 0.34	16.2 $\pm$ 1.2
Vehicle	18.9 $\pm$ 1.2	3.19 $\pm$ 0.28	16.9 $\pm$ 1.2
Corticosterone	19.5 $\pm$ 4.0	3.16 $\pm$ 0.38	16.8 $\pm$ 3.6
<hr/>			
% Difference CORT vs Naïve	1.6	1.43	
% Difference CORT vs Vehicle	3.2	-0.98	

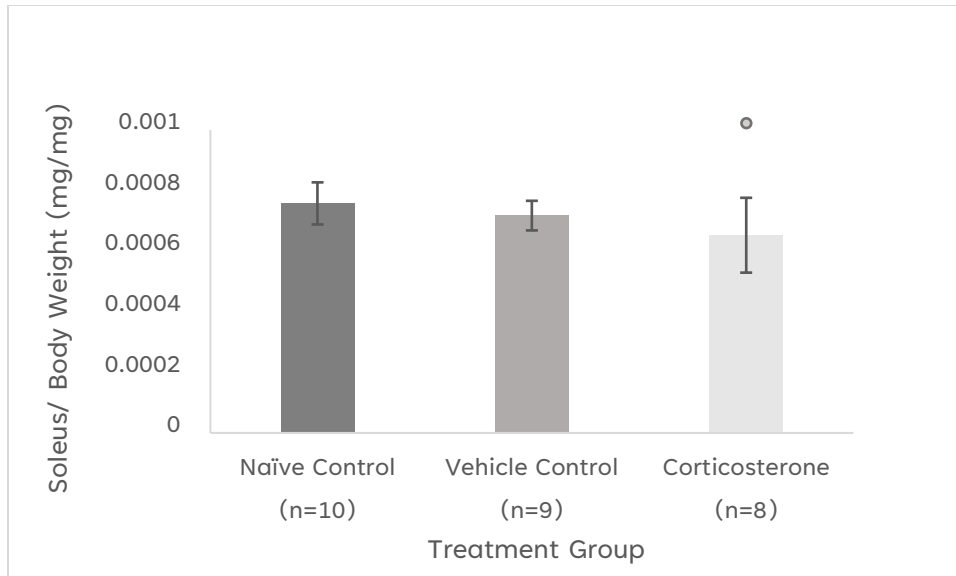
#### 4.2.3 Chronic Corticosterone Exposure Significantly Decreased Skeletal Muscle Wet Weight Normalized to Body Weight in Gastrocnemius/Plantaris but not Soleus

After 4 weeks of treatment, the body weight of mice was recorded prior to euthanasia, after which the gastrocnemius/plantaris muscle group and the soleus muscle were immediately excised and wet weights taken. The wet weight of the gastrocnemius/plantaris muscle group normalized to body weight decreased by 36% in the corticosterone treated mice compared to the naïve control ( $p < 0.0001$ ) (Figure 7a). The wet weight of the soleus normalized to body weight was also decreased by 15% in the corticosterone group compared to the naïve control, however it was not significant ( $p = 0.065$ ) (Figure 7b).



**Figure 7a. Gastrocnemius/Plantaris Muscle Weight**

Muscle wet weight of the gastrocnemius/plantaris muscle group normalized to body weight after 4 weeks of treatment. \*Significant difference ( $p \leq 0.05$ ) from naïve and vehicle control groups. Data are presented as mean  $\pm$  SD. n = 8-10 per group.



**Figure 7b. Soleus Muscle Weight**

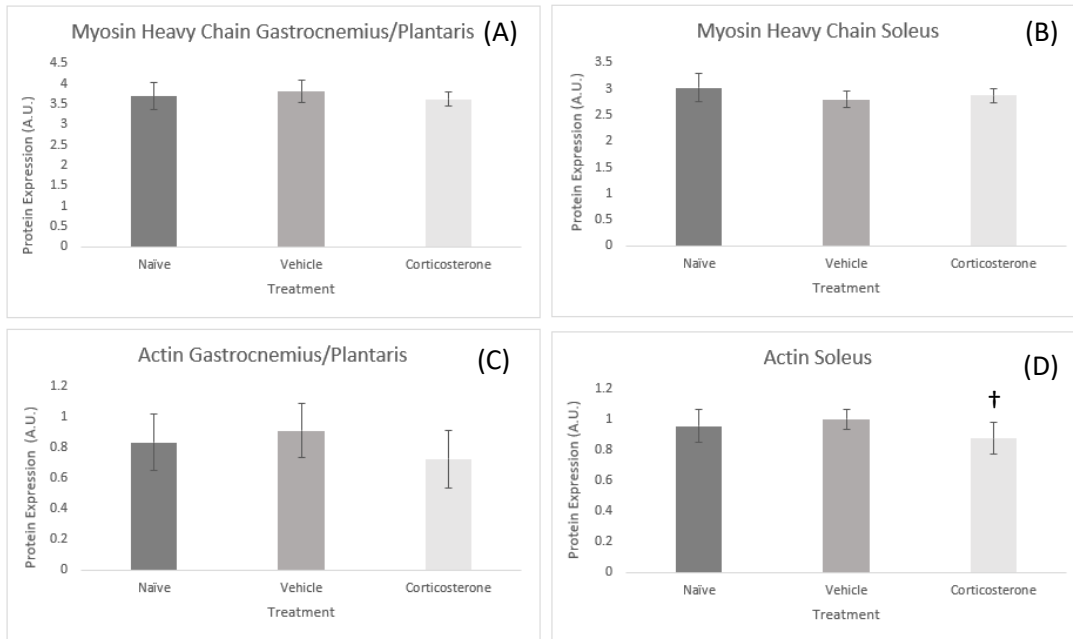
Muscle wet weight of the soleus muscle normalized to body weight after 4 weeks of treatment. There are no significant differences between groups. An outlier of 0.00096mg/mg is seen in the corticosterone group; it was kept in the analysis although it was identified as an outlier using Normal Q-Q plot. Data are presented as mean  $\pm$  SD. n = 8-10 per group.

### 4.3 Contractile Protein Content

#### 4.3.1 Coomassie G250 Gel Stain Results

To examine the effects of chronic corticosterone treatment on contractile protein content, Coomassie G250 gel staining was used to measure myosin heavy chain and skeletal muscle actin content. Based on optimization, 2 $\mu$ g of total protein was loaded per well. Adjusted band volume was normalized to a loading control on each gel to give the content of contractile protein relative to total protein loaded. In the gastrocnemius/plantaris muscle group, there was no statistically significant decrease in MHC (Figure 8A) or actin (Figure 8B) content ( $p=0.5$  and  $0.2$ , respectively), although the average actin content in corticosterone-treated mice was 14% lower than mice in the naïve control group. In the soleus, neither MHC (Figure 8B) or actin (Figure 8D) protein content was significantly decreased from the naïve control, although there was a

significant decrease in actin content of corticosterone-treated mice compared to the vehicle control of ~13% ( $p=0.046$ ).



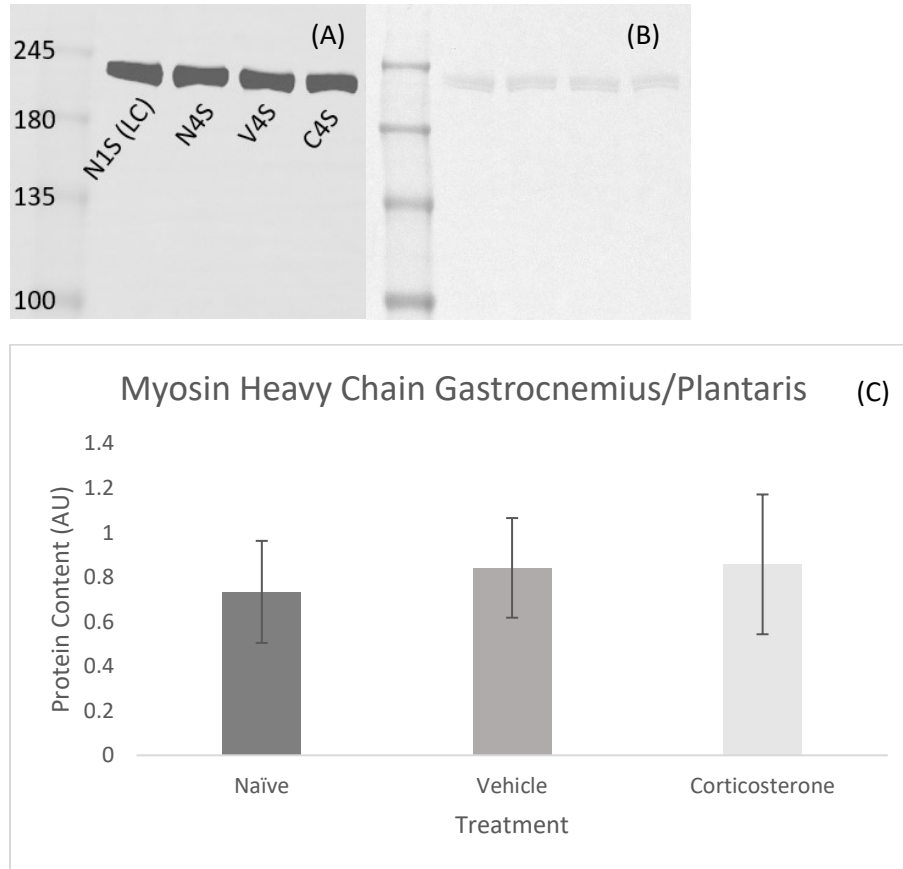
**Figure 8. Myosin and Actin in Coomassie Stained Gels.**

Protein expression in MHC and skeletal muscle actin in the gastrocnemius/plantaris and soleus in Coomassie G250 stained gels. (Panel A) MHC expression in gastrocnemius/plantaris (Panel B) MHC expression in soleus (Panel C) Actin expression in gastrocnemius/plantaris (Panel D) Actin expression in soleus. † Significant difference ( $p \leq 0.05$ ) from vehicle control group. Data are presented as mean  $\pm$  SD.  $n = 8-10$  per group.

#### 4.3.2 Myosin Heavy Chain is Unchanged Relative to Total Protein Content

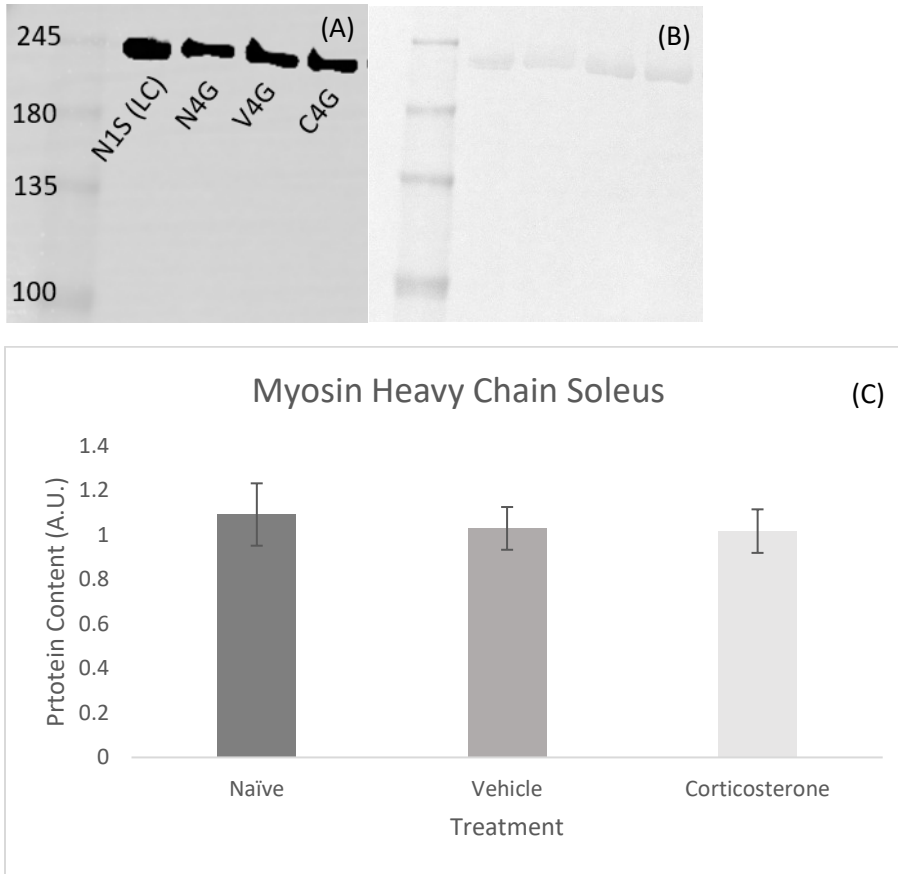
Western blotting of MHC was used in addition to Coomassie gel staining to examine the effects of chronic corticosterone treatment on myosin content. Based on optimization,  $1\mu\text{g}$  of total protein was loaded per well. Adjusted band volume was normalized to a loading control on each membrane to give the expression of MHC relative to total protein loaded. As with the gel stain results, no significant effect of

corticosterone treatment on the expression of MHC was detected in the gastrocnemius/plantar (p=0.57) (Figure 9) or soleus (p=0.38) (Figure 10).



**Figure 9. Myosin Heavy Chain Expression in Gastrocnemius/Plantaris Western Blot.**

A representative image of the western blot for protein expression of myosin heavy chain (panel A), the corresponding Coomassie R250 total protein stain (panel B), and normalized protein expressions (panel C) in gastrocnemius/plantar. Samples were separated on a 5% SDS-PAGE gel with 1 $\mu$ g of protein loaded per lane. Western blot lane labels represent naïve control sample (N), vehicle control sample (V), corticosterone sample (C), and loading control (LC). Samples were normalized to the loading control on each membrane. Data are presented as mean  $\pm$  SD. n = 8-10 per group.

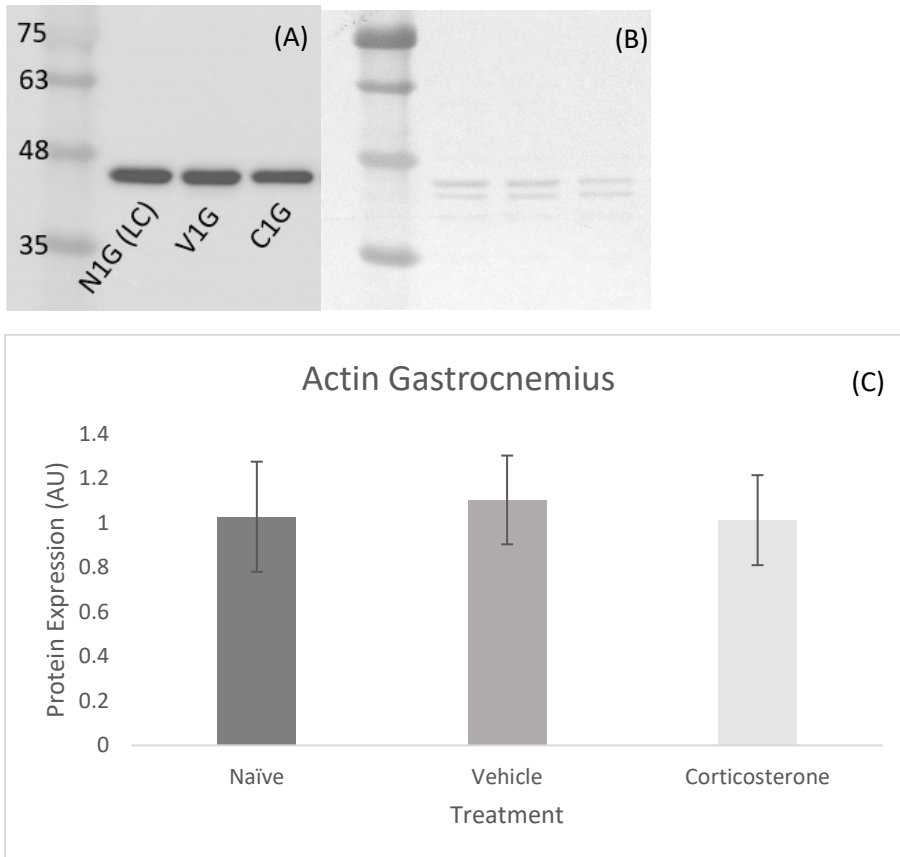


**Figure 10. Myosin Heavy Chain Expression in Soleus Western Blot.**

A representative image of the protein expression of myosin heavy chain (panel A), the corresponding Coomassie R250 total protein stain (panel B), and normalized protein expressions (panel C) in soleus. Samples were separated on a 5% SDS-PAGE gel with 1 $\mu$ g of protein loaded per lane. Western blot lane labels represent naïve control sample (N), vehicle control sample (V), corticosterone sample (C), and loading control (LC). Samples were normalized to the loading control on each membrane. Data are presented as mean  $\pm$  SD. n = 8-10 per group.

#### 4.3.3 Actin is Unchanged Relative to Total Protein Loaded

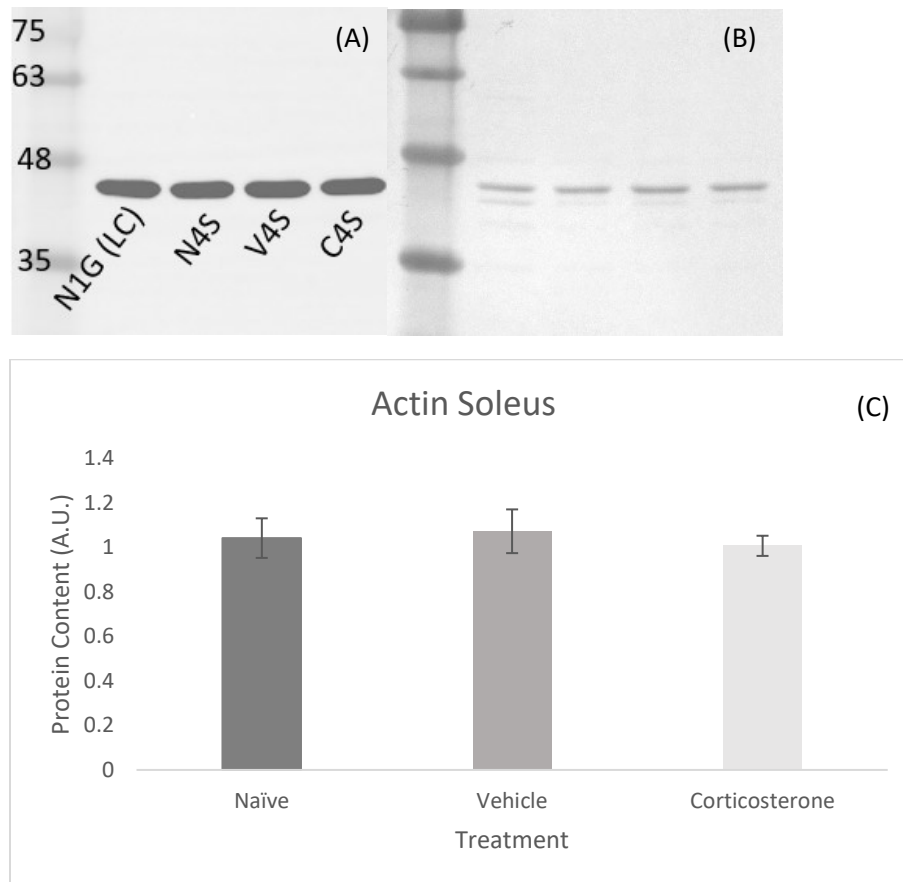
Western blotting of actin was also used to examine the effects of chronic corticosterone treatment on skeletal muscle actin content. Based on optimization, 1  $\mu\text{g}$  of total protein was loaded per well. Adjusted band volume was normalized to a loading control on each membrane to give the actin expression relative to total protein loaded. As with the gel stain results, no significant effect of corticosterone treatment on the expression of actin was detected in the gastrocnemius/plantaris ( $p=0.68$ ) (Figure 11) or soleus ( $p=0.32$ ) (Figure 12).



**Figure 11. Actin Expression in Gastrocnemius/Plantaris Western Blot.**

A representative image of the protein expression of actin (panel A), the corresponding Coomassie R250 total protein stain (panel B), and normalized protein expressions (panel C) in gastrocnemius/plantaris. Samples were separated on a 10% SDS-PAGE gel with 1  $\mu\text{g}$  of protein loaded per lane. Western blot lane labels represent naïve control sample (N), vehicle control sample (V), corticosterone sample (C), and loading control (LC). Samples

were normalized to the loading control on each membrane. Data are presented as mean  $\pm$  SD. n = 8-10 per group.



**Figure 12. Actin Expression in Soleus Western Blot.**

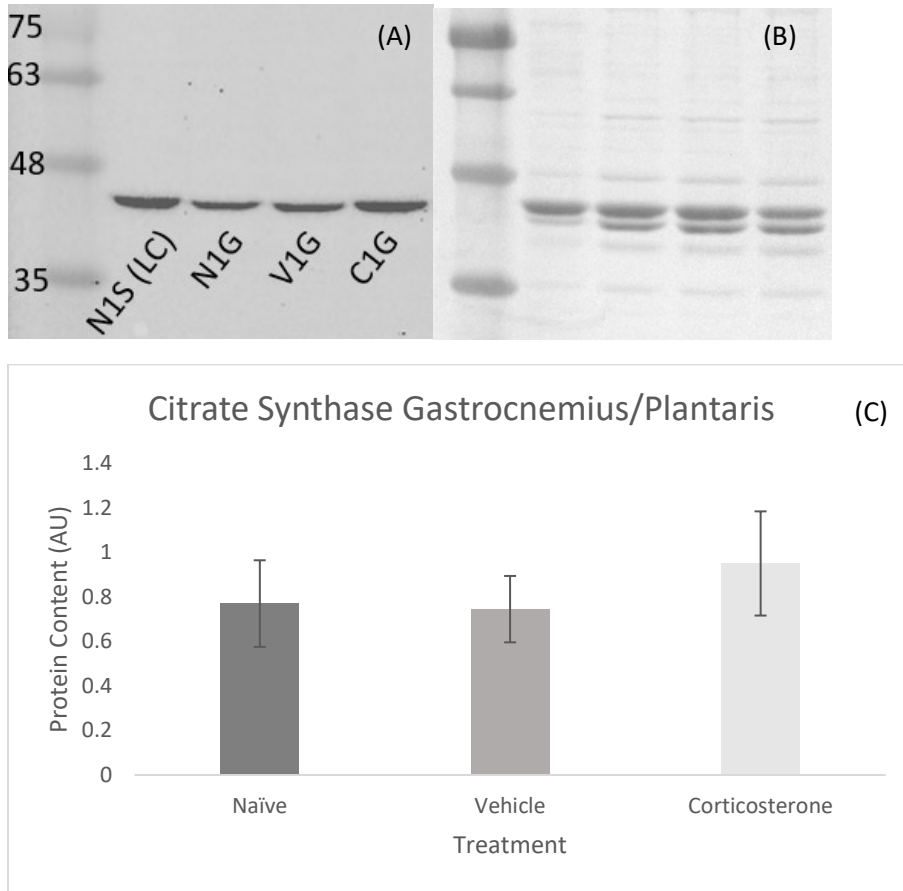
A representative image of the protein expression of actin (panel A), the corresponding Coomassie R250 total protein stain (panel B), and normalized protein expressions (panel C) in soleus. Samples were separated on a 10% SDS-PAGE gel with 1 $\mu$ g of protein loaded per lane. Western blot lane labels represent naïve control sample (N), vehicle control sample (V), corticosterone sample (C), and loading control (LC). Samples were normalized to the loading control on each membrane. Data are presented as mean  $\pm$  SD. n = 8-10 per group.



#### 4.4 Protein Biomarkers of Mitochondrial Content

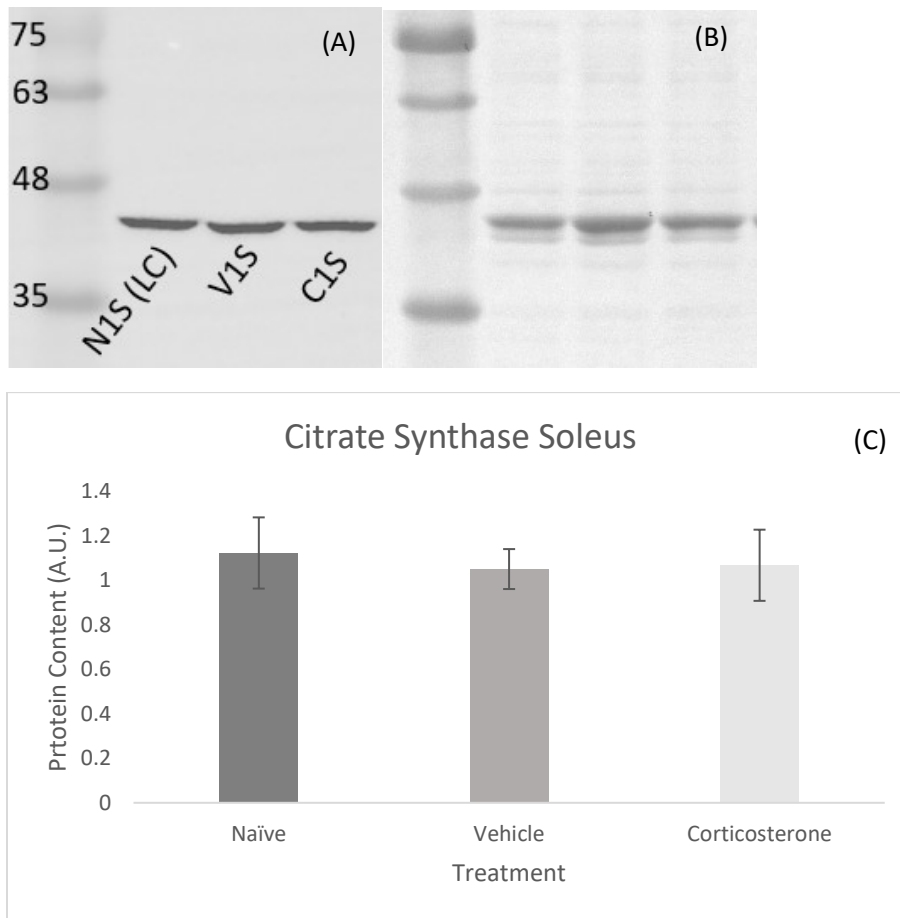
##### 4.4.1 Citrate Synthase Content is Increased in Gastrocnemius/Plantaris of Corticosterone-treated Mice Relative to Total Protein Content

Citrate synthase western blotting was used to examine the effects of chronic corticosterone treatment on functional mitochondrial content. Based on optimization, 5  $\mu$ g of total protein was loaded per well. Adjusted band volume was normalized to a loading control on each membrane to give the citrate synthase expression relative to the total protein loaded. There was a 21% increase in the average citrate synthase expression relative to total protein in the gastrocnemius/plantaris of corticosterone treated mice compared to naïve control mice, although it was not statistically significant ( $p=0.10$ ) (Figure 13). There was no significant effect of chronic corticosterone exposure on citrate synthase expression in the soleus muscle ( $p=0.55$ ) (Figure 14).



**Figure 13. Citrate Synthase Protein Expression in Gastrocnemius/Plantaris**

A representative image of the protein expression of citrate synthase (panel A), the corresponding Coomassie R250 total protein stain (panel B), and normalized protein expressions (panel C) in gastrocnemius/plantaris. Samples were separated on a 10% SDS-PAGE gel with 5 $\mu$ g of protein loaded per lane. Western blot lane labels represent naïve control sample (N), vehicle control sample (V), corticosterone sample (C), and loading control (LC). Samples were normalized to the loading control on each membrane. Data are presented as mean  $\pm$  SD. n = 8-10 per group.



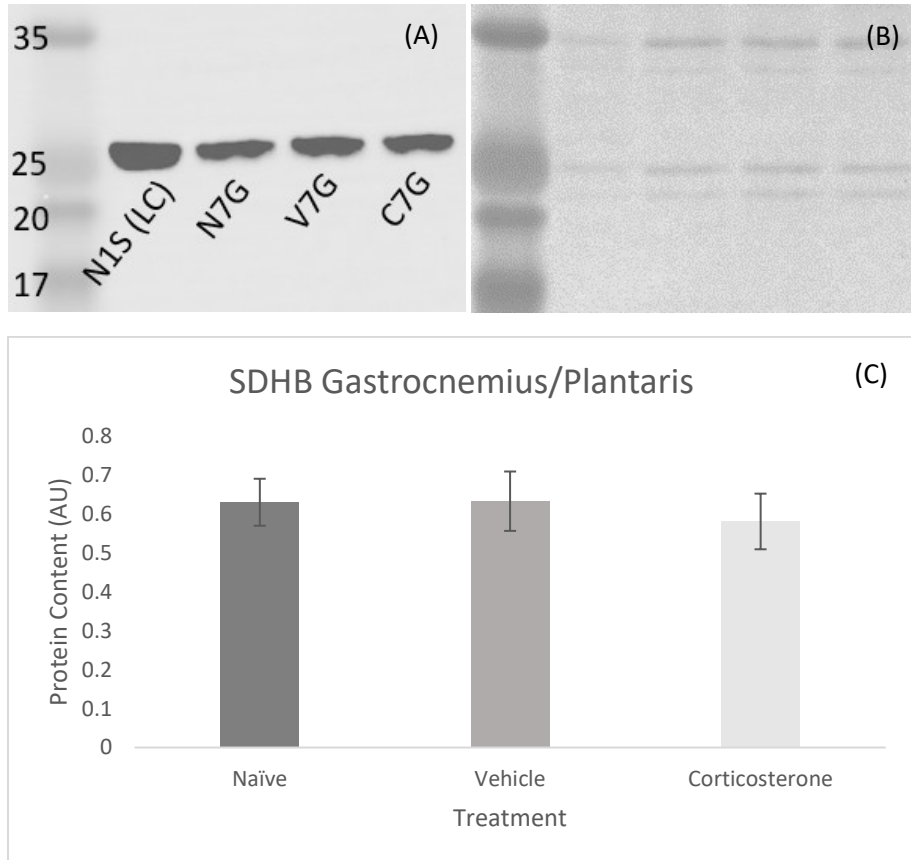
**Figure 14. Citrate Synthase Protein Expression in Soleus**

A representative image of the protein expression of citrate synthase (panel A), the corresponding Coomassie R250 total protein stain (panel B), and normalized protein expressions (panel C) in gastrocnemius/plantaris. Samples were separated on a 10% SDS-PAGE gel with 5 $\mu$ g of protein loaded per lane. Western blot lane labels represent naïve control sample (N), vehicle control sample (V), corticosterone sample (C), and loading control (LC). Samples were normalized to the loading control on each membrane. Data are presented as mean  $\pm$  SD. n = 8-10 per group.

#### 4.4.2 SDHB Decreases in Proportion to Total Protein Content

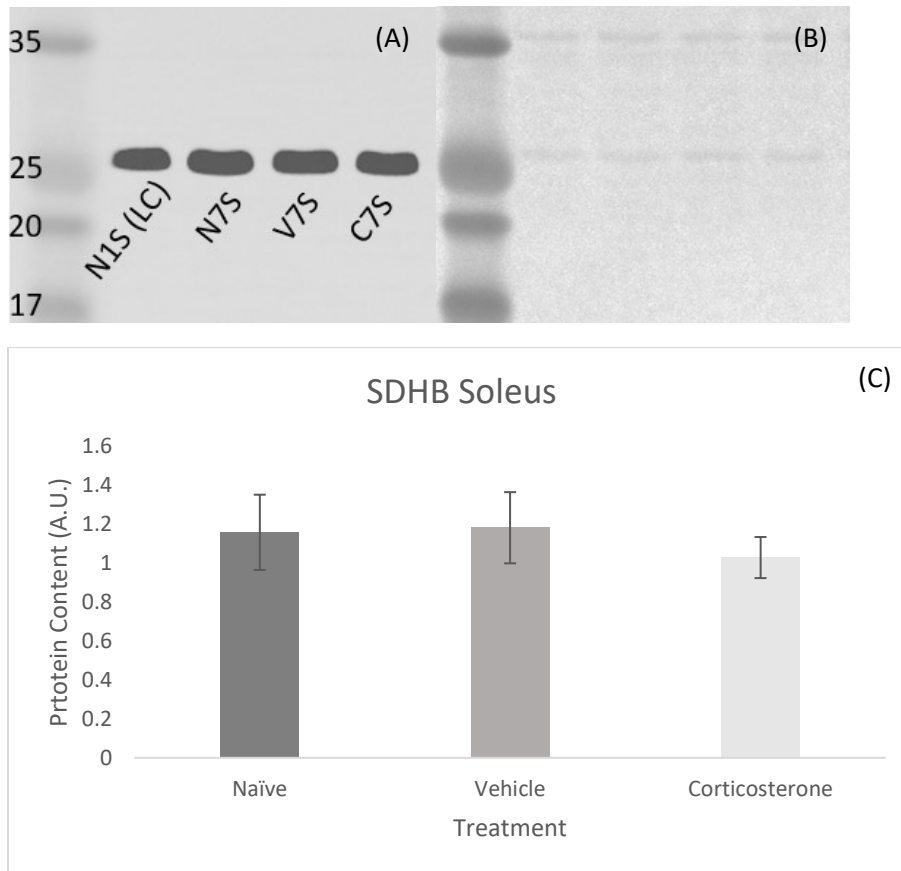
SDHB western blotting was used as a second measure of the effects of chronic corticosterone treatment on functional mitochondrial content. Based on optimization, 5  $\mu$ g of total protein was loaded per well. Adjusted band volume was normalized to a

loading control on each membrane to give the SDHB expression relative to the total protein loaded. There was no significant effect of chronic corticosterone exposure on SDHB expression in either the gastrocnemius/plantaris ( $p=0.28$ ) (Figure 15) or the soleus ( $p=0.18$ ) (Figure 16) muscle.



**Figure 15. SDHB Protein Expression in Gastrocnemius/Plantaris**

A representative image of the protein expression of SDHB (panel A), the corresponding Coomassie R250 total protein stain (panel B), and normalized protein expressions (panel C) in gastrocnemius/plantaris. Samples were separated on a 10% SDS-PAGE gel with  $5\mu\text{g}$  of protein loaded per lane. Western blot lane labels represent naïve control sample (N), vehicle control sample (V), corticosterone sample (C), and loading control (LC). Samples were normalized to the loading control on each membrane. Data are presented as mean  $\pm$  SD.  $n = 8-10$  per group.



**Figure 16. SDHB Protein Expression in Soleus**

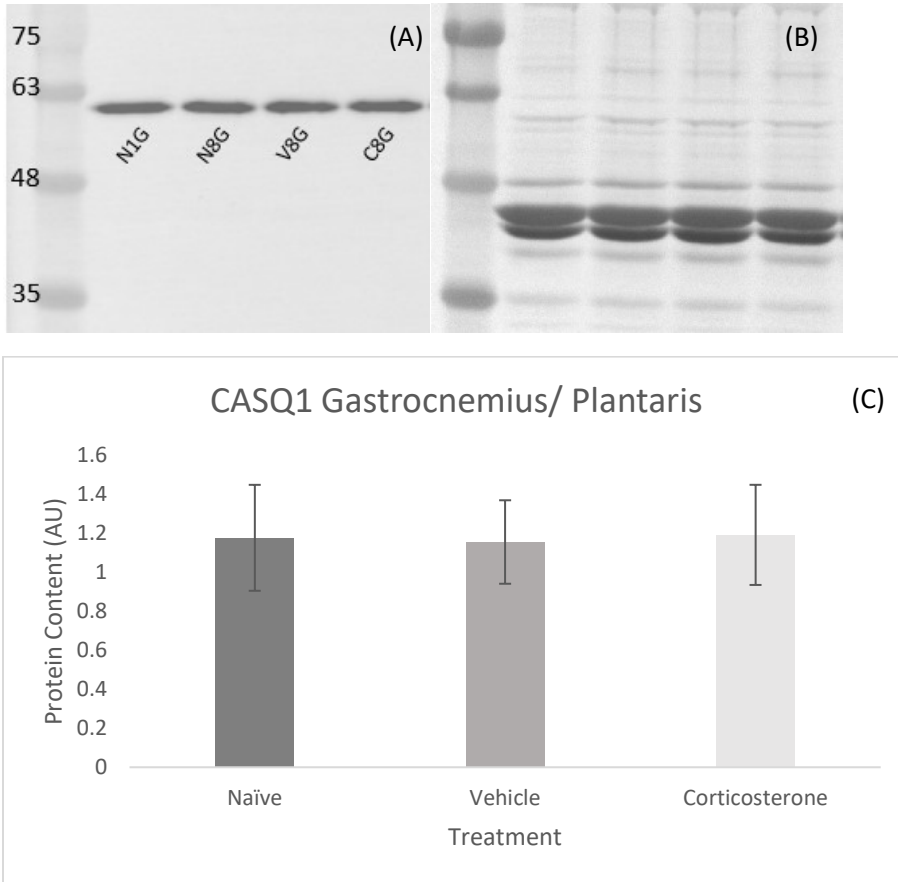
A representative image of the protein expression of SDHB (panel A), the corresponding Coomassie R250 total protein stain (panel B), and normalized protein expressions (panel C) in soleus. Samples were separated on a 10% SDS-PAGE gel with 5 $\mu$ g of protein loaded per lane. Western blot lane labels represent naïve control sample (N), vehicle control sample (V), corticosterone sample (C), and loading control (LC). Samples were normalized to the loading control on each membrane. Data are presented as mean  $\pm$  SD. n = 8-10 per group.

#### 4.5 Protein Biomarkers of Sarcoplasmic Reticulum Content

##### 4.5.1 CASQ1 Content is Decreased in Soleus of Corticosterone-treated Mice Relative to Total Protein Content

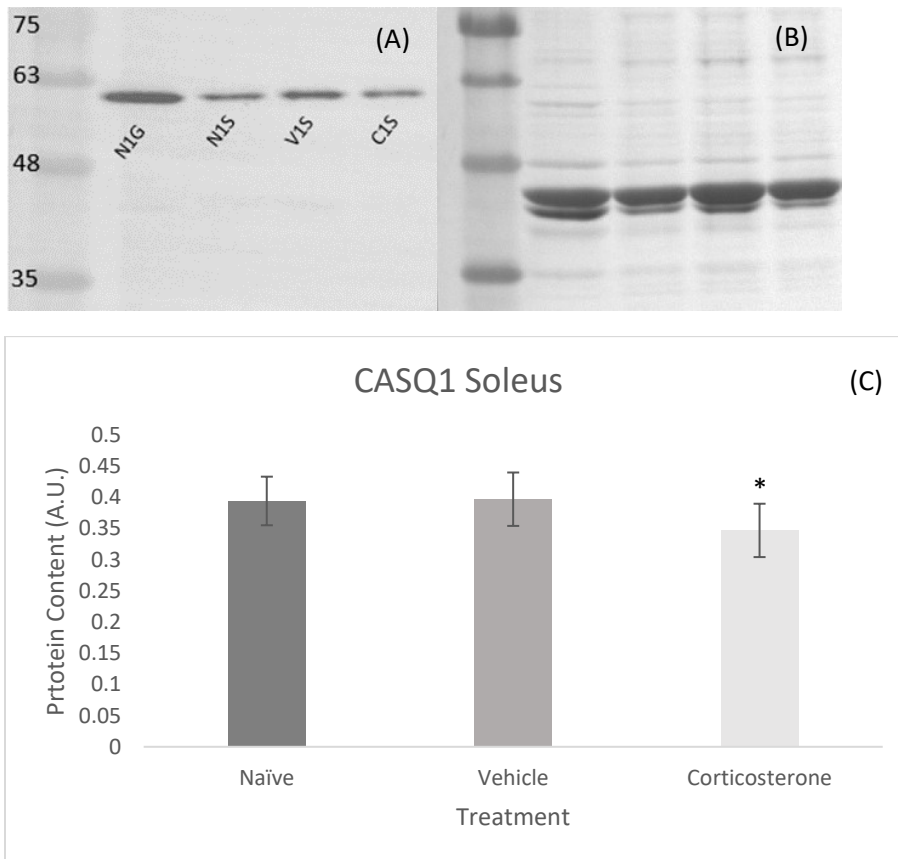
CASQ1 western blotting was used to examine the effects of chronic corticosterone treatment on the SR. 10  $\mu$ g of total protein was loaded per well. Adjusted band volume was normalized to a loading control on each membrane to give the CASQ1

expression relative to the total protein loaded. In the gastrocnemius/plantaris, there was no significant effect of chronic corticosterone treatment on CASQ1 expression ( $p=0.96$ ) (Figure 17). In the soleus, there was a significant decrease in CASQ1 expression in the corticosterone group versus the naïve control ( $p=0.048$ ), with the average CASQ1 expression of the corticosterone group being 13% lower than the naïve control group (Figure 18).



**Figure 17. CASQ1 Protein Expression in Gastrocnemius/Plantaris**

A representative image of the protein expression of CASQ1 (panel A), the corresponding Coomassie R250 total protein stain (panel B), and normalized protein expressions (panel C) in gastrocnemius/plantaris. Samples were separated on a 10% SDS-PAGE gel with 10 $\mu$ g of protein loaded per lane. Western blot lane labels represent naïve control sample (N), vehicle control sample (V), corticosterone sample (C), and loading control (N1G). Samples were normalized to the loading control on each membrane. Data are presented as mean  $\pm$  SD.  $n = 8-10$  per group.



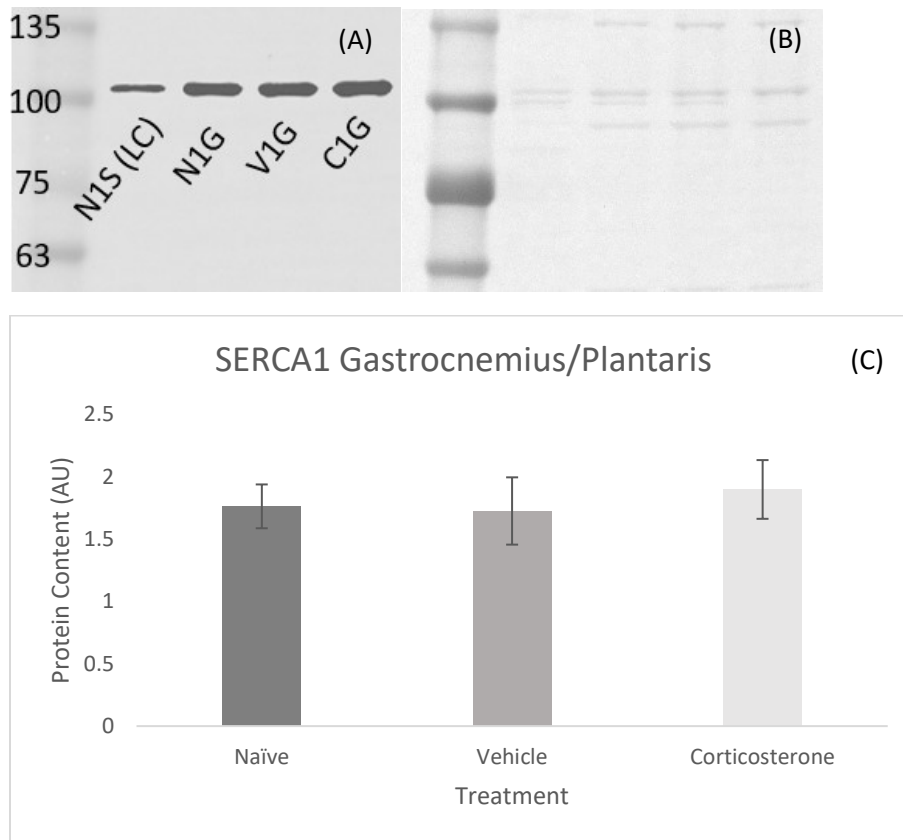
**Figure 18. CASQ1 Protein Expression in Soleus**

A representative image of the protein expression of CASQ1 (panel A), the corresponding Coomassie R250 total protein stain (panel B), and normalized protein expressions (panel C) in soleus. Samples were separated on a 10% SDS-PAGE gel with 10 $\mu$ g of protein loaded per lane. Western blot lane labels represent naïve control sample (N), vehicle control sample (V), corticosterone sample (C), and loading control (N1G). Samples were normalized to the loading control on each membrane. Data are presented as mean  $\pm$  SD. n = 8-10 per group. \*= p<0.05

#### 4.5.2 SERCA1 Content is Decreased in Soleus Relative to Total Protein Content

SERCA1 western blotting was used to examine the effects of chronic corticosterone treatment on the SR. 10  $\mu$ g of total protein was loaded per well. Adjusted band volume was normalized to a loading control on each membrane to give the SERCA1 expression relative to total protein loaded. In the gastrocnemius/plantaris,

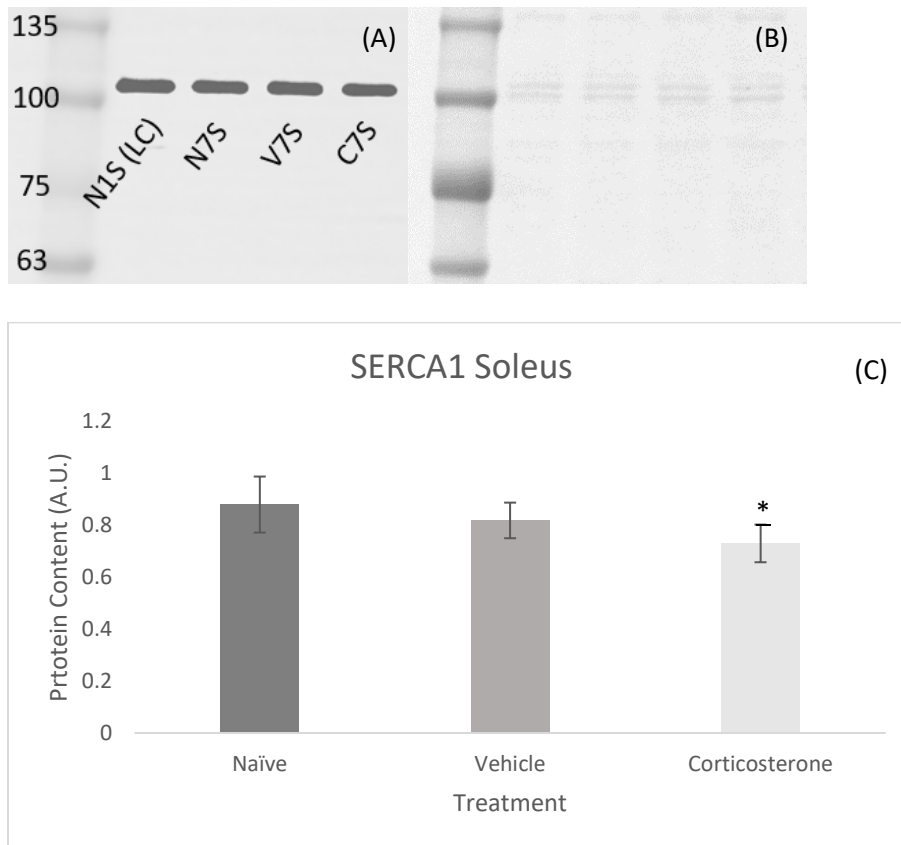
there was no significant effect of chronic corticosterone treatment on SERCA1 expression ( $p=0.32$ ) (Figure 17). In the soleus, there was a significant decrease in SERCA1 expression in the corticosterone group versus the naïve control ( $p<0.01$ ), with the average SERCA1 expression of the corticosterone group being ~19% lower than the naïve control group (Figure 18).



**Figure 19. SERCA1 Protein Expression in Gastrocnemius/Plantaris**

A representative image of the protein expression of SERCA1 (panel A), the corresponding Coomassie R250 total protein stain (panel B), and normalized protein expressions (panel C) in gastrocnemius/plantaris. Samples were separated on a 7.5% SDS-PAGE gel with 3 $\mu$ g of protein loaded per lane. Western blot lane labels represent naïve control sample (N), vehicle control sample (V), corticosterone sample (C), and loading control (LC). Samples were normalized to the loading control on each membrane. Data are presented as mean  $\pm$  SD.  $n = 8-10$  per group.





**Figure 20. SERCA1 Protein Expression in Soleus**

A representative image of the protein expression of SERCA1 (panel A), the corresponding Coomassie R250 total protein stain (panel B), and normalized protein expressions (panel C) in soleus. Samples were separated on a 7.5% SDS-PAGE gel with 3 $\mu$ g of protein loaded per lane. Western blot lane labels represent naïve control sample (N), vehicle control sample (V), corticosterone sample (C), and loading control (LC). Samples were normalized to the loading control on each membrane. Data are presented as mean  $\pm$  SD. n = 8-10 per group. \* = p<0.05

## Chapter 5. Discussion

This study examined the effects of chronic endogenous glucocorticoid administration on skeletal muscle structure in C57BL/6 mice using corticosterone treatment in drinking water. Chronically elevated glucocorticoid levels can occur as a by-product of stress, chronic treatment with glucocorticoids in a clinical setting-- such as through treatment of autoimmune disorders like rheumatoid arthritis with (often synthetic) glucocorticoids such as dexamethasone-- or they may occur as a result of increased endogenous glucocorticoids through diseases such as Cushing's disorder. Whatever the cause, prolonged periods of elevated glucocorticoids are associated with a wide range of deleterious effects on the body, including skeletal muscle atrophy. While in a broad sense, it is generally accepted that chronic glucocorticoid treatment and/or chronically elevated endogenous glucocorticoids will lead to muscle atrophy, the effects seen at different time points and different levels of glucocorticoids vary, and so the continued study of this phenomenon is vital. Furthermore, research into the effects of chronic corticosterone treatment on the key structures of functionally different muscle groups over various time periods and at different glucocorticoid levels is underdeveloped. To our knowledge, this is the first study aimed at determining the effect of chronic corticosterone on skeletal muscle atrophy with respect to 1) comparing gastrocnemius/plantaris to soleus, and 2) the specific effects on the contractile protein and biomarkers of mitochondrial and sarcoplasmic reticulum content.

To investigate the adaptations of different skeletal muscle groups to chronic corticosterone treatment, the soleus and gastrocnemius/plantaris muscle group were isolated in a mouse model to determine contractile protein content and indicators of mitochondrial content and sarcoplasmic reticulum content. The outcomes can be helpful in examining the effects of chronically elevated endogenous glucocorticoids on humans and may have implications in the effect of chronic low-dose treatment with glucocorticoids in a medical setting. Based on tissue weights and results from muscle protein expression, there is a greater effect of chronic corticosterone treatment on the

skeletal muscle mass of gastrocnemius/plantar muscles than soleus muscles. Interestingly, a selective decrease in indicators of sarcoplasmic reticulum content and function is seen in soleus muscles as a result of chronic corticosterone treatment, indicating that the sarcoplasmic reticulum, and potentially  $\text{Ca}^{2+}$  handling, may be affected by chronic corticosterone treatment before contractile and mitochondrial proteins.

### 5.1 Dosing effects

As mentioned in the limitations section, the dosing method chosen for this study (corticosterone treatment via drinking water) was selected as it has been previously validated as a model of chronic glucocorticoid administration and it helps reduce excess stress to the animal [25, 53, 105]. Although unreported in past studies, we found that corticosterone-treated mice drank significantly more water than the naïve or vehicle controls, which resulted in a higher average daily dose per mouse than anticipated (Appendix 9.6, Figure 21). Increased consumption of drinking water began on day 4 and escalated from days 10 through 20. On day 21 the concentration of corticosterone in water was reduced to 50 $\mu\text{g}/\text{mL}$  from 100 $\mu\text{g}/\text{mL}$  and drinking water consumption became similar to naïve and vehicle controls (Figure 5). While overconsumption of water did alter the dose of the treatment mice received, it was corrected after day 19 of the experiment and in the final 8 days of the experiment doses were much nearer the target 500 $\mu\text{g}$  per mouse per day.

Most past studies using the same corticosterone dose, delivery method, and housing temperature did not report measuring water intake or the increased dose of corticosterone consumed by the mice [53, 105]. A handful of studies reported an increase in water intake using the same dose and housing temperature, but none reported on the magnitude of this increase in water consumption or the corresponding increase in corticosterone dose which would be a direct result [42, 106, 107]. Although Do et al. (2019) and Kinlein et al. (2017) reported a significant increase in treatment

water consumption, neither reported the dose of corticosterone received and only indicated that plasma corticosterone levels were sustained at >400ng/mL [106, 107].

Given the magnitude of the increased water intake in corticosterone-treated mice over naïve and vehicle controls, this represents an important factor that should be taken into account in future studies. The water consumption and corticosterone dose administered should be monitored and reported to ensure accuracy and reproducibility in future studies.

## 5.2 Sample population considerations

The weight of the C2 study mouse soleus is 0.029 grams. This is an outlier, as determined by Normal Q-Q plotting and interquartile range, with the next highest value soleus weight being 0.021g and remaining values all below 0.020g. The inclusion of this soleus muscle does not effect the significance calculations of the soleus study samples, but potentially lessens the observed decrease in muscle mass and protein content in the corticosterone group. The removal of an outlier should also be based on a proven collection error, data entry error, or other observed variation from the set parameters of the study. We do not have any record indicating sufficient grounds for exclusion of the outlier; for this reason, the outlier has been included in the analysis.

## 5.3 Overall effect of treatment on muscle wet weight and total protein content

Skeletal muscle mass is made up of approximately 20% protein [116]. We were able to isolate approximately 15-18% of the gastrocnemius/plantaris and soleus muscles as protein, indicating good recovery of the total protein present in the muscle (Tables 1 and 2). The amount of protein recovered from the muscle samples also decreases more or less in parallel with the muscle mass (Table 1 and 2). The same amount of relative protein between groups should therefore indicate lower total protein in smaller muscles, so a corresponding decrease in the total protein content of each indicator protein is expected in treatment groups where the muscle mass is reduced (i.e., corticosterone treatment group) (Figure 6). Further analysis of the relative protein

content of selected indicator proteins when loading equal total protein for each sample is used to examine any differences in the effect of treatment on functionally different muscle groups and look for evidence of targeted effects of chronic corticosterone treatment on various muscle structures.

#### 5.4 Atrophy effect on functionally different muscle groups

As suggested by previous studies on the effect of chronic glucocorticoid treatment and chronic corticosterone treatment, our study revealed atrophy in the skeletal muscle of C57BL/6N mice (Figure 6). Interestingly, the effect of chronic corticosterone treatment on muscle mass appears to be greater in the gastrocnemius/plantaris muscle group than in the soleus muscle (Figure 6, Figure 7). The average muscle wet weight of the gastrocnemius/plantaris normalized to body weight in chronic corticosterone-treated mice was significantly decreased by 36% compared to control (Figure 6), and although the average soleus muscle wet weight also decreased by ~15%, it was not statistically significant (Figure 7).

There are many contradictory findings in the literature regarding the differing effects of atrophy- both in glucocorticoid treatment and other atrophy models- on these two functionally different muscle groups. One potential reason for the greater degree of atrophy observed in the gastrocnemius/plantaris in this study is the difference in recruitment of these two muscle groups. Although it was not measured, it is possible that there was decrease in voluntary movement in our corticosterone mice compared to vehicle controls. This is supported by various studies indicating chronic stress or chronic glucocorticoid treatment reduces voluntary movement in mouse models [50, 51, 52]. As a very active species, mice will typically run long distances when presented the option under normal physiological conditions [50]. In hypertrophy studies, mice which ran more had increased gastrocnemius muscle mass but not soleus muscle mass, indicating the increased recruitment of the gastrocnemius over the soleus in running [75]. Multiple studies have indicated that there is an increase in protein degradation in skeletal muscles, including the medial gastrocnemius, of rodents over periods of disuse around 1

week [118, 119]. Since gastrocnemius/plantaris is used less than the soleus, it is likely catabolized first. The over 2X greater loss of muscle mass seen in the gastrocnemius/plantaris represents a clearly larger effect of chronic corticosterone treatment on this muscle group than the soleus.

## 5.5 Contractile Protein

The contractile proteins myosin and actin are the main components of the thick and thin filaments, respectively, of the sarcomere. They are also by far the most abundant proteins in the skeletal muscle, and an essential component of muscle structure [112]. As the two main components of the contractile unit, myosin and actin are widely studied in various atrophy models, however, there are conflicting reports regarding the relative rate of decrease of myosin and actin in most atrophy models, including chronic stress and chronic corticosterone treatment [102, 110]. It is therefore still debated whether myosin and actin degrade at the same rate in chronic stress atrophy, or whether one or the other may be selectively degraded. Our results highlight one of the causes for this disagreement in results: the method used to isolate and quantify contractile proteins, especially myosin, has a major impact on the reported effect of treatment.

As previously reported by Leinwand et al, many groups fail to properly account for the insolubility of the myosin heavy chain when attempting to isolate muscle proteins for quantification by gel staining or western blot [110]. In total protein staining of muscle studies, it is not uncommon to see SDS-PAGE or western blots in which the MHC band is far lighter than it should be given how large a portion of the total protein it represents in skeletal muscle. This failure to properly extract MHC can cause significant effects of treatment to be missed. To account for this, our group adapted the appropriate method of solubilizing MHC prior to centrifugation with 600mM KCl in the extraction buffer to improve the isolation of insoluble MHC [110]. We used two methods of detection for actin and myosin to test for differences in the observed effect of treatment based on quantification method.

Neither the SDS-PAGE/Coomassie G250 stained gels nor the MHC westerns indicated a significant difference in the amount of relative MHC between treatment groups, indicating that MHC decreases proportionally with the decrease in total protein. There was some variability in results between the protein quantification using gel staining and protein quantification using western blotting. In the Coomassie G250-stained gels, there was no observable difference in the average MHC expression of the corticosterone treatment group compared to naïve and vehicle controls in the gastrocnemius/plantaris or soleus, whereas western blotting of MHC indicated a slight, non-significant increase in the average MHC expression of corticosterone-treated gastrocnemius/plantaris of around 15% over naïve control. Leinwand et al. (2012) previously concluded that MHC protein expression is better quantified using gel staining rather than western blotting [110]. We therefore conclude that MHC seems to decrease proportionally with the decrease in total protein and muscle mass after 4 weeks of corticosterone treatment.

As with MHC, neither the SDS-PAGE/Coomassie G250 stained gels nor the actin western blots indicated a significant difference in the amount of relative actin between treatment groups, indicating that actin decreases proportionally with the decrease in total protein. The SDS-PAGE/Coomassie G250 results also indicated a possible non-significant decrease in actin content relative to total protein in the corticosterone treatment group versus naïve and vehicle controls, although there was a high degree of variability. This may indicate that actin content is reduced more than myosin content under chronic stress conditions, possibly as result of the different degradation pathways involved in the breakdown of myosin and actin in skeletal muscle, however the current protocol lacks the sensitivity/power to confirm this [30].

## 5.6 Mitochondrial Content

Chronic stress has been reported to result in mitochondrial dysfunction via dysregulated exchange between mitochondria and endoplasmic reticulum or reduced mitochondrial biogenesis and quality control [26, 27]. Previous studies have indicated

that mitochondrial content is decreased in more extreme atrophy models such as denervation [28], however, the present study utilized a less robust model of atrophy. Citrate synthase and SDHB content were both included as indicators of functional mitochondrial content, as they are key components of the Krebs cycle and have been validated as biomarkers in previous studies [18, 28, 29]. Our results found that the relative citrate synthase content increased by 21% (though not significantly,  $p=0.10$ ) in the corticosterone treatment group compared to naïve and vehicle controls in the gastrocnemius/plantaris, while no effect of treatment was observed in the soleus (Figure 13, 14). Given the decrease in muscle mass and total protein content in the gastrocnemius/plantaris muscle group, this may indicate a possible preservation of mitochondrial content during chronic corticosterone-induced atrophy, although the current study lacks the sensitivity to confirm this.

To corroborate the results of citrate synthase expression, SDHB was also measured as a biomarker of mitochondrial content. SDHB content of the corticosterone treatment group was not significantly different from naïve or vehicle controls in either the gastrocnemius/plantaris or soleus (Figure 15, 16) and unlike citrate synthase showed no evidence of a trend toward increased protein content in the corticosterone treatment group. Reduction in mitochondrial content may be restricted to more extreme forms of atrophy, such as denervation models.

### 5.7 Sarcoplasmic Reticulum Content

The effect of chronic glucocorticoid treatment on the SR in skeletal muscle is poorly understood. Although it is widely accepted that chronic glucocorticoid treatment results in muscle myopathy and muscle weakness, it is uncertain how functional alterations seen in these models are related to adaptations in the SR. The volume of the sarcoplasmic reticulum alone is not the best indicator of SR function, and so it is beneficial to instead measure important indicators of SR function such as CASQ1 and SERCA1 [113, 114]. CASQ1 is the most abundant  $\text{Ca}^{2+}$  binding protein in skeletal muscle and has a wide range of functions in the SR including: maintaining a sufficient amount of



Ca<sup>2+</sup> in the SR, sensing and regulating the release of Ca<sup>2+</sup> from the SR into the cytosol, regulating formation of terminal cisternae, and regulating Ca<sup>2+</sup> entry into the SR [115]. The relative protein content of CASQ1 was significantly reduced in the corticosterone treatment group in the soleus but not the gastrocnemius/plantaris (Figures 17, 18). The same pattern was seen in SERCA1 in both gastrocnemius/plantaris and soleus (Figures 19, 20).

This decrease in key SR proteins in the soleus but not in the gastrocnemius/plantaris group that experienced a higher degree of muscle wasting may suggest that SR dysfunction characterized by a reduction in calsequestrin and SERCA may be a precursor to or even a contributing factor of corticosteroid induced muscle myopathy. Loss of SERCA1 activity and function has been identified as a characteristic of many muscle atrophy and dysfunction models, and overexpression of the SERCA1 protein has been suggested as a way to improve muscle function [45, 64, 67]. A reduction in SR functional proteins CASQ1 and SERCA1 and expected corresponding decrease in activity may be an early indicator of atrophy [120, 121]. The decrease in these two proteins in soleus but not gastrocnemius/plantaris may also be due to recruitment differences in the two muscle groups.

## Chapter 6. Conclusion

Chronic stress and chronic treatment with synthetic and endogenous stress hormones (i.e. glucocorticoids) in a clinical setting produces a range of negative effects on the body and skeletal muscle tissue. The effect of chronic corticosterone treatment on major skeletal muscle features (contractile protein, mitochondria, and SR) in functionally different muscle groups is also poorly understood. Chronic oral corticosterone treatment via drinking water in C57BL6/N mice is a model of chronic stress in humans and may also provide insight into the effect of chronic low-dose treatment with glucocorticoids in a clinical setting. The effect of 500µg/mouse/day corticosterone treatment over 4 weeks on the gastrocnemius/plantaris and soleus suggests a greater effect of treatment on muscle mass in the gastrocnemius/plantaris muscle group than the soleus muscle. Atrophy was induced in the gastrocnemius/plantaris but not the soleus based on muscle wet weight and total protein content. In the gastrocnemius/plantaris muscle group, chronic corticosterone induced atrophy without demonstrating a significant specific effect on the contractile protein or indicators of mitochondrial and SR content. In the soleus, while no significant muscle wasting occurred, decreases in key SR functional proteins CASQ1 and SERCA1 may indicate SR dysfunction. This research supplements the need for better characterization of the effects of chronic corticosterone treatment on different skeletal muscles to determine the effects of atrophy and Ca<sup>2+</sup> handling on different muscle groups and key structures within them.

## Chapter 7. Future Directions

The present study opens the door for further studies to examine the differing effects of chronic corticosterone treatment on functionally different skeletal muscle groups. Specifically, future studies should include longer treatment time, improved matching of target corticosterone treatments, and potentially larger sample sizes. Using a larger sample size to examine the effects of chronic corticosterone treatment on activities of key contractile, SR, and mitochondrial proteins would permit more statistical power for the analysis of changes in skeletal muscle function. Any future studies using drinking water drug delivery should select the appropriate dose in the drinking water to better match the targeted dose delivery with the volume of water consumed. In addition, monitoring and reporting the water consumption and dose of the treatment to ensure reproducibility and accuracy in interpreting results is critical. Finally, future studies should include both male and female mice to better understand the effects of corticosterone and sex on skeletal muscle.

## Chapter 8. References

1. Gensler, L. S. Glucocorticoids. *Neurohospitalist* 3, 92–97 (2013).
2. The RECOVERY Collaborative Group. Dexamethasone in hospitalized patients with Covid-19 - Preliminary Report. *N Engl J Med.* (2020) Published online Jul 17 2020: <https://doi.org/10.1056/NEJMoa2021436>
3. Gianfrancesco M, Hyrich KL, Al-Adely S, et al. Characteristics associated with hospitalisation for COVID-19 in people with rheumatic disease: data from the COVID-19 Global Rheumatology Alliance physician-reported registry. *Ann Rheum Dis.* 79, 859-866 (2020).
4. Brenner EJ, Ungaro RC, Geary RB, et al. Corticosteroids, but not TNF antagonists, are associated with adverse COVID-19 outcomes in patients with inflammatory bowel diseases: results from an international registry. *Gastroenterology.* 159, 481-491 (2020).
5. Kuo, T., Harris, C. A. & Wang, J.-C. Metabolic functions of glucocorticoid receptor in skeletal muscle. *Molecular and Cellular Endocrinology* 380, 79–88 (2013).
6. Krozowski, Z. *et al.* The type I and type II 11 $\beta$ -hydroxysteroid dehydrogenase enzymes. *The Journal of Steroid Biochemistry and Molecular Biology* 69, 391–401 (1999).
7. Joëls, M., Karst, H. & Sarabdjitsingh, R. A. The stressed brain of humans and rodents. *Acta Physiol (Oxf)* 223, e13066 (2018).
8. Kanda F, Okuda S, Matsushita T, Takatani K, Kimura KI, Chihara K. Steroid myopathy: pathogenesis and effects of growth hormone and insulin-like growth factor-I administration. *Horm Res.* 56(Suppl 1):24–28 (2001).
9. Haus, J. M., Carrithers, J. A., Carroll, C. C., Tesch, P. A. & Trappe, T. A. Contractile and connective tissue protein content of human skeletal muscle: effects of 35 and 90 days of

simulated microgravity and exercise countermeasures. *American Journal of Physiology-Regulatory, Integrative and Comparative Physiology* 293, R1722–R1727 (2007).

10. Buliman, A., Tataranu, L., Paun, D., Mirica, A. & Dumitrache, C. Cushing's disease: a multidisciplinary overview of the clinical features, diagnosis, and treatment. *J Med Life* 9, 12–18 (2016).

11. Beaupere, C., Liboz, A., Fève, B., Blondeau, B. & Guillemain, G. Molecular Mechanisms of Glucocorticoid-Induced Insulin Resistance. *Int J Mol Sci* 22, 623 (2021).

12. Löfberg E., Gutierrez A., Wernerman J., Anderstam B., Mitch W.E., Price S.R., Bergström J., Alvestrand A. Effects of high doses of glucocorticoids on free amino acids, ribosomes and protein turnover in human muscle. *Eur. J. Clin. Investig.* 32:345–353 (2002).

13. Curtis J.R., Westfall A.O., Allison J., Bijlsma J.W., Freeman A., George V., Saag K.G. Population-based assessment of adverse events associated with long-term glucocorticoid use. *Arthritis Rheum.* 55,420–426 (2006).

14. Sato, A. Y. *et al.* Glucocorticoids Induce Bone and Muscle Atrophy by Tissue-Specific Mechanisms Upstream of E3 Ubiquitin Ligases. *Endocrinology* 158, 664–677 (2017).

15. Pin, F., Couch, M. E. & Bonetto, A. Preservation of muscle mass as a strategy to reduce the toxic effects of cancer chemotherapy on body composition. *Current Opinion in Supportive and Palliative Care* 12, 420–426 (2018).

16. Martin, L. *et al.* Cancer cachexia in the age of obesity: skeletal muscle depletion is a powerful prognostic factor, independent of body mass index. *J Clin Oncol* 31, 1539–1547 (2013).

17. Robinson, P. C. & Morand, E. Divergent effects of acute versus chronic glucocorticoids COVID-19. *The Lancet Rheumatology* 3, e168–e170 (2021).

18. Jacobs, R. A., Díaz, V., Meinild, A.-K., Gassmann, M. & Lundby, C. The C57Bl/6 mouse serves as a suitable model of human skeletal muscle mitochondrial function. *Experimental Physiology* 98, 908–921 (2013).
19. Gomez-Sanchez, E. & Gomez-Sanchez, C. E. The Multifaceted Mineralocorticoid Receptor. *Compr Physiol* 4, 965–994 (2014).
20. Liu, D. *et al.* A practical guide to the monitoring and management of the complications of systemic corticosteroid therapy. *All Asth Clin Immun* 9, 1–25 (2013).
21. Allen, D. L., McCall, G. E., Loh, A. S., Madden, M. C. & Mehan, R. S. Acute daily psychological stress causes increased atrophic gene expression and myostatin-dependent muscle atrophy. *Am J Physiol Regul Integr Comp Physiol* 299, R889–898 (2010).
22. Valenzuela, C. A. *et al.* Chronic stress inhibits growth and induces proteolytic mechanisms through two different nonoverlapping pathways in the skeletal muscle of a teleost fish. *Am J Physiol Regul Integr Comp Physiol* 314, R102–R113 (2018).
23. Schakman, O., Gilson, H. & Thissen, J. P. Mechanisms of glucocorticoid-induced myopathy. *J Endocrinol* 197, 1–10 (2008).
24. Gehlert, S., Bloch, W. & Suhr, F. Ca<sup>2+</sup>-dependent regulations and signaling in skeletal muscle: from electro-mechanical coupling to adaptation. *Int J Mol Sci* 16, 1066–1095 (2015).
25. Gasparini, S. J. *et al.* Continuous corticosterone delivery via the drinking water or pellet implantation: A comparative study in mice. *Steroids* 116, 76–82 (2016).
26. Wang, J., Yang, X. & Zhang, J. Bridges between mitochondrial oxidative stress, ER stress and mTOR signaling in pancreatic  $\beta$  cells. *Cell Signal* 28, 1099–1104 (2016).

27. Suliman, H. B. & Piantadosi, C. A. Mitochondrial biogenesis: regulation by endogenous gases during inflammation and organ stress. *Curr Pharm Des* 20, 5653–5662 (2014).
28. Adhihetty, P. J., O’Leary, M. F. N., Chabi, B., Wicks, K. L. & Hood, D. A. Effect of denervation on mitochondrially mediated apoptosis in skeletal muscle. *J Appl Physiol* (1985) 102, 1143–1151 (2007).
29. Marzetti, E. et al. Mitochondrial death effectors: relevance to sarcopenia and disuse muscle atrophy. *Biochim Biophys Acta* 1800, 235–244 (2010).
30. Schiaffino, S. Losing pieces without disintegrating: Contractile protein loss during muscle atrophy. *Proc Natl Acad Sci U S A* 114, 1753–1755 (2017).
31. Biga, L. M. et al. Anatomy and Physiology- 1st Edition: 10.5 Types of Muscle Fibers. *Oregon State University* (2019).
32. Menconi, M., Gonnella, P., Petkova, V., Lecker, S. & Hasselgren, P.-O. DEXAMETHASONE AND CORTICOSTERONE INDUCE SIMILAR, BUT NOT IDENTICAL, MUSCLE WASTING RESPONSES IN CULTURED L6 AND C2C12 MYOTUBES. *J Cell Biochem* 105, 353–364 (2008).
33. Desler, M. M., Jones, S. J., Smith, C. W. & Woods, T. L. Effects of dexamethasone and anabolic agents on proliferation and protein synthesis and degradation in C2C12 myogenic cells. *Journal of Animal Science* 74, 1265 (1996).
34. Barel, M. et al. Exercise training prevents hyperinsulinemia, muscular glycogen loss and muscle atrophy induced by dexamethasone treatment. *Eur J Appl Physiol* 108, 999–1007 (2010).

35. Shang, Y. *et al.* An Ultrashort Peptide-Based Supramolecular Hydrogel Mimicking IGF-1 to Alleviate Glucocorticoid-Induced Sarcopenia. *ACS Appl. Mater. Interfaces* 12, 34678–34688 (2020).
36. Marzetti, E. *et al.* Mitochondrial death effectors: relevance to sarcopenia and disuse muscle atrophy. *Biochem Biophys Acta* 1800, 235–244 (2010).
37. Larsen, S. *et al.* Biomarkers of mitochondrial content in skeletal muscle of healthy young human subjects. *The Journal of Physiology* 590, 3349–3360 (2012).
38. Volodin, A., Kostin, I., Goldberg, A. L. & Cohen, S. Myofibril breakdown during atrophy is a delayed response requiring the transcription factor PAX4 and desmin depolymerization. *PNAS* 114, E1375–E1384 (2017).
39. Hunter, R. B., Mitchell-Felton, H., Essig, D. A. & Kandarian, S. C. Expression of endoplasmic reticulum stress proteins during skeletal muscle disuse atrophy. *Am J Physiol Cell Physiol* 281, C1285–1290 (2001).
40. Yamada, T., Ashida, Y., Tatebayashi, D., Abe, M. & Himori, K. Cancer Cachexia Induces Preferential Skeletal Muscle Myosin Loss When Combined With Denervation. *Front. Physiol.* 11, (2020).
41. Schertzer, J. D., Green, H. J., Fowles, J. R., Duhamel, T. A. & Tupling, A. R. Effects of prolonged exercise and recovery on sarcoplasmic reticulum Ca<sup>2+</sup> cycling properties in rat muscle homogenates. *Acta Physiol Scand* 180, 195–208 (2004).
42. Cassano, A. E. *et al.* Anatomic, Hematologic, and Biochemical Features of C57BL/6NCrl Mice Maintained on Chronic Oral Corticosterone. *Comparative Medicine* 62, 13 (2012).
43. Agrawal, A., Suryakumar, G. & Rathor, R. Role of defective Ca<sup>2+</sup> signaling in skeletal muscle weakness: Pharmacological implications. *J Cell Commun Signal* 12, 645–659 (2018).



44. Beard, N. A., Laver, D. R. & Dulhunty, A. F. Calsequestrin and the calcium release channel of skeletal and cardiac muscle. *Progress in Biophysics and Molecular Biology* 85, 33–69 (2004).
45. Murphy, R. M., Larkins, N. T., Mollica, J. P., Beard, N. A. & Lamb, G. D. Calsequestrin content and SERCA determine normal and maximal Ca<sup>2+</sup> storage levels in sarcoplasmic reticulum of fast- and slow-twitch fibres of rat. *J Physiol* 587, 443–460 (2009).
46. Damiani E, Volpe P & Margreth A. Coexpression of two isoforms of calsequestrin in rabbit slow-twitch muscle. *J Muscle Res Cell Motil* 11, 522–530 (1990).
47. Paolini C, Quarta M, Nori A, Boncompagni S, Canato M, Volpe P, Allen PD, Reggiani C & Protasi F. Reorganized stores and impaired calcium handling in skeletal muscle of mice lacking calsequestrin-1. *J Physiol* 583, 767–784 (2007).
48. Delp, M. D., Duan, C., Mattson, J. P. & Musch, T. I. Changes in skeletal muscle biochemistry and histology relative to fiber type in rats with heart failure. *J Appl Physiol* 83, 1291–1299 (1997).
49. Smith, I. C., Bombardier, E., Vigna, C. & Tupling, A. R. ATP consumption by sarcoplasmic reticulum Ca<sup>2+</sup> pumps accounts for 40-50% of resting metabolic rate in mouse fast and slow twitch skeletal muscle. *PLoS One* 8, e68924 (2013).
50. DeVallance, E. et al. Effect of chronic stress on running wheel activity in mice. *PLoS One* 12, e0184829 (2017).
51. Mul, J. D. Voluntary exercise and depression-like behavior in rodents: are we running in the right direction? *Journal of Molecular Endocrinology* 60, R77–R95 (2018).
52. Nagai, M., Nagai, H., Numa, C. & Furuyashiki, T. Stress-induced sleep-like inactivity modulates stress susceptibility in mice. *Sci Rep* 10, 19800 (2020).
53. Karatsoreos, I. N. et al. Endocrine and Physiological Changes in Response to Chronic Corticosterone: A Potential Model of the Metabolic Syndrome in Mouse. *Endocrinology* 151, 2117–2127 (2010).

54. Ruderman N.B. Muscle Amino Acid Metabolism and Gluconeogenesis. *Annual Review of Medicine*, 7147 (1975).
55. Hellhammer, D. H., Wüst, S. & Kudielka, B. M. Salivary cortisol as a biomarker in stress research. *Psychoneuroendocrinology* 34, 163–171 (2009).
56. Planche, K. et al. Diurnal Cortisol Variation According to High-Risk Occupational Specialty Within Police: Comparisons Between Frontline, Tactical Officers, and the General Population. *Journal of Occupational and Environmental Medicine* 61, e260 (2019).
57. Cortisol blood test Information | Mount Sinai - New York. Mount Sinai Health System <https://www.mountsinai.org/health-library/tests/cortisol-blood-test>.
58. Becker, D. E. Basic and Clinical Pharmacology of Glucocorticosteroids. *Anesth Prog* 60, 25–32 (2013).
59. Löfberg, E. et al. Effects of high doses of glucocorticoids on free amino acids, ribosomes and protein turnover in human muscle. *European Journal of Clinical Investigation* 32, 345–353 (2002).
60. Vieira, T. M. M., Loram, I. D., Muceli, S., Merletti, R. & Farina, D. Recruitment of motor units in the medial gastrocnemius muscle during human quiet standing: is recruitment intermittent? What triggers recruitment? *J Neurophysiol* 107, 666–676 (2012).
61. Oya, T., Riek, S. & Cresswell, A. G. Recruitment and rate coding organisation for soleus motor units across entire range of voluntary isometric plantar flexions. *J Physiol* 587, 4737–4748 (2009).
62. Zhong, H., Roy, R. R., Siengthai, B. & Edgerton, V. R. Effects of inactivity on fiber size and myonuclear number in rat soleus muscle. *J Appl Physiol* 99, 1494–1499 (2005).

63. Protasi, F., Paolini, C., Canato, M., Reggiani, C. & Quarta, M. Lessons from calsequestrin-1 ablation in vivo: much more than a Ca<sup>2+</sup> buffer after all. *J Muscle Res Cell Motil* 32, 257–270 (2011).
64. Xu, H. & Van Remmen, H. The SarcoEndoplasmic Reticulum Calcium ATPase (SERCA) pump: a potential target for intervention in aging and skeletal muscle pathologies. *Skeletal Muscle* 11, 25 (2021).
65. Kang, W., Tong, T. & Park, T. Corticotropin releasing factor-overexpressing mouse is a model of chronic stress-induced muscle atrophy. *PLoS One* 15, e0229048 (2020).
66. Edwards, S. J. et al. Short-term step reduction reduces citrate synthase activity without altering skeletal muscle markers of oxidative metabolism or insulin-mediated signaling in young males. *Journal of Applied Physiology* 131, 1653–1662 (2021).
67. Braun, J. L., Geromella, M. S., Hamstra, S. I., Messner, H. N. & Fajardo, V. A. Characterizing SERCA Function in Murine Skeletal Muscles after 35–37 Days of Spaceflight. *International Journal of Molecular Sciences* 22, 11764 (2021).
68. Lambolley, C. R. et al. Contractile properties and sarcoplasmic reticulum calcium content in type I and type II skeletal muscle fibres in active aged humans. *The Journal of Physiology* 593, 2499–2514 (2015).
69. Relaix, F. & Zammit, P. S. Satellite cells are essential for skeletal muscle regeneration: the cell on the edge returns centre stage. *Development* 139, 2845–2856 (2012).
70. Bodine, S. C. et al. Identification of Ubiquitin Ligases Required for Skeletal Muscle Atrophy. *Science* 294, 1704–1708 (2001).
71. Peters, D. G. et al. Skeletal Muscle Sarcoplasmic Reticulum Ca<sup>2+</sup>-ATPase Gene Expression in Congestive Heart Failure. *Circulation Research* 81, 703–710 (1997).
72. Ramamoorthy, S. & Cidlowski, J. A. Corticosteroids: Mechanisms of Action in Health and Disease. *Rheum Dis Clin North Am* 42, 15–31, vii (2016).

73. Herman, J. P. et al. Regulation of the hypothalamic-pituitary-adrenocortical stress response. *Compr Physiol* 6, 603–621 (2016).
74. Gallo-Payet, N. & Battista, M.-C. Steroidogenesis-adrenal cell signal transduction. *Compr Physiol* 4, 889–964 (2014).
75. Sakakima, H., Yoshida, Y., Suzuki, S. & Morimoto, N. The Effects of Aging and Treadmill Running on Soleus and Gastrocnemius Muscle Morphology in the Senescence-Accelerated Mouse (SAMP1). *The Journals of Gerontology: Series A* 59, B1015–B1021 (2004).
76. Lamboley, C. R., Wyckelsma, V. L., Perry, B. D., McKenna, M. J. & Lamb, G. D. Effect of 23-day muscle disuse on sarcoplasmic reticulum Ca<sup>2+</sup> properties and contractility in human type I and type II skeletal muscle fibers. *Journal of Applied Physiology* 121, 483–492 (2016).
77. Clarke, B. A. et al. The E3 Ligase MuRF1 degrades myosin heavy chain protein in dexamethasone-treated skeletal muscle. *Cell Metab* 6, 376–385 (2007).
78. Morgan, S. A. et al. 11 $\beta$ -HSD1 is the major regulator of the tissue-specific effects of circulating glucocorticoid excess. *Proceedings of the National Academy of Sciences* 111, E2482–E2491 (2014).
79. Boutilier, J. K. et al. Variable cardiac  $\alpha$ -actin (Actc1) expression in early adult skeletal muscle correlates with promoter methylation. *Biochim Biophys Acta Gene Regul Mech* 1860, 1025–1036 (2017).
80. Perrin, B. J. & Ervasti, J. M. The Actin Gene Family: Function Follows Isoform. *Cytoskeleton (Hoboken)* 67, 630–634 (2010).
81. Brotto, M. A., Biesiadecki, B. J., Brotto, L. S., Nosek, T. M. & Jin, J.-P. Coupled expression of troponin T and troponin I isoforms in single skeletal muscle fibers correlates with contractility. *American Journal of Physiology-Cell Physiology* 290, C567–C576 (2006).

82. Morgan, S. A. et al.  $11\beta$ -Hydroxysteroid Dehydrogenase Type 1 Regulates Glucocorticoid-Induced Insulin Resistance in Skeletal Muscle. *Diabetes* 58, 2506–2515 (2009).
83. Seene, T., Kaasik, P., Pehme, A., Alev, K. & Riso, E.-M. The effect of glucocorticoids on the myosin heavy chain isoforms' turnover in skeletal muscle. *J Steroid Biochem Mol Biol* 86, 201–206 (2003).
84. Rebuffe-Scrive, M., Krokiewski, M., Elfverson, J. & Bjorntorpe, P. Muscle and Adipose Tissue Morphology and Metabolism in Cushing's Syndrome. *The Journal of Clinical Endocrinology & Metabolism* 67, 1122–1128 (1988).
85. Pleasure, D. E., Walsh, G. O. & Engel, W. K. Atrophy of Skeletal Muscle in Patients With Cushing's Syndrome. *Archives of Neurology* 22, 118–125 (1970).
86. Fimbel, S. et al. Exercise training fails to prevent glucocorticoid-induced muscle alterations in young growing rats. *Pflügers Arch.* 424, 369–376 (1993).
87. Ferguson, G. T., Irvin, C. G. & Cherniack, R. M. Effect of corticosteroids on respiratory muscle histopathology. *Am Rev Respir Dis* 142, 1047–1052 (1990).
87. Barel, M. et al. Exercise training prevents hyperinsulinemia, muscular glycogen loss and muscle atrophy induced by dexamethasone treatment. *Eur J Appl Physiol* 108, 999–1007 (2010).
88. Goldman, A., Harper, S. & Speicher, D. W. Detection of Proteins on Blot Membranes. *Current Protocols in Protein Science* 86, 10.8.1-10.8.11 (2016).
89. Romero-Calvo, I. et al. Reversible Ponceau staining as a loading control alternative to actin in Western blots. *Analytical Biochemistry* 401, 318–320 (2010).
90. Gilda, J. E. & Gomes, A. V. Stain-Free total protein staining is a superior loading control to  $\beta$ -actin for Western blots. *Anal Biochem* 440, 186–188 (2013).

91. Aldridge, G. M., Podrebarac, D. M., Greenough, W. T. & Weiler, I. J. The use of total protein stains as loading controls: an alternative to high-abundance single protein controls in semi-quantitative immunoblotting. *J Neurosci Methods* 172, 250–254 (2008).
92. Jackson Laboratory. 000664 - B6 Strain Details. <https://www.jax.org/strain/000664>.
93. Capri, K. M. et al. Male C57BL6/N and C57BL6/J Mice Respond Differently to Constant Light and Running-Wheel Access. *Frontiers in Behavioral Neuroscience* 13, (2019).
94. Bryant, C. D. The blessings and curses of C57BL/6 substrains in mouse genetic studies. *Annals of the New York Academy of Sciences* 1245, 31–33 (2011).
95. Luine, V., Gomez, J., Beck, K. & Bowman, R. Sex differences in chronic stress effects on cognition in rodents. *Pharmacology Biochemistry and Behavior* 152, 13–19 (2017).
96. Rincón-Cortés, M., Herman, J. P., Lupien, S., Maguire, J. & Shansky, R. M. Stress: Influence of sex, reproductive status and gender. *Neurobiol Stress* 10, 100155 (2019).
97. Kitraki, E., Nalvarte, I., Alavian-Ghavanini, A. & Rüegg, J. Effects of pre- and post-natal exposure to bisphenol A on the stress system. *Endocrine Disruptors* 4, e1184775 (2016).
98. Kokras, N., Hodes, G. E., Bangasser, D. A. & Dalla, C. Sex differences in the hypothalamic–pituitary–adrenal axis: An obstacle to antidepressant drug development? *British Journal of Pharmacology* 176, 4090–4106 (2019).
99. Jiang, S., Postovit, L., Cattaneo, A., Binder, E. & Aitchison, K. Epigenetic Modifications in Stress Response Genes Associated With Childhood Trauma. *Frontiers in Psychiatry* 10, (2019).
100. Morgan, S. A. et al. Regulation of Lipid Metabolism by Glucocorticoids and 11 $\beta$ -HSD1 in Skeletal Muscle. *Endocrinology* 154, 2374–2384 (2013).
101. Periasamy, M. & Kalyanasundaram, A. SERCA pump isoforms: Their role in calcium transport and disease. *Muscle & Nerve* 35, 430–442 (2007).

102. Kayali, A. G., Young, V. R. & Goodman, M. N. Sensitivity of myofibrillar proteins to glucocorticoid-induced muscle proteolysis. *American Journal of Physiology-Endocrinology and Metabolism* 252, E621–E626 (1987).
103. Auclair, D., Garrel, D. R., Chaouki Zerouala, A. & Ferland, L. H. Activation of the ubiquitin pathway in rat skeletal muscle by catabolic doses of glucocorticoids. *American J Phys-Cell Physiol* 272, C1007–C1016 (1997).
104. Tipton, K. D., Hamilton, D. L. & Gallagher, I. J. Assessing the Role of Muscle Protein Breakdown in Response to Nutrition and Exercise in Humans. *Sports Med* 48, 53–64 (2018).
105. Donkelaar, E. L. van et al. Long-Term Corticosterone Exposure Decreases Insulin Sensitivity and Induces Depressive-Like Behaviour in the C57BL/6NCrl Mouse. *PLOS ONE* 9, e106960 (2014).
106. Do, T. T. H. et al. Glucocorticoid-induced insulin resistance is related to macrophage visceral adipose tissue infiltration. *J Steroid Biochem Mol Biol* 185, 150–162 (2019).
107. Kinlein, S. A., Shahanoor, Z., Romeo, R. D. & Karatsoreos, I. N. Chronic Corticosterone Treatment During Adolescence Has Significant Effects on Metabolism and Skeletal Development in Male C57BL6/N Mice. *Endocrinology* 158, 2239–2254 (2017).
108. SDHB succinate dehydrogenase complex iron sulfur subunit B [Homo sapiens (human)] - Gene - NCBI. <https://www.ncbi.nlm.nih.gov/ezproxy.lakeheadu.ca/gene/6390>.
109. Leduc-Gaudet, J. P. et al. Mitochondrial morphology is altered in atrophied skeletal muscle of aged mice. *Oncotarget* 6, 17923–17937 (2015).
110. Cosper, P. F. & Leinwand, L. A. Myosin heavy chain is not selectively decreased in murine cancer cachexia. *Int J Cancer* 130, 2722–2727 (2012).

111. Bowes, S. B., Jackson, N. C., Papachristodoulou, D., Umpleby, A. M. & Sönksen, P. H. Effect of corticosterone on protein degradation in isolated rat soleus and extensor digitorum longus muscles. *Journal of Endocrinology* 148, 501–507 (1996).
112. Augusto, V., Padovani, C., Eduardo, G. & Campos, R. Skeletal muscle fiber types in C57BL6J mice. *J. Morphol. Sci* 21, 89–94 (2004).
113. Swift, F. et al. Extreme sarcoplasmic reticulum volume loss and compensatory T-tubule remodeling after Serca2 knockout. *Proc Natl Acad Sci USA* 109, 3997–4001 (2012).
114. Knollmann, B. C. et al. Casq2 deletion causes sarcoplasmic reticulum volume increase, premature Ca<sup>2+</sup> release, and catecholaminergic polymorphic ventricular tachycardia. *J Clin Invest* 116, 2510–2520 (2006).
115. Woo, J. S., Jeong, S. Y., Park, J. H., Choi, J. H. & Lee, E. H. Calsequestrin: a well-known but curious protein in skeletal muscle. *Exp Mol Med* 52, 1908–1925 (2020).
116. Frontera, W. R. & Ochala, J. Skeletal Muscle: A Brief Review of Structure and Function. *Calcif Tissue Int* 96, 183–195 (2015).
117. Kohlmeier, M. Structure and function of amino acids. in Nutrient Metabolism (ed. Kohlmeier, M.) *Academic Press* 244–268 (2003). doi:10.1016/B978-012417762-8.50009-0.
118. Magne, H. et al. Contrarily to whey and high protein diets, dietary free leucine supplementation cannot reverse the lack of recovery of muscle mass after prolonged immobilization during ageing. *J Physiol* 590, 2035–2049 (2012).
119. Lang, S. M., Kazi, A. A., Hong-Brown, L. & Lang, C. H. Delayed recovery of skeletal muscle mass following hindlimb immobilization in mTOR heterozygous mice. *PLoS One* 7, e38910 (2012).
120. Afroze, D. & Kumar, A. ER Stress in Skeletal Muscle Remodeling and Myopathies. *FEBS J* 286, 379–398 (2019).



121. Qaisar, R., Qayum, M. & Muhammad, T. Reduced sarcoplasmic reticulum Ca<sup>2+</sup> ATPase activity underlies skeletal muscle wasting in asthma. *Life Sciences* 273, 119296 (2021).
122. Bers, D. M. Cardiac excitation–contraction coupling. *Nature* 415, 198–205 (2002).
123. Thomason, D. B., Baldwin, K. M. & Herrick, R. E. Myosin isozyme distribution in rodent hindlimb skeletal muscle. *Journal of Applied Physiology* 60, 1923–1931 (1986).
124. Gambara, G. et al. Gene Expression Profiling in Slow-Type Calf Soleus Muscle of 30 Days Space-Flown Mice. *PLOS ONE* 12, e0169314 (2017).
125. Ishihara, A., Roy, R. R., Ohira, Y., Iyata, Y. & Edgerton, V. R. Hypertrophy of rat plantaris muscle fibers after voluntary running with increasing loads. *Journal of Applied Physiology* 84, 2183–2189 (1998).
126. Meijer, O. C., de Kloet, E. R. & McEwen, B. S. Corticosteroid Receptors in *Encyclopedia of Stress (Second Edition)* (ed. Fink, G.) 594–605 (2007). doi:10.1016/B978-012373947-6.00097-0.
127. Prickaerts, J. & Steckler, T. Effects of glucocorticoids on emotion and cognitive processes in animals. *Techniques in the Behavioral and Neural Sciences* 15, 359–385 (2005).

## Chapter 9. Appendix

### 9.1 List of Abbreviations

11 $\beta$ -HSD1/2	11 $\beta$ -Hydroxysteroid Dehydrogenase Type 1/2
11-DHC	11-Dehydrocorticosterone
Acetyl CoA	Acetyl Coenzyme A
ACTH	Adrenocorticotrophic hormone
ADP	Adenosine diphosphate
ATP	Adenosine triphosphate
AVP	Arginine vasopressin
CASQ	Calsequestrin
CASQ1	Calsequestrin 1
CNS	Central nervous system
CORT	Corticosterone
CRF-OE	Corticotropin-releasing factor overexpressing
CRH	Corticotropin releasing hormone; corticotropin releasing factor; CRF
DEX	Dexamethasone
DTT	Dithiothreitol
ECL	Enhanced chemiluminescence
EDL	Extensor digitorum longus
GR	Glucocorticoid receptor
HOMA-IR	Homeostatic Model Assessment for Insulin Resistance
HPA Axis	Hypothalamic Pituitary Adrenal Axis
HRP	High frequency running program
IGF	Insulin-like growth factor
LFD	Left ventricular dysfunction
LRP	Low frequency running program
LUACF	Lakehead University Animal Care Facility
MR	Mineralocorticoid receptor
MURF-1	Muscle RING-finger protein-1
MYH, MHC	Myosin heavy chain
PFK	Phosphofructokinase
PVDF	Polyvinylidene fluoride
SDHB	Succinate Dehydrogenase Complex Iron Sulfur Subunit B
SDS-PAGE	Sodium dodecyl sulfate poly acrylamide gel
SERCA1/2/3	Sarcoplasmic/endoplasmic reticulum calcium ATPase 1/2/3
SNS	Sympathetic nervous system
SOL	Soleus
TA	Tibialis anterior
TBST	Tris buffered saline with 0.1% Tween 20
Tn	Troponin
UCMS	Unpredictable Chronic Mild Stress

## 9.2 Isoflourane Anaesthesia in Rodents



### Animal Care and Use Program Standard Operating Procedure

SOP # R-18-LUACF


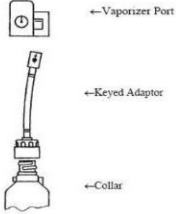
**Title:** Isoflourane Anaesthesia in Rodents

Species: Rats and Mice

1. Purpose:
  - 1.1. To describe the use of isoflourane anaesthesia to induce and maintain a surgical plane of inhalation anaesthesia in mice and rats.
2. Responsibility:
  - 2.1. Researcher
  - 2.2. Animal Care Technician or Veterinarian
3. Minimum Qualifications/Training Required:
  - 3.1. CCAC modules, Health & Safety Training, Facility Orientation
  - 3.2. Rodent handling training and/or experience
  - 3.3. Training and/or experience in general and inhalation anaesthesia of rodents
4. Materials:
  - 4.1. Anaesthesia machine (including vaporizer, tubing, breathing circuit (Mapleson E or other suitable for small rodents), oxygen tank, scavenger canister
  - 4.2. Nose cone, appropriate size for animal being anaesthetized
  - 4.3. Isoflourane anaesthesia, with key-fill adaptor
  - 4.4. Induction chamber
  - 4.5. Heating pad
  - 4.6. Eye lubricant (e.g. lacrilube, isoptotears)
  - 4.7. Subcutaneous fluids (0.9% saline or Lactate Ringers Solution), needles and syringes
5. Procedure:

For Occupational Health and Safety, isoflourane anaesthesia should be performed in a biosafety cabinet whenever possible. The nose cone should fit snugly to prevent gas from escaping. The induction chamber should be flushed with oxygen prior to opening. Refer to the MSDS sheets on the use of Isoflourane.

- 5.1. Rodents do not need to be fasted prior to anaesthesia. However, to ensure their mouths are empty of food, and not potentially blocking their airway, food should be removed from the cage 1 hour prior to anaesthesia. Water does not need to be removed.

- 5.2. Do a pre-anaesthetic evaluation of the animal to be anaesthetized. If any health concerns are noted, contact the Veterinarian prior to proceeding.
- 5.3. Ensure anaesthesia system is properly connected
  - 5.3.1. Induction chamber: inspect the chamber for cracks and ensure the lid closes securely. Attach one (blue) hose to the anaesthetic machine and one port on the induction chamber. Attach another hose (white) to the scavenger canister and the other port on the induction chamber.
  - 5.3.2. Mapleson E circuit: Ensure it is intact and ready to use, but do not hook up until animal is anesthetised in the induction chamber. Attach appropriate sized mask to the T-end of the tubing. When ready to use, attach thin end to oxygen out port on the anaesthetic machine. Attach thicker end to the white hose attached to the scavenger canister.
  - 5.3.3. Scavenger system: weigh canister without tubing before using, record weight. Do not use if the canister is over 50 grams from its original weight.
- 5.3.4. Fill vaporizer with isoflurane: Screw keyed adaptor onto isoflurane bottle collar. Unscrew top screw of vaporizer port. Place keyed adaptor into vaporizer port, ensuring that the holes are lined up. Tighten screw again. Lift isoflurane bottle and allow the liquid to pour into vaporizer. Fill to top line. Do not overfill. Loosen screw, remove keyed adaptor, and tighten screw. Remove keyed adaptor from isoflurane bottle and recap bottle with original cap. Keyed adaptor must remain with the vaporizer. Recheck the level of anaesthesia before starting. Recheck the level between animals or if the procedure is lengthy.
 
- 5.4. Turn oxygen on
  - 5.4.1. Refer to SOP R-19-LUACF-Safe Oxygen Use
  - 5.4.2. Ensure regulator is closed (turn counter clockwise until it feels loose)
  - 5.4.3. Gauge should read zero
  - 5.4.4. Turn tank valve on counter clockwise several turns to open
  - 5.4.5. Turn regulator clockwise until the pressure on the gauge reads 55 psi (red line)
- 5.5. Place a drop of eye lubricant in each eye of the animal
- 5.6. Place animal in induction chamber and seal lid
- 5.7. Place induction chamber on heating pad
- 5.8. Turn oxygen on at the anaesthetic machine to about 1 to 1.5 L/min. Allow the rodent to acclimatize to the chamber for about 1 minute on oxygen.
- 5.9. Turn the isofluroane gas on by pressing down on the white button and turning the dial on the vaporizer to 1%. Allow the rodent to adjust to this amount of gas for about 1 minute.
- 5.10. Slowly turn the dial by 1% increments until you reach 4% to 5%. Allow the rodent to rest at this level until it is not responding to a gentle rocking of the induction

- chamber. Monitor the breathing. It should go from rapid and shallow to slower, regular and deeper breaths as the animal goes under anaesthesia. Never leave an animal alone in the induction chamber.
- 5.11. Once the animal is under anaesthesia (not responding to gentle rocking, and breathing slow and regular), flush the chamber with oxygen by pressing the oxygen flush button on the anaesthesia machine several times. You will need to proceed quickly for the next steps so as not to allow sufficient time for the animal to wake up for anaesthesia.
  - 5.12. Unplug the oxygen hose (blue) from the outflow port on the anaesthesia machine and plug in the smaller hose of the Mapleson E circuit. You can leave this blue hose attached to the induction chamber.
  - 5.13. Unplug the scavenger (white) hose (leave it connected to the charcoal canister) from the induction chamber and attach it to the larger hose on the Mapleson E circuit.
  - 5.14. Take the rodent out of the induction chamber and place the nose into the appropriate sized nose cone of the Mapleson E circuit. Set the induction chamber with the blue hose attached aside.
  - 5.15. Keep the animal on the heating pad during the entire procedure to ensure warmth. Position and secure rodent for procedure as per AUP. Ensure that the nose is in the nose cone at all times. During the procedure, periodically check to ensure that the nose remains in the nose cone.
  - 5.16. Turn the isoflurane gas down to about 1.5% to 2% to maintain the rodent under anaesthesia. Monitor breathing, heart rate, toe pinch reflex, eye blink response, and mucous membrane color to ensure proper anaesthesia. Adjust from 1.5% to 4% isoflurane as needed to maintain adequate plane of anaesthesia.
  - 5.17. Administer subcutaneous fluids according to SOP R-20-LUACF-Subcutaneous Fluid Administration in Rodents. Place another drop of eye lubricant in each eye. Check the level of anaesthesia by toe pinch and blink response. If there is not response, and breathing is slow, deep and regular, you can proceed with the surgery or procedure intended. If there is a response, then wait and periodically check reflexes until there is no response and you have obtained a surgical plane of anaesthesia.
  - 5.18. Continue to monitor the level of anaesthesia periodically during the surgery or procedure by checking breathing, heart rate, toe pink, eye blink and mucous membrane color. The surgical plane of anaesthesia is indicated by deep slow regular breathing, steady heart rate, and absence of toe pinch or eye blink reflex (see chart below). The mucous membrane should be pink.
  - 5.19. Once the procedure is finished and you wish to recover the animal, turn the gas off (turn the dial on the vaporizer all the way to zero and ensure it clicks into place). Leave the oxygen on until the rodent's breathing becomes more rapid, about 1 to 2 minutes.
  - 5.20. Place another drop of eye lubricant in each eye and place the animal back in the cage. It is best to recover the animals alone, with no other animal in the cage, if possible. Turn the oxygen off at the anaesthetic machine by turning the dial and

watching the silver ball fall all the way to the bottom. Keep the animal warm until it is able to walk around the cage normally without stumbling. Until the animal is fully recovered (approximately 10 to 30 minutes), it should not be left alone.

- 5.21. Clean your station, including the induction chamber, anaesthetic machine tubing, and nose cone. Use a mild detergent (e.g. dawn dish soap, Accel cleaner on the chamber, tubing and nose cone, and rinse thoroughly with water. Allow to dry adequately before storing. Hang the tubing up for several hours to dry thoroughly.
- 5.22. Ensure a record of anaesthesia is filled out for each animal.
- 5.23. Depending on the AUP, the rodent should be rechecked at least 4 to 6 hours post-anaesthesia to ensure full recovery.

6. Reference Chart:

Table 1. Parameters to gauge level of anaesthesia in rodents.

	Too light	Surgical Plane	Too deep or problem
Heart beat	Fast, regular	Slower, regular	Irregular, very slow, absent
Respirations	Fast, regular, shallow	Slower, regular, deep	Irregular, very slow, strained, absent
Toe pinch reflex	Present, animal will pull leg back	absent	absent
Eye blink reflex	Animal will blink	Absent	absent
Mucous membrane color	pink	pink	Red, pale, grey, white, blue

Review/Approval:

Author: P. Alderson

ACC Chair: N. Luckai

Date of approval: March 27, 2015

### 9.3 Power Analysis

\*Conducted by Dr. Jocelyn Bel during initial experimental design.

The sample sizes were determined based on other studies being conducted using either corticosterone or mirabegron treatments in mice. Power analysis was performed using University of British Columbia's online statistics software (<https://www.stat.ubc.ca/~rollin/stats/ssize/n2.html>) with values reported by research in this area.

A power above 0.80 was desired from each analysis. A sample size of 10 mice in each group, will provide an n value adequate to determine the treatment effects.

Example of Power analysis for the corticosterone study van Donkelaar et al. (2014):

HOMA-IR:  $M_s1=37.1$ ,  $M_s2=6.8$ ,  $\sigma=4.5$ ,  $\text{power}=0.99$ ,  $\alpha=0.05$ ,  $n=5$

Therefore, this study chose a sample group of 10 mice per group in order for the effects between treatments to be observed.

### 9.4 Lees Lab Western Blot SOP

Western Blot

#### **Day 1 - Gel Preparation and Running**

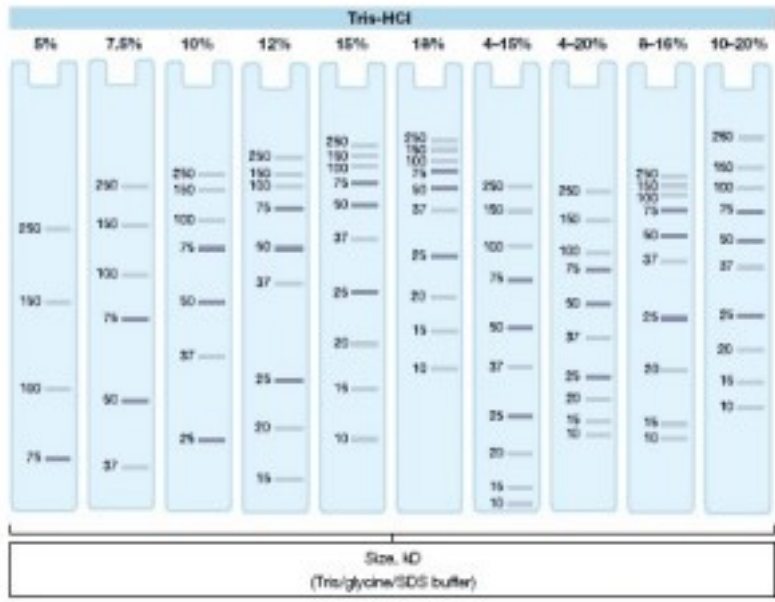
What you need:

- gel apparatus with sponges (bench)
- glass plates (2 sized (1.5mm), 2 short plates) (bench)
- 2 green plate holders (bench)
- combs same size as glass plates (bench)
- vacuum degasser
- 2x 50mL beakers (bench)
- 5ml and 10ml serological pipettes
- 2 transfer pipettes
- Distilled water (DW)
- 1.5M Tris pH 8.8 (4°C)
- 0.5M Tris pH 6.8 (4°C)
- 10% SDS (bench)
- 40% acrylamide (4°C)
- Ammonium persulfate (APS, bench) - catalyst
- TEMED (flammables cabinet, use in fume hood) - catalyst
- 20% methanol (bench, main stock bottles in flammables cabinet)

- 0.1% SDS (bench, main stock powder in flammables cabinet)
- standard ladder (molecular marker) (-20°C)
- gel running apparatus and container (bench)
- PowerPac for power source
- 10ml syringe with needle, or two more transfer pipettes (preference)
- Large styrofoam with ice
- Gel map with sample layout

1. Prepare your separating gel and stacking gel solutions **without catalysts** in separate 50ml beakers each with a stir bar.
  - a. Your separating gel percentage depends on the weight of your target protein. Use the chart in Figure 1 on the next page to choose the appropriate percentage of gel to make. Stock component volumes for various gel percentages are listed in Table 1.
  - b. Your stacking gel is always at 4%. Stock component volumes are listed in Table 2.

**Migration Pattern for Ready Gel Tris-HCl Gels**



<http://www.bio-rad.com/en-us/product/ready-gel-precast-gels/ready-gel-tris-hcl-precast-gels>



Figure 1: Sample migration pattern for different Tris-HCl gel percentages  
 Table 1. Separating gel stock components.

Stock Component	Volume (ml)				
	5%	7.5%	10%	12%	15%
Distilled Water	12.3	10.93	9.68	8.68	7.18
1.5M Tris, pH 8.8	5	5	5	5	5
10% SDS	0.2	0.2	0.2	0.2	0.2
40% Acrylamide	2.5	3.75	5	6	7.5

*Note: The percentage of acrylamide determines the percentage of gel you are making. So, if you have 30% acrylamide to start, you will need to adjust volumes accordingly. For example, for a 10% gel, you will need 6.67ml of 30% acrylamide, and 8.01ml of DW. The DW is to make up the final volume of the solution to ~20ml.*

Table 2. Stacking gel stock components.

Stock Component	Volume (ml)
	4%
Distilled Water	12.68
0.5M Tris, pH 6.8	5
10% SDS	0.2
40% Acrylamide	2

*Note the use of a different Tris buffer compared to the separating gel.*

2. Mix both solutions on the stir plate and place both beakers into the vacuum degasser. Put the lid on and turn the vacuum pump on. Leave the pump running for 20 minutes to remove any air bubbles from the solutions.
3. During this time, obtain glass plates from drying rack on bench. If there is anything to clean off, use a kimwipe with DW. Be sure to check for any chips or cracks in the plates that may result in gel leakage.
4. Place the glass plates into the green holders with the doors open, making sure both plates lay flush with the surface of the bench, and with each other. Next, while applying slight pressure to the tops of the glass plates, close the doors.
5. Place the well combs between the glass plates. Measure 11mm from the bottom of the well comb and place a mark. This is your pour line for your separating gel. Remove the combs and set aside.
6. Place the glass plates that are in the green holders onto the sponges of the gel apparatus. Clip them in. Ensure they are sitting flush on the sponges.
7. Prepare 10% APS in a 1.5ml eppendorf tube: add 0.1g APS to 1ml DW. Triturate until dissolved. Make fresh daily.
8. After the 20 minutes of degassing, carefully remove the separating gel only and replace the chamber lid to protect the remaining stacking gel.
9. In the fume hood, add 20 $\mu$ l TEMED to the separating gel. Quickly move the beaker to a stir plate and mix gently so as not to introduce bubbles. While mixing, add 100 $\mu$ l 10% APS and continue to mix for 30 seconds.
10. Using a transfer pipette, pipette gel mixture quickly between the plates, moving back and forth between the two sets of plates after each pipette-full. Fill each set of plates just over your marker line. As the gel polymerizes, it will shrink slightly.
11. Carefully overlay the separating gel with 20% methanol using a syringe or a second transfer pipette. Allow to polymerize for 30 mins. *\*Tip: leave your transfer pipette in your beaker containing left over gel solution. If this is polymerized after 30 minutes, your gel between the plates will be too.*
12. During this time, make up your 1 X Running Buffer and 1 X Transfer Buffer. Recipes are at the end of this document. Store at 4°C until use. Do not make further than one week in advance.
13. Once the poured separating gel is polymerized, keep the gels on the apparatus and pour the methanol down the sink. Rinse the empty area between the plates three times with 0.1% SDS using a syringe or new transfer pipette. Ensure all SDS is emptied from this area by tilting the apparatus to the side and holding kimwipes to the top edge of the glass plates to absorb any last drops.
14. In the fume hood, add 20 $\mu$ l TEMED to the stacking gel. Quickly move the beaker to a stir plate and mix gently so as not to introduce bubbles. While mixing, add 100 $\mu$ l 10% APS and continue to mix for 30 seconds.

15. Using a transfer pipette, overlay the separating gel with the stacking gel solution, filling to the top of the plates. Insert your gel combs on an angle slowly so as not to introduce bubbles or displace too much gel solution. Allow to polymerize for 30 mins. *Tip: If you need to stop here, you can store your gels for up to 3 days at 4°C. Remove the gels from the apparatus while keeping them in their glass plates with the well combs in place. Wrap them in several layers of wet paper towel that has been soaked with DW and place in a Ziploc bag. Label and move to 4°C.*
16. During this polymerization step, remove your prepped samples from -80°C to thaw in either the bead bath or heat block at 37°C. If a white precipitate is present after thawing, keep them at 37°C until they are clear. This should only take a few minutes. Put all samples along with your molecular marker (ladder) into a tube holder on ice.
17. Fill a Styrofoam box with ice. Use the clear container as a mold and pack ice around container. Remove the container and set Styrofoam box aside for now.
18. Once the gel is polymerized, remove the combs by gently pulling them straight up and out. Remove the glass plates carefully from the holders and place them onto the middle section of the apparatus (containing the electrodes). The short plates of each set should be facing each other. Place this section into the beige middle part with clear “doors”. The doors should be open while the electrode section is being inserted. Apply gentle downward pressure to the electrode section while closing the doors. Place this in the clear container.
19. Fill the middle section between the two gels with 1X Running buffer first, then continue filling the clear container about half way full. Use a transfer pipette to carefully “wash out” wells with 1X Running buffer before loading.
20. Begin loading your samples and ladder into the wells of the gel, vortexing each one just before loading. You should load the wells of the gel closest to you first, and then turn the gel container to load the other gel.  
*Typically, 5ul of ladder is loaded into the first well on your left. All wells should be filled to ensure the samples run straight down. Follow your gel map.*
21. Place the gel container into your ice mold in the Styrofoam box. Pack the ice around the container. Fill up the rest of the gel container with 1X Running buffer, being careful not to pour directly on top of your loaded samples.
22. Place the lid onto the container (black to black electrode, red to red electrode). Plug the cords into the PowerPac and turn on. Turn the voltage up to 200V and press the button that looks like a man running. Make sure to observe bubbles in the running buffer, signifying the gel is running. Check the current to make sure that everything is running correctly. The amperage should be around 60mA per gel (120mA for 2 gels) at the beginning of the run, and should drop to 30mA per gel by the end. If

- these values are significantly off, there could be something wrong with the running buffer.
23. The samples are condensed into a solid blue line (dye front) while they run through the stacking gel. This ensures that all samples enter the separating gel at the same time, and therefore have the same amount of time to run through the gel. Periodically confirm ice is pushed against the apparatus to ensure buffer is kept cold during run.
  24. Allow your gel to run until the blue dye front completely runs off the bottom of the gel. This typically takes just over 1 hour. While this is happening, gather your transfer supplies.

### **Gel Transfer**

What you need:

- transfer apparatus and container (bench)
- 2x cassettes (bench)
- 2 larger plastic containers for soaking filter paper, sponges
- 2 plastic containers for soaking membranes (bench)
- 2 plastic containers for soaking the gels (bench)
- 4x black sponges (bench)
- 4x filter paper (bench)
- 2x nitrocellulose or PVDF membrane (bench)
- flat forceps (bench)
- 1x transfer buffer (4°C)
- ice pack (freezer section of Lees Lab small white fridge)
- stir bar
- gel wedge

25. Just before the run is complete, obtain all your transfer sandwich supplies and containers. Fill all the necessary containers with 1X Transfer buffer.
26. Cut two membranes from the nitrocellulose or PVDF roll using the filter paper as a size guide. Be careful not to touch the membrane with your gloves. Keep the blue protective paper on while cutting.
  - a. Nitrocellulose: carefully remove the blue protective paper using flat forceps and place the membranes into separate containers with 1 X Transfer Buffer
  - b. PVDF: carefully remove the blue protective paper using flat forceps and place the membranes into separate containers with methanol for 30 seconds to activate the membrane. After 30 seconds, rinse the membranes with DW then cover with 1 X Transfer Buffer.
27. In another set of plastic containers, place two sponges and two filter papers in each of two containers.

28. Once the gel is finished running, bring the entire container to the sink and dump out the running buffer. **Do not reuse this buffer.** Disassemble the apparatus to remove the glass plates.
29. Using the gel wedge, release the gel from the big plate so the gel is kept on the short plate. Cut the stacking gel off using the wedge and discard into the chemical waste bucket marked for gels that had samples with DTT run through them. Make a nick in the top left corner (the corner containing your ladder) for the first gel.
30. Place the short plate with the gel on it over the top of a container with 1 X Transfer Buffer. By allowing the buffer to make contact with the gel, it should take the gel off of the plate itself. If this does not work, or if the gel stayed on the big plate rather than the short plate, use the wedge to gently lift the gel off of the plate and place into the buffer. Repeat with second gel in a separate plastic container, making a nick in the opposite corner from the first gel.
31. Place all plastic containers on the belly dancer for at least 15 minutes, with slight agitation. This is necessary to equilibrate all components of the transfer “sandwich”
32. While these components are soaking, wash the running apparatus. To do this, re-assemble without the glass plates and fill the container with DW. Discard and repeat for a total of 3 times. Allow to dry on the drying rack or paper towel. **Do not hang.** Immediately clean the glass plates and place in drying rack with other glass plates to avoid possible damage.
33. Assemble the sandwiches out of buffer on paper towel on the bench in the following order: clear side down, sponge, filter paper **\*add more transfer buffer on top of the filter paper using a transfer pipette to keep things wet**, membrane (move with forceps) **\*add more transfer buffer again**, gel (move with gel wedge, place so that the ladder remains on your left, ensure no bubbles) **\*add more transfer buffer**, filter paper, **\*add more transfer buffer.**
34. Use a 50ml tube to roll out any bubbles in the sandwich layers. Complete the sandwich by placing the second sponge onto the filter paper. Close the sandwich and repeat with the second one.
 

*Tip: Close the sandwich over the clear container to allow any excess transfer buffer to drip into the container.*
35. Place the sandwiches in the centre of the transfer apparatus with the black side of the cassettes facing the black side of the apparatus. Place the apparatus in the clear container, add a stir bar, and place the ice pack in the unfilled space in the container.
36. Fill the container up to just below the edge with fresh 1X Transfer buffer.
 

*Tip: You can pour transfer buffer from the plastic containers that had the sponges, filter paper, and membranes, into the clear container, but NOT from the plastic container that had the gel in it.*

37. Move the apparatus to the clear door fridge onto a stir plate. Turn the stir plate on to low, making sure the stir bar moves easily. Place lid on top, red to red electrode and black to black electrode.
38. Turn the PowerPac on to 30V and run overnight. The amperage should reach 90mA by the end of the transfer. **Note:** you can also transfer for one hour on the bench at 100V. The amperage should reach 350mA by the end of the transfer.

## **Day 2 – Ponceau S, Blocking, and Primary Antibody**

What you need:

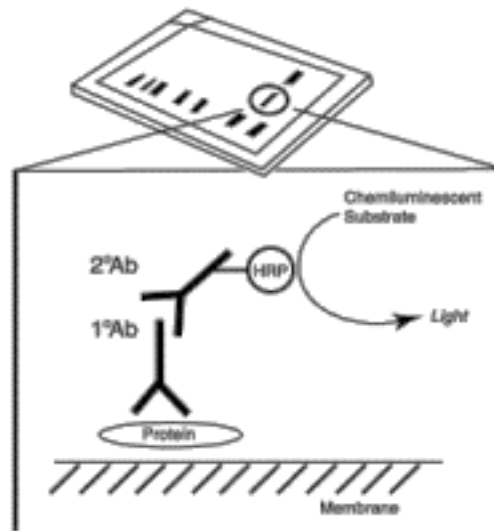
- 2x plastic containers (bench)
- flat forceps (bench)
- scalpel (bench)
- ruler
- glass plate (not one that is used for gel pouring)
- Ponceau S stain (bench, in the dark)
- 0.1M NaOH (bench)
- 1 X TBST (bench)
- 1 clear plastic sheet (bench)
- milk powder or BSA (antibody dependent)
- primary antibody (storage conditions dependent on antibody)
- 50ml conical tube

39. Press stop on the power supply, turn off the stir plate and return the apparatus to the bench. Clean any spilled buffer on the stir plate immediately and remove from the fridge for storage at room temperature.
40. On paper towel on the bench, open the sandwich (black side down). If the transfer was successful, you will see the ladder on the membrane. Cut the nick in the ladder corner again (or the opposite of this for your second gel) and flip the membrane so that the ladder is on your left and place in a container.
41. Rinse the membranes with DW quickly then discard and add Ponceau S to the container (enough to cover the membrane). Place on belly dancer at low speed for 5 minutes.
42. During this staining, wash the transfer apparatus. Rinse 3 times by filling the apparatus with distilled water. Observe the wires inside the apparatus as deposits can build up here causing an improper transfer. If present, gently clear off using a kimwipe wet with DW. Follow this up with 2 more rinses of the apparatus/container with distilled water. Allow to dry on the drying rack.

43. Discard the Ponceau stain and rinse the membranes with DW until all residual background red is gone, and only red bands remain. Scan this image on the computer.
  - a. Plug the scanner into the USB port of the computer, then open the scanner program
  - b. Lay membranes face down on the surface, ensuring no bubbles
  - c. Lay a clear plastic sheet over the membranes, ensure no bubbles are present, and close the scanner
  - d. Select "Document" scan
  - e. After the scan completes, the image is saved automatically. Check to make sure the picture is clear before de-staining the membrane
  - f. Remove the membranes from the scanner surface and clean gently with 70% ethanol and kimwipes
44. Place the membrane on the back of a glass plate (choose one that is not used for gel pouring) and cut out your area of interest using a scalpel. Start by cutting any excess membrane off that was not used in the transfer. **Note:** if you have proteins of interest that are different enough molecular weights from each other (for example, 60kDa and 46kDa) and have run far enough apart to safely separate, you can now cut the membrane into these respective pieces using a scalpel and ruler, being careful to only touch the ruler's edge to the membrane while using it. You can now proceed with each piece as if they are their own blot.
45. Destain the membranes by adding 0.1M NaOH to the container with agitation. It should destain within minutes.
46. Discard and rinse with DW, then wash the membrane for five minutes on the belly dancer at medium speed in 1 X TBST (recipe in Buffers section, this should be made in advance and stored at room temperature)
47. During this wash step, prepare your blocking solution. Make sure to check the antibody information sheet of the antibody you will use to choose the appropriate blocking solution. Typically, 5% milk in 1 X TBST is sufficient, but BSA is also sometimes used. Skim milk is in a bag in the weigh room and BSA is kept at 4°C. Make this fresh daily. Typically, 25ml is used per full membrane. **Note:** if you have cut your blots into smaller pieces and are using the Perfect Western containers, you may use 12.5mL per blot.
48. Once the wash step is complete, discard the 1 X TBST. If you have cut your blots into smaller pieces, move them to the coloured Perfect Western containers. Add the appropriate volume of blocking solution to the container. Place on the belly dancer at room temperature on a low speed for 1 hour. *\*Tip: If after you complete your western it comes out with nonspecific antibody binding, you can increase your blocking percentage to 8% to attempt to eliminate that.*
49. Just before the blocking step is complete, make up the primary antibody in a 15ml tube. The antibody information sheet should suggest a starting concentration for the antibody, as well as what to make it in. Typically, 5ml

of antibody solution (5% milk or BSA made in 1 X TBST) is made per full membrane. **Note:** if you have cut your blots into smaller pieces and they fit into a strip container, you may use 2mL per blot. Otherwise, use 5mL in the coloured Perfect Western containers.

50. Once the blocking step is complete, if you are using the entire blot, place the membranes in the coloured Perfect Western containers. This container requires 5ml of antibody solution. If you have cut your blots into smaller pieces, place them into the strip container. Add your antibody solution and place the container of choice on the rocker in the fridge (4°C) at a low speed. Leave overnight.



*The information sheet that comes with your antibody has suggested blocking percentages as well as antibody concentrations. It also lists species reactivity, meaning which animal species they can detect. Ensure the antibody you choose is specific for the species of your sample. Some primary antibodies are specific to multiple animals. Your secondary antibody is made to target your primary antibody based on the animal that your primary antibody was made in. So, if your primary antibody is a goat anti-rat IL-6, it is detecting rat IL-6 in your sample, and was made in a goat. This means your secondary antibody must be anti-goat.*

### **Day 3 - Secondary antibody**

What you need:

- 2x plastic containers
- 1 X TBST (bench)
- milk powder or BSA (antibody dependent)
- secondary antibody (storage conditions dependent on antibody)



51. Remove membranes from the fridge and place in plastic containers. Add 1 X TBST to cover and wash the membranes for a total time of 25 mins (medium speed on the belly dancer), changing the buffer every 5 minutes (discard down drain).
52. During the last wash, prepare the secondary antibody as per the antibody information sheet. Typically, 25ml of solution (usually in 5% milk made in 1 X TBST) is used per full membrane. If you have cut your blots into smaller pieces, you may make up 12.5mL of solution per piece and again use the coloured Perfect Western containers.
53. Following washes, discard the 1 X TBST. If you have smaller membrane pieces, move them to the coloured Perfect Western containers. Add the appropriate volume of secondary antibody solution. Place on belly dancer for 1 hour at room temperature at a low speed.
54. Discard the secondary antibody solution and perform wash steps as per step 49.
55. During the final wash steps, prepare your detection solution (If using enhanced chemiluminescence, continue as below) and set up the Biorad ChemiDoc Imaging system. **Note:** this system requires 5 minutes to warm up.
  - a. An alternative to enhanced chemiluminescence is Super Signal. Prepare this as per manufacturer's instructions. Typically, it is 2mL of each solution mixed together per full size membrane. This is stored at the bench.

### **Enhanced Chemiluminescence (ECL)**

What you need:

- 1XTBST (bench)
- 1.0M Tris pH 8.5 (4°C)
- DW
- 30% H<sub>2</sub>O<sub>2</sub> (4°C)
- Coumeric acid - light sensitive (-20°C)
- Luminol - light sensitive (-20°C)
- 2 x clear plastic sheets (bench)
- 2 x 50mL tubes, one wrapped in tinfoil (bench, tinfoil in autoclave room) -plastic sheets
- kimwipes
- 1ml pipette and tips
- flat forceps for membrane handling

\*Take out coumeric acid and luminol, wrap in tinfoil and thaw on bench

Label two 50ml tubes as “Solution 1” and “Solution 2”. Add components listed below and keep solution 2 covered with tinfoil.

Solution 1		Solution 2	
Component	Volume	Component	Volume
1.0M Tris pH 8.5	2mL	1.0M Tris pH 8.5	2mL
30% H <sub>2</sub> O <sub>2</sub>	12uL	90mM Coumeric acid	88uL
Distilled Water	8mL	250mM Luminol	200uL
		Distilled Water	8mL

### Imager System Set-Up

- a. Turn on the ChemiDoc imager (one power button at the front)
  - b. Press anywhere on the screen to bring up the selection of users
  - c. Select your name (or create a new user if you haven't yet)
  - d. Ensure you are in the “Camera” section of the program rather than “Gallery”
56. After the final wash, discard the wash buffer. Using the flat forceps, move the membranes to a clear plastic sheet after holding the corner of each membrane to a kimwipe to remove excess wash buffer.
  57. Pour ECL solutions together into one 50ml tube and mix by inverting. Pipette the mixed ECL directly onto the membranes, being sure to cover every part of it. Continue for one minute. **Note:** if you are using Super Signal, you incubate the membranes for 5 minutes rather than one.
  58. Dab excess solution from membranes onto kimwipe by touching the corner of the membrane to the kimwipes, handling with the flat forceps. Place membranes onto a clean clear plastic sheet and move to imager.
  59. Open the drawer on the imager, slide out the tray and place the sheet with the membranes on top. Gently move the tray back into position and monitor the screen to check that the membranes are centered.
  60. Once you are happy with the placement of the membranes, close the drawer.
  61. Select “Chemiluminescence” by clicking on “Application” on the left of the screen and selecting that option under the “Blots” category.
  62. Select “Auto Optimal” by clicking on “Exposure” on the left of the screen and selecting “Auto”. This will auto-expose your membranes, finding the optimal time for signal detection.
  63. Click the camera icon at the bottom left of the screen.

64. Once the image has been taken, a large version of it will pop up on the screen. Ensure there are no saturated spots. These will be red in colour. You can also do this by going into "Gallery" by clicking that button on the top left of the screen, clicking on the image, and clicking "Image Info" at the bottom of the screen. If the pixels have a range topping out at 65,535, there is saturation somewhere on your image. In this same window, you will see exposure time. To fix the saturation, make note of the exposure time and go back to the "Camera" by clicking this button on the top left of the screen. Click "Exposure" and select "Manual". Fill in an exposure time of slightly less than the previous listed time. Click the camera icon to take a new image. Repeat this until no saturation is present.
65. Once you are satisfied with the image taken, without moving the membranes, change the Application type to "Colorimetric" under the "Blots" category. Change the Exposure back to "Auto-Optimal". Click the camera icon. This is your picture for your marker.
66. Go into the Gallery and rename all images taken. Here you can also merge the marker image with the exposed image by selecting both (they will have a check mark in the top right corner) and clicking "Merge" along the bottom of the screen. You can also save this.
67. Connect a USB to the machine. Click all images and select "Send/Save". Select which file type you would like to export (for example, Image Lab is the file type used during analysis with the BioRad Image Lab program) and select your listed USB. All images will be copied over.
68. Log out and turn off the system if no one else is using it that day.
69. The membranes can now be discarded or stored at 4°C in 1 X TBST until a decision is made about possible re-probing. The membrane can be stripped and re-probed for another target if necessary. Note: If you are storing your membranes, perform one 5 minute wash in 1 X TBST before storing in fresh 1 X TBST.

## Buffers and Reagents

### Tris 0.5M pH 6.8

Tris Base - 0.914g

Tris HCl – 14.67g

dH<sub>2</sub>O - 200mL

Directions - Add Tris base and Tris HCl to ~150mL of dH<sub>2</sub>O, stir to dissolve completely. Adjust pH to 6.8 using concentrated HCl and adjust final volume to 200mL. Check pH and store in 4°C.

### **Tris 1.0M pH 8.5**

Tris Base – 17.44g

Tris HCl – 8.84g

dH<sub>2</sub>O - 200mL

Directions - Add Tris base and Tris HCl to ~150mL of dH<sub>2</sub>O, stir to dissolve completely. Adjust pH to 8.5 using concentrated HCl and adjust final volume to 200mL. Check pH and store in 4°C.

### **Tris 1.5M pH 8.8**

Tris Base – 30.78g

Tris HCl - 7.38g

dH<sub>2</sub>O - 200mL

Adjust pH to 8.8 if necessary using concentrated HCl. Store in 4°C.

Directions – start with 100ml distilled water plus Tris base and Tris HCl. Mix well then pH with 6M or 12N HCl (this should be minor if the pH meter is calibrated and working correctly). Measure the resulting volume with a graduated cylinder, and top up the volume to 190ml with distilled water. Check the pH again. You may need to adjust the pH slightly. Do this, then measure the volume again and top up to 200mL with distilled water.

### **10% SDS**

Sodium dodecylsulfate (SDS) - 10g

dH<sub>2</sub>O - 100mL

### **0.1% SDS**

Sodium dodecylsulfate (SDS) – 0.1g

dH<sub>2</sub>O - 100mL

### **4x Reducing Loading Buffer**

0.5M Tris pH 6.8 - 10mL

dH<sub>2</sub>O – 4.06mL

SDS – 2g

Bromophenol blue – 5mg

Glycerol - 10mL \*add last!

-make 1ml aliquots and store at -20°C. Before use, add 110ul β-mercaptoethanol or DTT to 1ml (final conc = 0.1M).

### **1x Running Buffer**

Glycine – 14.4g  
Tris Base - 3g  
SDS – 1g \*add after water!  
dH<sub>2</sub>O – 1L  
store at 4°C

### **1x Transfer Buffer**

Glycine – 2.93g  
Tris Base – 5.82g  
dH<sub>2</sub>O – 800ml  
Methanol - 200ml  
store at 4°C

### **10x TBS**

Tris Base – 5.56g  
Tris HCl – 24.24g  
dH<sub>2</sub>O – 800mL  
-check pH, adjust with HCl to pH 7.6  
NaCl - 87.6g  
Make up to 1L with dH<sub>2</sub>O, check pH again, adjust if needed (should be minor, if at all).

### **1x TBST**

dH<sub>2</sub>O – 900mL  
10xTBS – 100mL  
Tween 20 – 1mL \*use syringe for this

### **Ponceau Stain**

dH<sub>2</sub>O - 475mL  
Acetic acid - 25mL  
Ponceau - 0.5g

\*Note - light sensitive

## **Luminol**

Luminol - 0.44g

DMSO - 10mL

Directions - Dissolve luminol in DMSO by vortexing. Pipette 250uL into eppendorf tubes and store in -20°C. \*Note - light sensitive

## **Coumeric Acid**

Para-coumeric acid - 0.15g

DMSO - 10mL

Directions - Dissolve coumeric acid in DMSO by vortexing. Pipette 100uL into eppendorf tubes and store in -20°C. \*Note - light sensitive

## 9.5 Coomassie G250 Membrane Staining SOP



### QC Colloidal Coomassie Stain

#### Ordering Information

Catalog #	Product
161-0803	QC Colloidal Coomassie Stain, 1 L

#### Introduction

Bio-Rad's QC colloidal Coomassie stain is a ready-to-use single-bottle protein stain that does not require the mixing of any components or addition of any alcohols. It is a special formulation of Coomassie G-250 that provides maximum sensitivity with low background for a wide variety of acrylamide gel chemistries. The QC colloidal Coomassie stain can reliably detect BSA in amounts down to 3 ng.

The QC colloidal Coomassie stain does not contain any methanol or acetic acid, which must be disposed of as hazardous waste.

#### Kit Contents

Kit contains 1 L of QC colloidal Coomassie stain, which is sufficient to stain 10 Criterion™ gels or 20 Mini-PROTEAN® gels.

#### Storage Conditions

The QC colloidal Coomassie stain should be stored and used at room temperature. Do not freeze or refrigerate the stain.

#### User-Supplied Materials

- Deionized water
- Shallow tray with cover for gel staining and destaining
- Ethanol and acetic acid, if gel fixation is desired

#### Staining Protocol

This protocol provides the maximal sensitivity while maintaining low background levels and provides the most consistent and robust results. This protocol allows detection of amounts down to 3 ng of BSA.

Gel Size	Fixing Solution*, ml	QC Colloidal Coomassie Stain, ml	Water Washes, ml
Criterion	100	100	100
Mini-PROTEAN	50	50	50

\* 40% ethanol, 10% acetic acid

#### Gel Fixation

Fixation is recommended for maximum sensitivity and staining of low molecular weight proteins <20 kDa.

- Prepare fixing solution (40% ethanol, 10% acetic acid)
- Remove gel from cassette and rinse in a shallow staining tray with deionized water

- Fix gel for 15 min with gentle agitation
- Discard the fixing solution
  - Dispose of fixing solution properly
- Alternatively, the gel can be fixed with 50% methanol and 10% acetic acid with no loss in sensitivity. Fixing can be replaced with three 5 min water washes or no wash at all, but sensitivity will be reduced.

#### Gel Staining

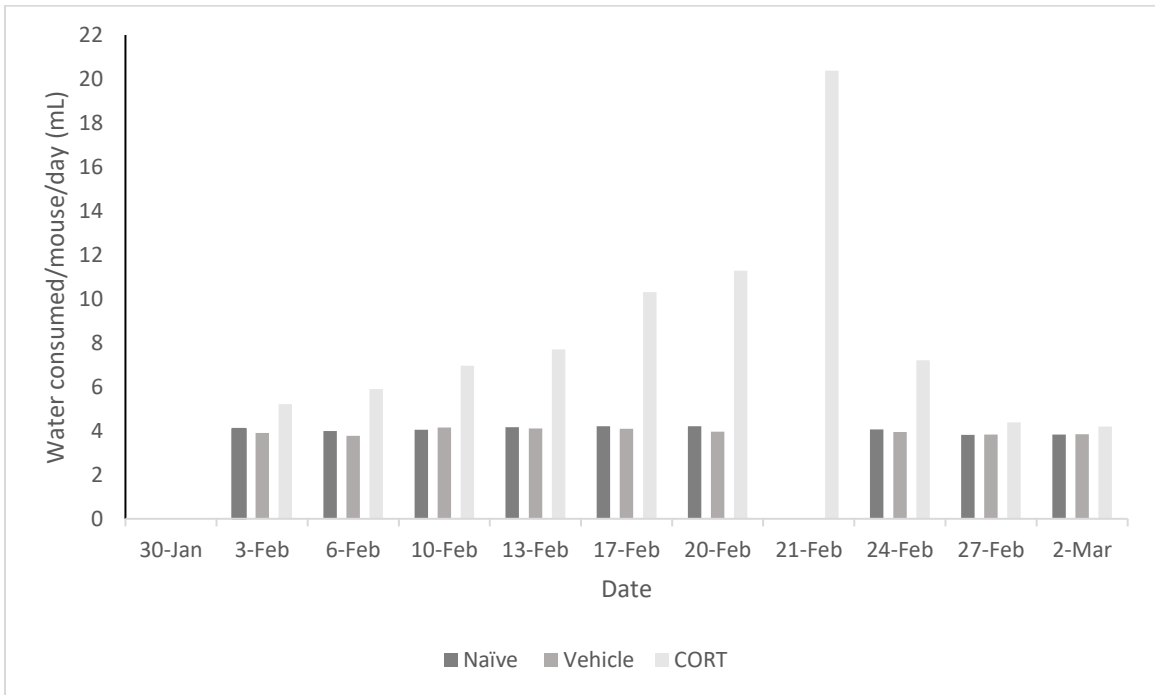
- Rinse the gel in a shallow staining tray with deionized water
- Add QC colloidal Coomassie stain to the gel and incubate with gentle agitation at room temperature for 1–20 hr
  - Maximum sensitivity is obtained after staining for 10–20 hr. Staining for 16 hr allows detection of amounts <10 ng of BSA
  - If rapid staining is desired, gels may be stained for only 1 hr with a slight reduction in sensitivity
  - Cover the staining container to reduce evaporation of the staining solution

#### Gel Destaining

- Discard the staining solution
  - QC colloidal Coomassie stain is formulated without methanol or acetic acid, which need to be disposed of as hazardous waste
- Destain the gel in deionized water. Destain for 1–3 hr with gentle agitation. Change the water at least three times
  - Highest signal-to-background levels are obtained with 3 hr of destaining
  - If rapid destaining is desired, destain 1 hr with 3 changes of water; signal-to-background decreases slightly
- Destained gels are now ready for imaging and analysis
  - Gels can be stored in water for up to 3 days without a significant decrease in sensitivity

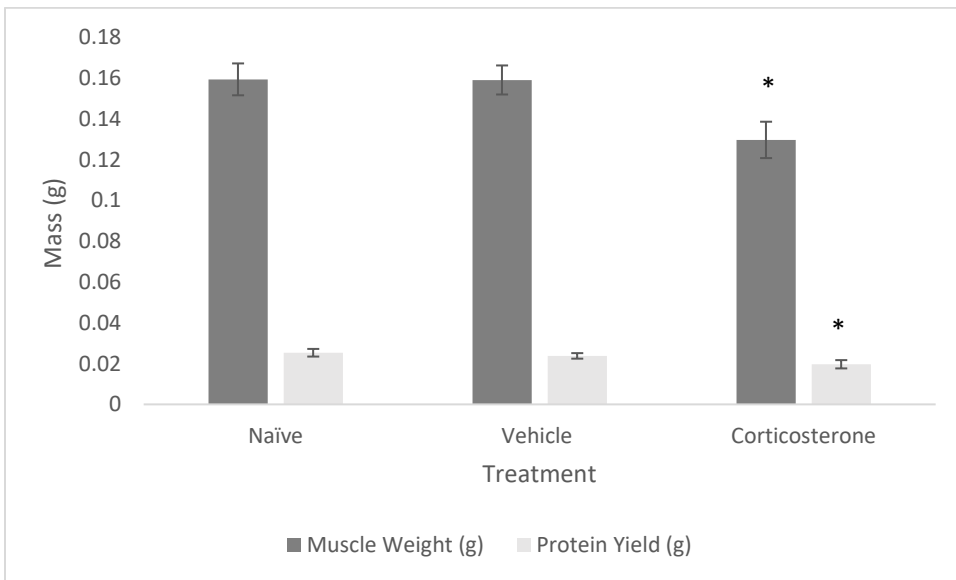


## 9.6 Additional Tables and Figures



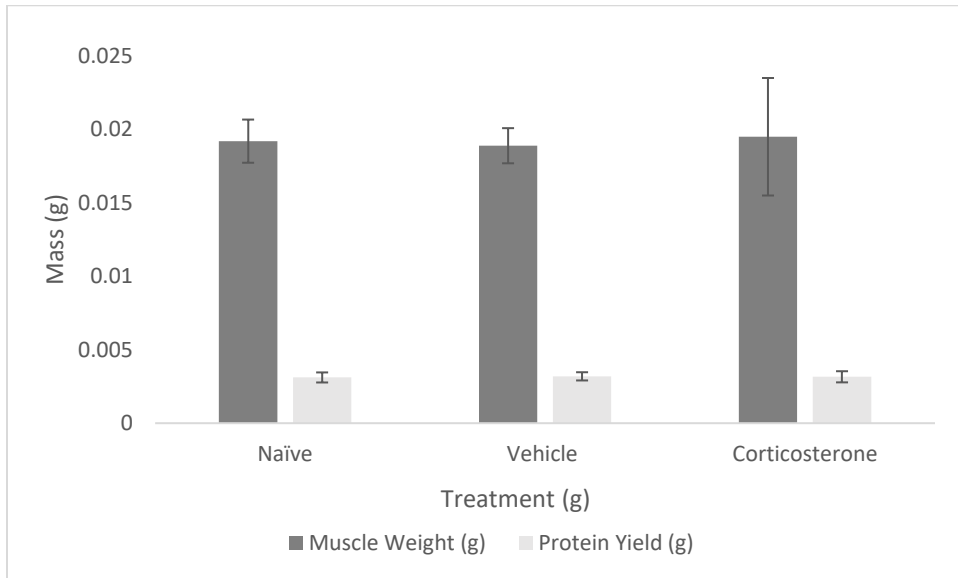
**Figure 21: Water consumption per mouse per day in each treatment group**

Average water consumption per mouse per day over the 4 week treatment period. Amount consumed found by dividing consumption per cage by number of mice and days since water was refreshed.



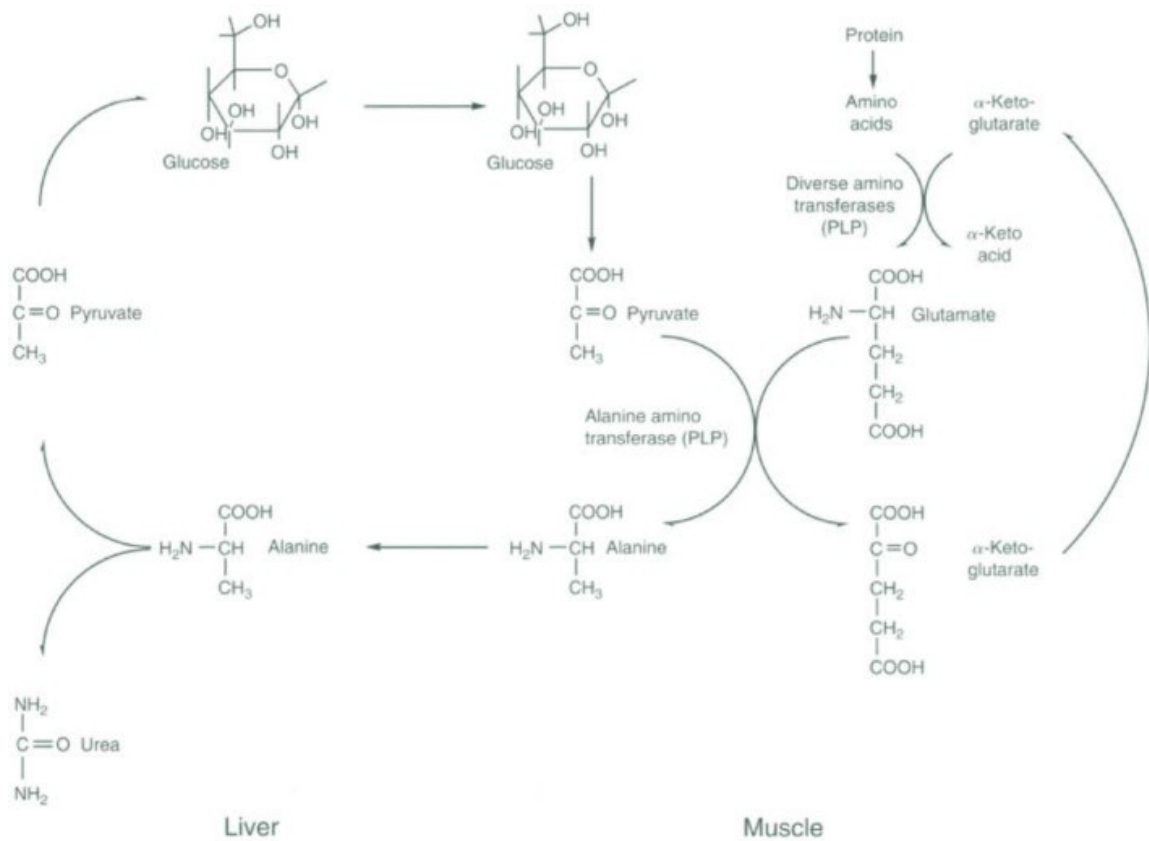
**Figure 22: Muscle Wet Weight vs Protein yield in Gastrocnemius/Plantaris.**

Muscle wet weight of the gastrocnemius/plantaris compared to protein yield.  
\*Significant difference ( $p \leq 0.05$ ) from control groups. Data are presented as mean  $\pm$  SD.  
n = 8-10 per group.



**Figure 23: Muscle Wet Weight vs Protein yield in Soleus.**

Muscle wet weight of the gastrocnemius/plantaris compared to muscle yield. Data are presented as mean  $\pm$  SD. n = 8-10 per group.



**Figure 24: Muscle Protein Degradation via the Alanine Cycle.**

The alanine cycle allows muscle proteins to be broken down as a source of energy for gluconeogenesis in the liver. In muscle atrophy, muscle protein degradation is increased in rodents. Image taken from Kohlmeier 2003 [117].

**Table 3:** Muscle mass and protein yield in milligrams of combined left and right gastrocnemius/plantaris muscles of each mouse. Percent yield indicates percent of muscle wet weight recovered as protein.

Sample	Muscle Mass (mg)	Protein Yield (mg)	Percent Yield (%)
N1G	167	28.8	17.3
N2G	150	23.4	15.6
N3G	152	26.6	17.5
N4G	168	26.7	15.9
N5G	162	25.2	15.5
N6G	173	26.2	15.2
N7G	152	22.2	14.6
N8G	162	26.2	16.2
N9G	151	23.7	15.7
N10G	156	24.0	15.4
V1G	154	23.3	15.1
V2G	163	24.0	14.7
V3G	150	22.8	15.2
V4G	161	23.4	14.5
V5G	174	27.2	15.6
V6G	149	23.9	16.0
V7G	161	21.9	13.6
V8G	159	23.8	15.0
V9G	160	23.7	14.8
C1G	138	19.4	14.1
C2G	129	19.7	15.3
C3G	122	23.1	19.0
C4G	133	19.3	14.5
C5G	119	16.5	13.9
C6G	118	17.3	14.7
C7G	145	21.9	15.1
C8G	133	20.1	15.1

**Table 4:** Muscle mass and protein yield in milligrams of combined left and right soleus muscles of each mouse. Percent yield indicates percent of muscle wet weight recovered as protein.

Sample	Muscle Mass (mg)	Protein Yield (mg)	Percent Yield (%)
N1S	21	3.38	16.1
N2S	19	3.37	17.7
N3S	17	2.36	13.9
N4S	21	3.24	15.4
N5S	20	3.38	16.9
N6S	19	3.47	18.2
N7S	18	2.94	16.4
N8S	21	3.36	16.0
N9S	17	2.80	16.5
N10S	19	2.85	15.0
V1S	18	2.72	15.1
V2S	20	3.09	15.4
V3S	17	2.78	16.4
V4S	20	3.23	16.2
V5S	20	3.42	17.1
V6S	19	3.51	18.5
V7S	17	3.13	18.4
V8S	20	3.56	17.8
V9S	19	3.27	17.2
C1S	21	2.98	14.2
C2S	29	2.81	9.7
C3S	17	3.86	22.7
C4S	17	3.10	18.2
C5S	16	2.67	16.7
C6S	17	2.91	17.1
C7S	21	3.45	16.4
C8S	18	3.50	19.4